Republic of Iraq

Ministry of Higher Education

And scientific Research

University of Babylon

College of Engineering

Mechanical Engineering Department

Wind Tunnel Testing for New Multi –Blades Vertical Rotor to Improve the Output Power in Hilla City

A Thesis

Submitted to the College of Engineering / University of Babylon in Partial Fulfillment of the Requirements a ward of Degree of Master in Engineering / Mechanical Engineering / Power

BY

Ekhlas Qnber Ayuz Mohammed

Pro.Dr. Dhirgham A H Alkhafaji

Pro.Dr. Salwan Obaid Waheed Khafaji

2022 A.D. **1444 A.H.**

بسم الله الرحمن الرحيم

(وَمِنْ آيَاتِهِ أَنْ يُرْسِلَ الرِّيَاحَ مُبَشِّرَاتٍ وَلِيُذِيقَكُمْ مِنْ
رَحْمَتِهِ وَلِتَجْرِيَ الْفُلْكُ بِأَمْرِهِ وَلِتَبْتَغُوا مِنْ فَضْلِهِ
وَلَعَلَّكُمْ تَشْكُرُونَ)

صدق الله العلي العظيم

سورة الروم أية (٤٦)

Supervisors' Certificate

We certify that this thesis entitled ***"Wind Tunnel Testing For New Multi-Blades Vertical Rotor To Optimize The Output Power On Babylon City"*** *was prepared by* ***"Ekhlas Qnber Ayuz"*** *is the result of her own research and under our supervision at the Mechanical Engineering Department, University of Babylon-Iraq, as a partial Fulfillment of requirement for the degree of Master of science in Mechanical Engineering.*

Signature:

Name: Pro.Dr. Dhirgham A H Alkhafaji and

Title: Supervisor

Data: / /

Signature:

Name: Prof. Dr. Salwan Obaid Waheed Khafaji

Title: Supervisor

Data: / /

DEDICATION

To the one who led the hearts and minds of humankind to the safe harbor, the first teacher of mankind the Prophet Muhammad (Sala Allah alleyh w alh wsllm).

To the one who honored me by bearing his name, my father, may God Almighty have mercy on him who exert dearly and precious in order to achieve me a high academic degracadem.

For my great mother's soul, may God Almighty have mercy on her.

To who was my shadow when I get tired my faithful husband.

To the seed of the heart and Tomorrow's hope my daughter and my son.

To my brothers, sisters an honorary source and their sons.

To the brothers who bring me together through the field of work my generous colleagues.

To every heart that walked with me the path of achievement.

To all of these I dedicate this study.

Acknowledgements

Foremost, my grateful thanks to Allah (be glorious) for all the blessings bestowed upon me, and giving me the power and energy to conduct this humble work. I would like to express my deepest gratitude to my supervisors Prof. Dr. Dhirgham Al-Khafaji and Prof. Dr. Salwan Waheed Khafaji for their efforts, encouragement to me, and valuable comments and suggestions. Without their support and careful guidance, this dissertation would not have been possible.

Special thanks go to all my professors in the Mechanical Department at Babylon University for their support and teaching during my graduate studies. I would finally to solely extend piles of thanks to friends in the Mechanical Department to for their advice and cooperation that motivated me in a way or another.

Ekhlas 2022

Abstract

Increasing environmental concerns have led to a demand for more environmentally friendly energy options. Worldwide, wind energy is one of a clean, renewable source of green electricity. Fossil fuel is one of our most important sources of energy and its quantities are decreasing. However, wind is a renewable resource that can as stand by source with fuel. Wind turbines are used to harness the wind to generate energy. For domestic use, most Horizontal- axis wind turbines (HAWTs) are unattractive due to manufacturing complexity and cost. Vertical- axis wind turbines (VAWTs) are ideal for urban applications due to their versatility, aesthetics, low noise and safety. To improve the performance of vertical axis wind turbines, multi-blade vertical axis wind turbines (sim-Savonius)with six arms with six sliding rotating bucket(half) this give flexibility to change the momentum through change of length of arm and angles of blades have been designed and tested in this study experimentally, manufactured and studied to verify their performance. The turbine blade is (half-cylinder blade). The hybrid wind turbine sim Savonius tested with different wind speeds (1.5m/s, 2.5m/s, 3m/s) and radius (30cm, 40cm, 50cm) for the first turbine, (40cm, 50cm, 55cm) for the hybrid turbine. The graphical relationship was established between power coefficient (Cp) and terminal velocity ratio (TSR) and between power coefficient (Cp) and blade angles. It is observed that the performance of wind turbines depends to a large extent on wind speed, blade locations, number of blades and blade angle. The maximum value of the power coefficients of the hybrid turbine (Cp = 31.111%) is observed at (R = 50 cm, r = 30 cm) and 1.5 m/s for blade radius and wind speed, respectively, specifically at TSR = 2.8, blade angle (Θ) = 45˚ and the number of blades equals six. ,where the percentage increase in the power factor between the multi-blade hybrid turbine (MBHYVAWT) and the vertical axis wind turbine that contains six blades (VAWT-b6) = 1.383%, and between

(MBHYVAWT) and (VAWT-b3) = 2.7%. The wind speed database for Hilla city for the past 31 years was also analyzed using (Weibull probability distribution), and the rated speed (V_R), cut-in speed (V_I) and cut-off speed (V_O) of the turbine were obtained. The cut-in speed (V_I) of the turbine was the minimum wind speed at which the machine begins to produce power. The turbine's rated speed (V_R) was the lowest wind speed corresponding to its rated power. The cut-off velocity (V_O) of a turbine was the wind speed at which the turbine is shut off (there is no power in the system). The power duration curve was also determined based on the velocity duration curve, which was plotted between the speed and time percentage values. Once the velocity axis cubed, we will have a force curve, where the area under this curve was proportional to the amount of energy available per year. The energy was found for four years (1988, 1998, 2008 and 2018) to be (3.104, 1, 2.370 and 2.783) watts, respectively.

TABLE of CONTENTS

NOMENCLATURES

Symbol	Description	Unit
A	The projected area	m^2
a	is the straight line's slope	
b	is the intercept (is the intersection distance of the straight line with the y axis)	
C_P	The power coefficient	-------
C_T	The torque coefficient	-------
c	Weibull scale parameter	m/s
E	Kinetic energy	Watt
F	Force	N
f_i	is the frequency of wind speed	-------
k	Weibull shape parameter (dimensionless)	-------
m	Mass	kg
N	The rotational speed	RPM
n	Number of blades	------
P	The theoretical available power	Watt
P_T	the actual value of the power of the turbine	Watt
R	Radius of rotor	cm
T	The rotor torque	N.m
V	Wind velocity	m/s
$V_{I,R,O}$	Cut in speed, Rated speed, Cut off speed	m/s
$\bar{V}$	Arithmetic mean of wind speed	m/s
v_i	wind speed	m/s
$\boldsymbol{v}$	The air volume	m^3

Greek Symbols

Symbol	Description	Unit
ρ_a	Density of air	Kg/m^3
λ	Tip speed ratio	-------
ω	The angular velocity	Rad/s
$\emptyset$	The percentage of calm speed	-------

Abbreviations

Abbreviations	Definition
VAWT	Vertical- axis wind turbine
HAWT	Horizontal- axis wind turbine
TSR	Tip speed ratio
VAWT- b6	Vertical- axis wind turbine is six blades
VAWT- b3	Vertical- axis wind turbine is three blades
MBHYVAWT	Multi-blade hybrid- vertical- axis wind turbine

CHAPTER ONE

INTRODUCTION

Introduction

1.1 Back ground

Wind energy is among the most important renewable energy sources for generating electricity, and its adoption has grown rapidly since 2000.Wind turbines are one of the first devices of extracting energy from natural sources.While it is not possible to generate high consistent electricity from a wind turbine due to fluctuating weather and wind speeds, a small wind turbine can be used to power small appliances at home. A wind turbine is a machine that converts the kinetic energy of the wind into mechanical energy. As a result, wind turbine power generation is entirely dependent on the interaction of the rotors and the wind. Thus, the wind turbine's key performance characteristics, such as power production and load, are specified by the aerodynamics forces produced by the wind [1].

Wind turbines are classified into two types: horizontal-axis wind turbines and vertical-axis wind turbines. HAWTs are employed in a wide variety of countries for medium- to large-scale energy projects, and the vast majority of commercial installations worldwide are based entirely on these turbines. From the other side, HAWTs are not considered a feasible alternatives for harnessing wind energy in metropolitan settings, where certain wind is less density, considerably more turbulent, and chaotic. Therefore, it is preferred to use VAWT due to its numerous advantages, including low cost, simple blade structure, ease of setting and maintenance, and capacity to utilize wind from all different direction, without requiring a steering system [1].

1.2 Brief history

Human attempts to harvest wind energy date all the way back to prehistoric times, when ships and vessels were propelled by sails. Later on, wind energy aided humanity by supplying electricity to milling grain and water pumps.Technology evolved through different stages of development from these primitive and heavy equipment to the efficient and sophisticated machinery of today.The origins of employing wind for mechanical energy are debated. Some say it comes from Babylonia. During the 17th century B.C., the Babylonian ruler Hammurabi sought to use energy from the wind for irrigation [2]. Others argue that wind turbines originated in India [1]. In Arthasastra, a classical Sanskrit text authored in the fourth century B.C. by Kautiliya, references are made to lifting water using wind-powered contrivances [3]. The earliest documented wind mill design dates all the way back to 200 B.C. During this time period, the Persians grind grains using wind mills. The Dutch pioneered the manufacture of these mills, led by renowned designer Jan Adriaenszoon. They improved the design significantly and invented several new mill kind. "Tjasker and smock" mills are examples of this [1], as illustrated in Fig. (1.1).

Fig. (1.1) The windmills of the Netherlands [1]

By the mid-1700s, these wind mills had made their way to America, courtesy of Dutch settlers. This is followed by wind turbine for water pumping, which is still regarded as among the most successful use of wind energy. By the mid-1800s, the so-called American multi-bladed wind turbine made its appearance in wind energy history as illustrated in Fig. (1.2).

Fig. (1.2): American multi blades Windmill [1]

Between 1850 and 1930, almost six million of these devices were installed in the United States alone. The era of wind electric generators began close to 1900's. The first modern wind turbine, specifically designed for electricity generation, was constructed in Denmark in 1890. Grandpa's Knob, in Rutland, Vermont, was the first location to install the turbine in 1941 [4]. G.J.M. Darrieus, a French engineer, proposed the Darrieus turbine design in 1920, that was patented in the United States in 1931 [5]. In comparison to the more common horizontal axis rotor, Darrieus turbines featured narrow curved blades that rotated around a vertical axis. Julius D. Madaras developed a turbine based on the Magnus effect during the same time period. Magnus effect is obtained mostly from the force acting on a spinning cylinders in an air stream. Another notable breakthrough during this period was the invention of the Savonius rotors in Finland by S.J. Savonius. This rotor was created by splitting a cylinder longitudinally and arranging the parts radial on a vertical shaft. The rotor's transverse cross-section resembled a 'S ' [6]. The rotor was propelled forward by the differences in drag forces operating on its convex and concave faces toward the wind.

1.3 Types of wind turbine

There are numerous ways to classify current wind turbines, including the orientation of the rotational axis, the drag or lift forces acting on the blade, and the power output of the turbines (Figure 1.3) [7]. There are two primary types of WTs based on the rotational axis:

1.3.1. Wind turbines with a horizontal axis (HAWT).

The rotor axis of HAWTs is "parallel to the ground" and parallel to the wind direction. These turbines are typically fitted with a self-starter and a yaw system that directs the blades into the direction of the wind. The energy output of these turbines is dependent on the average wind speed

at the site and the amount of wind turbulence [8]. The optimal aerodynamic efficiencies of these turbines has been reported to be between 40% and 55% under steady wind conditions [9]. HAWTs are commonly employed in big wind farm applications, particularly indistant and offshore sites with clean and undisturbed wind. In comparison, HAWTs are just not considered a successful design for urban areas due to the high cut-in wind speed, erratic nature of the wind,and negative public impression of these large devices [10].

1.3.2. Wind turbines with a vertical axis (VAWT).

The axis of rotation of the VAWT is "perpendicular" to the wind and ground directions. These are relatively simple turbines that do not require a yaw system or a self-starting technology (except, Darrieus turbines). VAWTs have a low cut-in wind velocity and noise level, making them suitable for installation in urban settings where towering structures are prohibited. Fig. (1.4) represents the types of turbines. Wind turbines are also classified according to the aerodynamic forces acting on their blade surfaces (drag and lift) forces.

In general the aerodynamic force acting on drag-based WTs is parallel to the direction of wind, whereas the force acting on lift-based WTs is a perpendicular to the direction of wind. While HAWTs and Darrieus turbines are entirely based on lift. Savonius turbines and several other designs of VAWT are dependent on drag forces. Although drag-based turbine are simple in design, they are poor efficiency. From the other hand, lift-based turbines are more complicated and generate more energy per unit area from the wind [11].

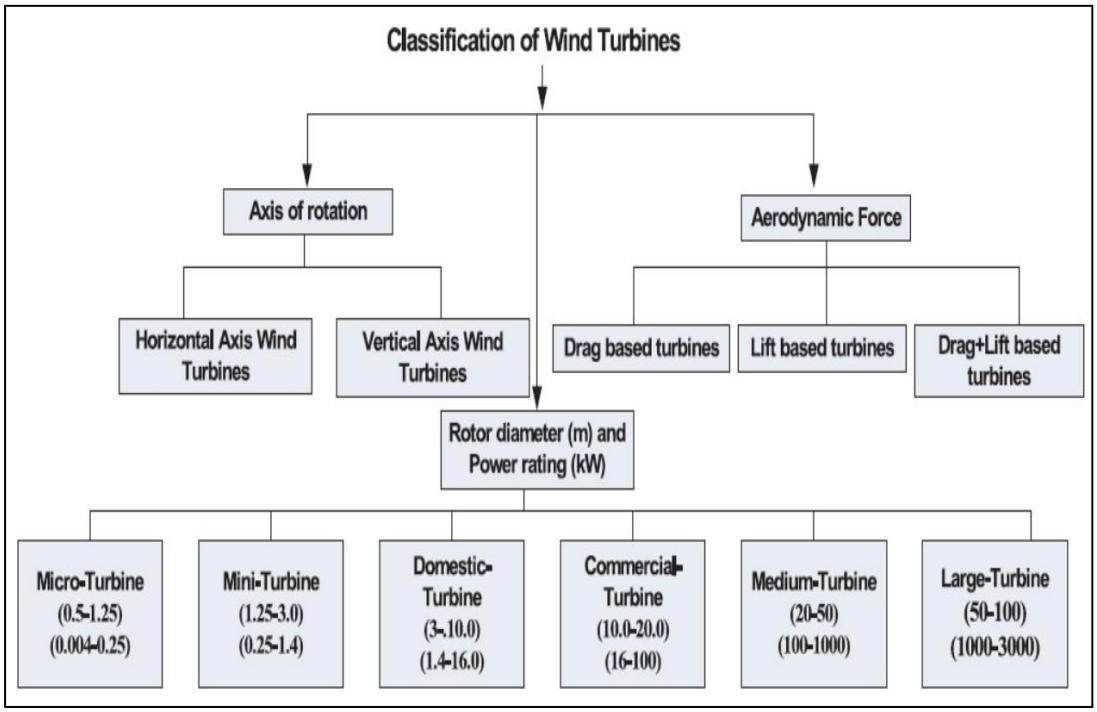

Fig. (1.3) Classifications of wind turbines [7].

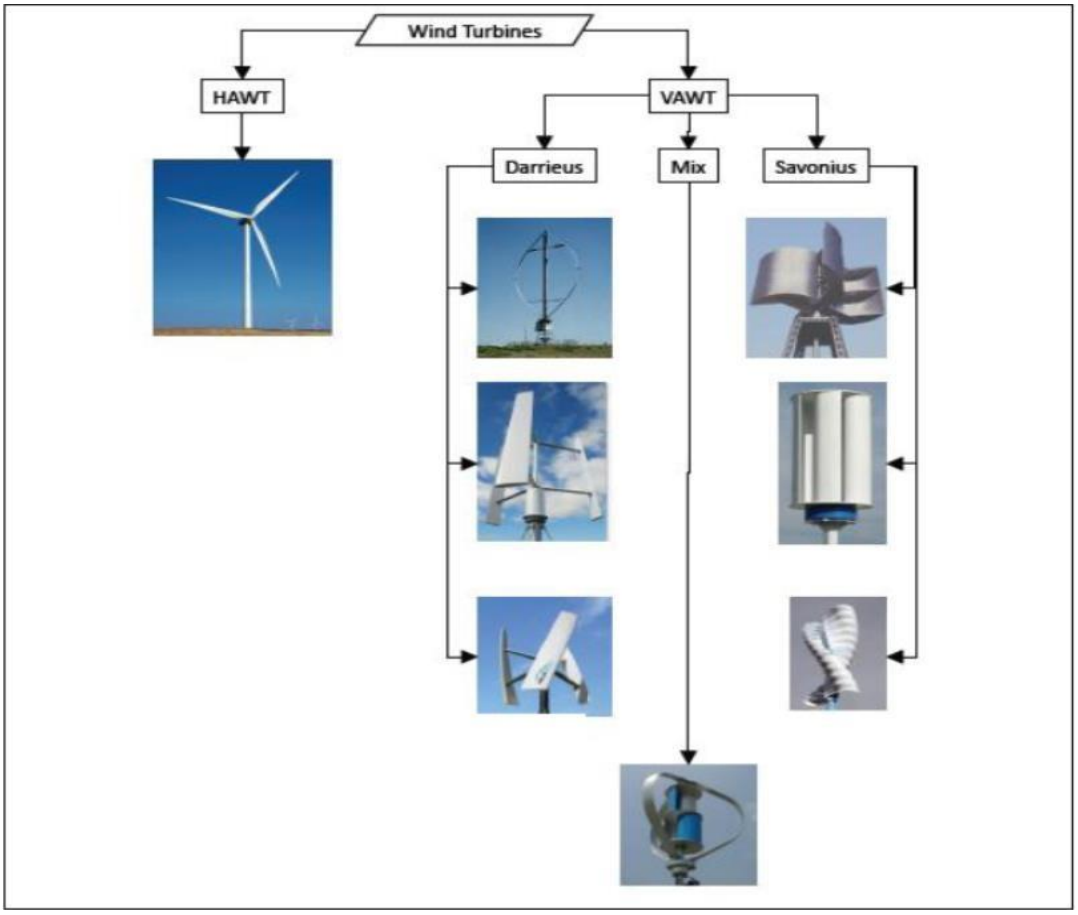

Fig. (1.4) Wind turbine types [70]

1.4 Advantage and disadvantage of vertical Axis wind turbine

1.4.1. Advantage of Vertical Axis Wind [70]

1- The generator, gearbox, and other components can be mounted on the ground, eliminating the need for the tower and making maintenance easier.

2 -The turbines do not have to face into the wind in order to be functional. In a vertical arrangement, air can move the blades in any direction or at any speed. This is advantageous on areas with changeable wind directions.

3- Expandability: The design may be scaled down to extremely small size, even smaller than those seen on urban rooftops. While not all renewable energy technologies have a place in cities, vertical turbines offer a viable alternative to hydrocarbon-based energy.

4- Less expensive to manufacture, easier to install, and transport as compared to horizontal axis turbines.

5- Operate under severe weather conditions, including changeable winds and even mountainous conditions. Where they can provide power to mountain lodges .

6- More quiet than a horizontal axis wind turbine in operation. Since, vertical axis wind turbines are well suited for rooftop installation, making them particularly beneficial in residential and urban areas. Additionally, they can be constructed in areas where higher structures are restricted by legislation .

7- Designed with low-speed blades, which reduces the risk of injury to people and birds.

1.4.2. Disadvantage of Vertical Axis Wind [70]

1. They are less efficient than wind turbines with horizontal axis. Due to the increased drag created by their blades rotating into the wind, the majority of them are just half as efficient as horizontal ones .

2. Airflow near the ground and other objects can produce turbulent flow, introducing vibrational difficulties. This could include noise and bearing wear, which could result in increased maintenance or a shorter service life.

3. Support (Guy wires) may be required to support the machine.

1.5 Commercial concept

Global warming, energy shortages, fast depletion of fossil fuels, and exponential rise in energy consumption in a number of emerging countries have created an ideal environment for widespread adoption of renewable energy technology. Wind energy has emerged as one of the most rapidly growing renewable energy technology, with total capacity reaching 487GW (about 4% of electricity in the world) by the end of 2016 [12]. Wind energy will meet around 18% of global electrical needs by 2050, according to the 2013 IEA roadmap [13]. The development of an efficient wind turbine (WT) and resource evaluation methodology for an urban regions are critical to expanding the penetration of wind energy technology in cities and semi-urban areas [14, 15]. Wind power installations have increased significantly in recent years. Wind energy generation system research and developments were at a high level, attracting worldwide attention. The cumulative installed wind energy capacity (MW) in the world is depicted in Fig. (1.5) [16, 17].

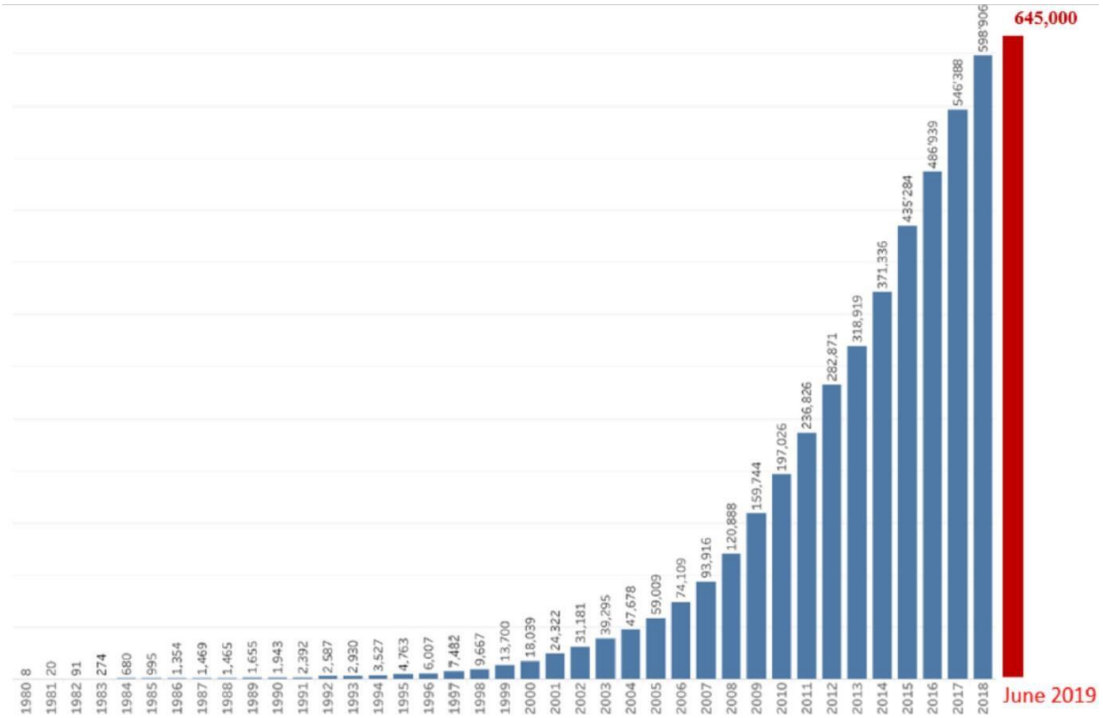

Fig. (1.5) Global cumulative installed wind power capacity (MW) [16, 17].

According to the reference [16], cumulative installed wind capacity power hit 599 MW in 2018 and rose by 7% to 645 MW in 2019 [17]. The development of wind energy-related system technology must be sustainable in order to contribute to climate mitigation, economic advantages, and energy security [18]. Wind energy has a global technological capacity five times that of current global energy generation (i.e. forty times that of global power demands in the best-assumed scenario) [19].

1.5.1. Importance of wind power to dominate power sector growth.

The World Wind Energy Council (WWEC) presented many scenarios that suggested wind energy systems might meet 20% of global electricity demand by 2030 [20]. As the Paris Agreement's aims call for a carbon-free electricity supply by 2050, wind energy would play a critical role in achieving this goal. By 2030, 2110 GW of generated capacity might be

achieved, which would be comparable to 20% of global needs. It is anticipated to generate over 2.4 million employment. Within the next ten years, an investment of approximately €200 billion is anticipated [20]. This is supported by a number of critical aspects, including the substantial fall in the cost of wind energy systems, which increases the practicality of their deployment and makes them economically viable. Wind energy power systems are increasingly likely to be capable of supplying electricity; Fig. (1.6) illustrates the cumulative generated capacity estimated and forecast in 2030 [20].

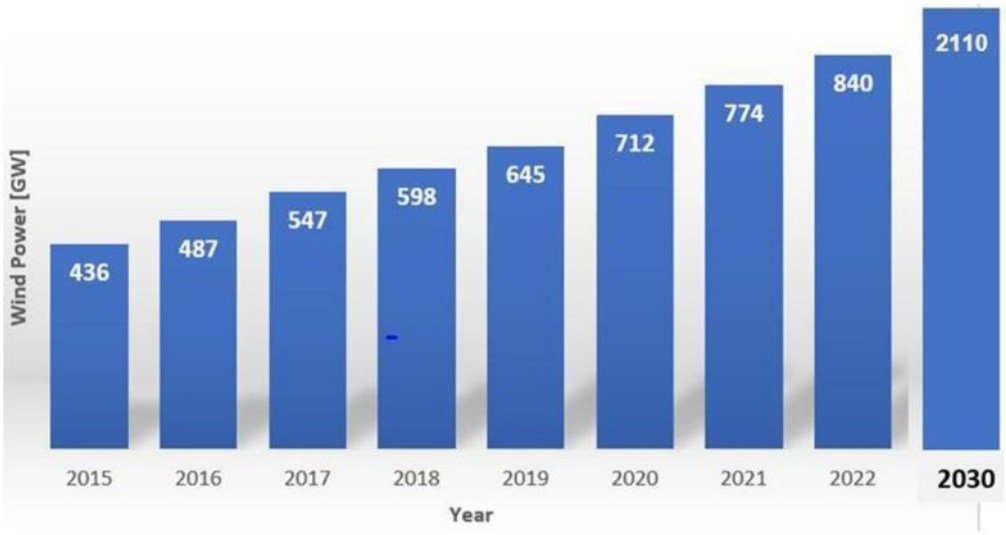

Fig. (1.6) Expected cumulative generated capacity in 2030 In GW [20].

1.5.2. Wind energy's future in Europe

Fig. (1.7) demonstrates that the total amount of wind energy generated by 2018 was 178.8GW [21]. This has expanded to 183.7GW by 2019, surpassing natural gas production. The combined onshore and offshore1 wind capacity installations in Europe were the same as in 2018, while onshore installations were lower.

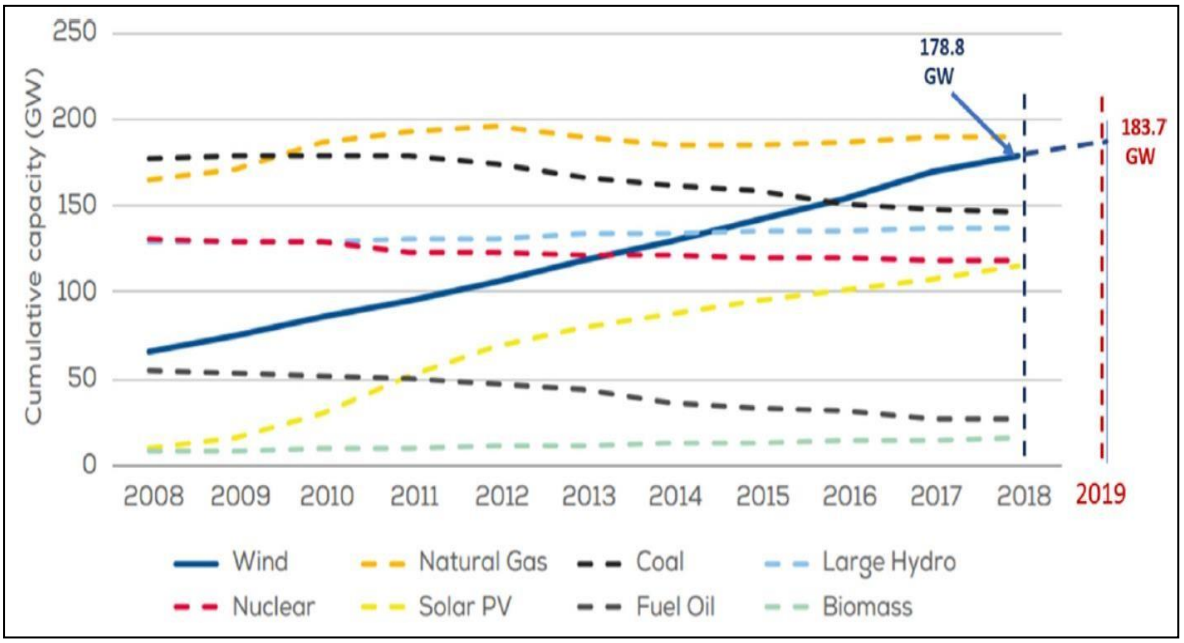

Fig. (1.7) Total European Union power generation capacity from 2008 to 2018 [21].

1.6. Aim of thesis

The purpose of this study is to design and testing a new model of a vertical turbine placed on the roofs of buildings working with low wind speeds to generate electrical power in the low wind speed regions like Babylon zone. The study involved testing of new configuration of vertical axis wind turbine with (three and six) a buckets (blades) and Multi-blade hybrid- vertical- axis wind turbine. The test involved the following parameters or steps:

1- Examine the effects of changing the rotor radius on the performance of the turbine.

2- Examine the effects of changing the angle of the blades with the x-axis on the performance of the turbine.

3- To test the effect of the number of blades on the performance of the turbine.

4- Hybrid turbine test and comparison with previous cases.

5- Analyzing the wind speed database for the Babylon province, which obtained from the Iraqi Meteorological Authority for the last 31 years from (1989 to 2019), the database are cut in velocity, the rated velocity and cut out velocity).

6- Relying on the velocity duration curve and the power duration curve, to find the power generated from wind energy for the Babylon city for the previous four years (1988, 1998, 2008 and 2018).

CHAPTER TWO

LITERATURE REVIEW

Chapter two
Literature Review

This chapter introduces the literature review of previous publications considered in the process of making some important decisions and publications related to the survey. The purpose is to put the research conducted in this article into perspective and appropriate context. Thereview also included an assessment of the contributions and deficiencies of the relevant published materials available, thus exposing areas that require further research (VAWT) technology.

2.1 Experimental Studies

Sad et al (2021) [22], developed a new configuration for multistage Savonius rotors that utilize twisted blades. Accordingly, single- stage, two-stage, three-stage, and 4-stage Savonius rotor with twist blades are explored and compared to a single-stage rotor with matching aspect ratios of 1 to 4. These findings of this research indicated that the new multistage rotor design with twisted blades greatly increased output power. The highest power coefficient for a two-stage rotor is 0.253; for a four- stage rotor, it is 0.261; and for a single-stage rotor, it is approximately
0.223. Additionally, the multistage rotor with twisting blades greatly reduced torque and thrust coefficient fluctuations throughout the cycle. This significantly reduced mechanical noise and vibrations during operation. Additionally, creating single-stage rotors with fewer aspect ratios and combining them into a multi-stage design was simpler and more cost effective than making a single-stage rotors with a higher aspect ratio. As a result, for practical applications, multistage Savonius rotors withtwisting blades are highly recommended.

Liew et al (2020) [23], This study proposed utilising small three- blade Savonius wind turbines with the Internet of1Things (IoT) to monitor environmental and operating variables. Thus, Internet of Things (IoT) technologies are proposed to characterise, regulate, and monitor wind turbine systems globally. This allows remote control over a secure Internet connection. Several factors affected the wind turbine's reliability. First, a gadget was needed to analyse wind turbine rotation data at any moment. Due to the curvature of the blades, when going against the wind, they feel reduced drag force (F convex) than when moving with the wind (F concave). Therefore, the half-cylinder with the concave side facing the wind would experience greater drag than the other half-cylinder, forcing the rotor to spin. The three-blade Savonius wind turbine consisted of three 120° half cylinders relative to one another.

Al-Asbahi et al (2020) [24], designed and build a hybrid power production system that uses wind turbines and solar panels to improve electric energy efficiency. The adopted system attempted to growrenewable energy sources to satisfy demand for polluted and scarce traditional fuels (such as oil, natural gas, and coal). The implementedhybrid design included an improved design for VAWT (Vertical Axis Wind Turbine), which compared two VAWT designs, namely the cupshape and Savonius in terms of performance and efficiency .Two solar panels complement electricity generation, especially in hot, low-wind situations. The system can create 75.05W and 18.2W, according to experiments. For these outcomes, their research presented a PMSG (permanent magnet synchronous generator) design with a stator made of 9 copper-wound coils and a stator Rotor made of rare earth magnets (shaft).

M. Zahir Hussain et al (2020) [25]. Introduced a system that can charge the battery while the vehicle was running, that is, withoutstopping the charging of the vehicle. To use the wind energy, vertical axis wind turbines (VAWT) are used. It was placed inside the front grille of the vehicle, where there will be air flow, which will push the turbine and therefore generate power. The system was reduce the time and money required to charge electric vehicles.

Brandetti et al (2020) [26]. Studied experimental applying variable loads to (VAWT). The experiment was carried out in an open wind tunnel equipped with two-bladed Darrieus VAWT with active independent blade pitch control. Variable load was achieved by dynamically changing the pitch angle of each blade and keeping the tunnel wind speed constant. They use strain gauges to measure blade load, and hot wires to measure the upper and lower wind speeds of the rotor. As a result, the induction of the turbine could be controlled by changing the pitch of the blades. The experimental database allowed the verification of new dynamic models for VAWT and make it publicly available for research purposes.

Al-Ghriybah et al (2019) [27]. This research reviewed the most recent and successful power augmentation systems for the Savonius wind rotor. It was noticed that for the conventional and modified Savonius rotors, the augmentation systems contributed to the power coefficient enhancement. To overcome the negative torque generated on the returning blade, the suggested designs were used.

Vergaerde et al (2019) [28] Wind tunnel tests have beencarried out on single and paired H-type Darrieus vertical axis wind turbines. The turbines arranged in pairs closely spaced, the rotor diameters

shaft to shaft are 1.2 and 1.3, and they rotate in opposite directions. Two rotation directions are studied, one of which is facing (inside) the blades move with the incoming wind, and the facing blades moved against the wind. Wind tunnel testing confirmed that the power coefficient of the paired configuration has a net increase compared to the power coefficientof a single turbine. They discovered the power factor was between 13% and16%, which was consistent with the numerical studies in the literature. In addition to the distance between the turbines, the increase in power also depended on the tip speed ratio and the direction of rotation.

Ayati (2019) [29]. An improved formulation of the Double Multiple Streamtube (DMST) model for the prediction of the flow quantities of vertical axis wind turbines was implemented in his study (VAWT). The latest formulation was strengthened by the fact that it makes the (DMST) valid for any induction element, i.e. any combination of rotor strength and tip speed ratio. Compared to VAWT power measurements obtained at Princeton's High Reynolds number test center, the predictions of the two DMST formulations are compared over a variety of tip speed ratios, rotor solidities, and Reynolds numbers, including those experienced by full-scale turbines. The findings reveal that when rotor loading was mildor heavy, the new DMST formulation displayed improved overallefficiency compared to the traditional one.

Salunkhe et al (2018) [30]. With the support of the vertical axis wind turbine, this paper focuses on the use of air on highway dividers. This air enters the blade of the vertical axis wind turbine tangentially and rotates the turbine in just one direction. In order to produce electrical energy, the solar system is used and often installed in a manner that diverts vehicle air to the turbine. To produce electricity, the generator with the gear

mechanism was attached to the shaft of the vertical axis wind turbine. A battery was used to store the electrical output of the vertical axis turbine and the solar system. This stored energy can also be used for street lights, toll gates, etc. This method basically requires the integration of two energy systems, meaning if any source fails to produce, another source will proceed to generate electricity and will give the load continuous power. For the generation of electricity, renewable energy sources such as solar and wind are used.

Driss et al (2015) [31]. Analyzed the global characteristics of the Savonius wind rotor with various external overlaps. In particular, it is reported evaluating the overall output of the rotor on the basis of the power and torque generated. The purpose of the work was to refine the Savonius wind rotor's experimental conditions and to develop them. It refers to a policy of long-term energization that is the concept of lasting growth and environmental conservation. It has been suggested to modify other geometrics in the future Savonius wind rotor efficiency optimization parameters.

Bhayo et al (2015) [32] Three wind S-rotor models were analysed in this study. Model 1 is a modified Savonius rotor with a single stage and zero offset zero overlaps; model 2 is a single-stage wind rotor with three blades; and model 3 is a conventional Savonius rotor with a double stage. Three output coefficient and dynamic torque coefficient models were created, constructed, and characterized. Model 1, Model 2, and Model 3 have maximum power coefficients of 0.26, 0.17, and 0.21 at
TSRs of 0.42, 0.39, and 0.46, respectively. Model 1 refines aspect ratio, increasing power coefficient by 24%. Model 1, Model 2, and Model 3 have maximum dynamic torque coefficients of 0.81, 0.56, and 0.67 at minimal TSR correspondence of 0.28, 0.21, and 0.17. All three types have high

torque coefficients because they are measured on rotors with higher applied torque.

Loganathan et al (2014) [33]. This research examines a vertical axis wind turbine with semicircular blades at cyclonic domestic wind rates. A 16-bladed rotor was built and tested in a wind tunnel at various wind speeds. A cowling system directs airflow from the back blades into the atmosphere to boost turbine performance. Another 8-bladed rotor was created to study how blade number affects power production. Cowling system aerodynamic efficiency was examined. Each design has wind speed-dependent maximum power curves. The results showed that the 16-bladed wind turbine could provide domestic wind power. The results show that the cowling system significantly increases rotor rpm. The cowling system increases 16-bladed rotor speed by 26% compared to the baseline arrangement. Rotor speed increased 40% for the 8-bladed rotor with the cowling unit. The cowling system can boost the power output of this cyclonic vertical axis wind turbine, especially with fewer blades.

2.2 Experimental and Numerical Studies

Abdel Salam et al (2021) [34]. The purpose of this article is to offer a numerical analysis of the performance of a suggested hybrid (VAWT) rotor. This suggested hybrid wind rotor employed twisting Savonius blade with a modified rotor blades in conjunction with 2/3 Darrieus blades. The numerical simulations was used to investigate the impacts of the blade's attachments angle, radius ratio, and blade count. The Darrieus blades used are straight and have an airfoil profile similar to thatof the NACA0021. It is discovered that "the radius ratio variation" has a greater effect on the performance of the hybrid rotors tested than the attachment angle variation. Additionally, searching for the optimal blade

design at = 0.43 demonstrates that altering the attachment angle and radius ratio can greatly improve hybrid rotor performance. Additionally, it is determined that the suggested hybrid rotor provides C p max. = 0.49 for three-bladed rotors at ϕ= 60 and β= 0.43.

Melani et al (2020) [35] This study proposed a method that combines experimental and numerical methods to analyze the flow field around a 2-blade H-Darrieus turbine moving under different tip speedratios (TSRs).A better understanding of the actual angle of attack during VAWT movement is essential for selecting the correct wing and effective design conditions.A high-fidelity unsteady CFD model of the two-blade H- Darrieus rotor is established It is verified against the unique experimental data collected using particle image velocimetry (PIV).In order to reconstruct the angle of attack change when the rotor rotates one revolution, three different methods (described in detail in the study) are then applied to the calculated CFD flow field.Combine the generated AoA trend with the available blade force data to evaluate the corresponding lift and drag coefficients when the rotor rotates one revolution, and correlate them with the most obvious flow macro-structure and the occurrence of dynamic stalls**.**

Jiang et al (2020) [36] In this research, the deflector located in front of the dual VAWT system is designed and tested with the purpose of improving the performance of the system. First, the power output of the dual VAWT system with and without baffles was quantified in the wind tunnel experiment. It was found that the dual VAWT configuration can increase the power of wind turbines at medium and high tip speed ratios, while the use of baffles improves the performance of wind turbines at low tip speed ratios. Secondly, the deflector affects the performance of the wind turbine, which is a function of the direction of rotation of the two rotors.

Compared with the upwind inward layout, the low wind speed increases the power output by 38.6% compared to the downwind inward layout. Inanother test, the influence of the position of the deflector is determined, and the results showed that placing the deflector closer to the rotor is more beneficial to their performance.Carried out three-dimensional CFD simulation to supplement the experiment, verified the CFD simulation with wind tunnel experimental data, and obtained good simulation data Consistent with the subject. It was found that the deflector contributed to the torque generation by changing the local flow and causing a greater angle of attack and relative speed of the blades. In addition, the blocking effect of the deflector also limits the fluid separation at low speed ratios. Enhanced power output.

LeBlanc (2018) [37]. The turbine is modeled with a two-dimensional actuator cylinder model to predict turbine output and blade loading. A test campaign is conducted to provide a baseline of installed turbine loads. The turbine produces a significant amount of drag that has not been modeled such as struts, strut links, three-dimensional effects, and most likely effects such as dynamic stall. These issues cause the calculated loads of the blades to be much higher than the model predicts. While upwind versus downwind loads transfer, and how this varies with a fixed pitch angle, it is shown to follow modeling trends. Steps are being taken in further research to minimize the drag of these areas on the experimental model, and attempts will also be made to incorporate some of the existing and currently overlooked flow effects, such as struts and dynamic stalls in the numerical model.

Malge et al (2017) [38]. The new blade design and permanent magnet rotor technology of the Savonius VAWT have enhanced its overall power generation .This permanent magnet rotor helps to minimize the

overall spinning force needed to rotate the blades, in particular the wind speed at which the turbine will rotate at low wind speed. The result will be accomplished in this project, which will support the future growth of digital technology (VAWT). This turbine would help to increase the output of electricity from renewable energy sources. Effective manufacturing of this VAWT which helps to reduce friction losses during rotation of the rotor blades .The newly developed blades are simple, powerful and lightweight in construction. It has the ability to catch wind from any direction and can endure any weather conditions. The key benefit of this Savonius (VAWT) is that its expense is minimal and can be easily affordable for commercial power generation.

2.3 Numerical Studies

Anthony et al (2020) [39]. The aim of this work is to develop and analyze wind flow modifier (WFM) modeling for a vertical axis wind turbine (VAWT) in low wind profile urban areas. A simulation is used to compare the efficiency of an efficient C-shaped rotor with a low aspect ratio and a proposed involute-type rotor. Additionally, the WFM model is modified to provide a stack of smaller diameter tubes from the wind inlet tothe outlet. It increased wind velocity and its efficacy is evaluated using an involute turbine. The rotor blade output is monitored numerically using a realizable K-" model in the (CFD) ANSYS Fluent software tool. Thisviscous model with an optimum three-blade rotor sweep area of 0.96 m2 is used to simulate turbine rotational speeds between 50 and 250 rpm. The lift–drag coefficient, the lift–drag powers, the torque, the power coefficient,and the power at different turbine speeds are all measured. As a result, the maximum power coefficient for the drag force rotor is 0.071, while the lift force involute rotor was 0.22. Additionally, the proposed WFM with an involute rotor significantly increased the maximum power coefficient to an

appreciable 0.397 at 5 m/s wind speed, allowing for more efficient configuration in low wind profile areas.

Jie Su et al (2020) [40]. This article attempts to propose a new VAWT structure with V-shaped blades to increase power output at a medium speed ratio. Verifies the feasibility of Reynolds average Navier- Stokes SST k-ω turbulence model applied to VAWT. Then, the SSTk-ω model is used to conduct a comprehensive study on the aerodynamic performance of this V-type VAWT. The results showed that the maximum increase in power coefficient obtained in the best V-shaped blade is about 24.1%. In addition to greatly improving power efficiency, V-shaped blades have also been shown to reduce damage caused by side loads on wind turbines. In addition, the flow structure on the blade surface was studied,the mechanism of dynamic stall, and the reason for the increase in power is explained. Moreover, it is found that the V-shaped blade can effectively suppress flow separation and delay the dynamic stall in the middle of the blade, and the undesired blade tip effect may be more serious than the conventional straight blade. Finally, it is concluded that the current work can be applied to the design and optimization of VAWT blade.

Siddiqui (2020) [41]. This study conducted using high-precision computational fluid dynamics (CFD) simulation, and the effects of tip velocity ratio (TSR), ground clearance, and turbulence intensity (TI) on the performance parameters of the power factor (Cp)) and average torque (T). The main conclusions of this work are as follows: By mounting at the optimum height, the VAWT ceiling performance can greatly reduce the impact of ground shear. The surface mounted VAWT output is affected by the following factors: They have been in close, open terrain conditions. Compared with higher speed ratio (TSR) (3.5 – 4.5), lower TSR (1.5 –2.5)

shows the best performance under variable turbulence intensity. According to reports, TSR 3.0 can provide the corresponding maximum Cp of 0.361**.**

Longo et al (2020) [42]. Computational fluid dynamics (CFD) was used to assess the effect of surrounding buildings on the performance of a roof-mounted, 2-bladed Savonius vertical-axis wind turbine (VAWT). A preliminary simulation campaign is conducted, specifically depicting the surrounding area and using an advanced Reynolds-Averaged Naiver-Stokes (RANS) model. The final objective is to replicate the effect of the surrounding buildings and to reliably predict the energy output of thesystem. This is an important feature of the increasingly up-to-date framework of smart cities, which includes the use of wind energy. Outcomes suggested that the resulting energy output of the system is remarkably different from ideal conditions and that accounting for the localtopography is an aspect of great relevance.

Vergaerde et al (2020) [43]. Closely spaced vertical-axis counter-rotating wind turbines (VAWTs) demonstrated a large increase in power relative to the same insulation turbines. It therefore makes sense to research their capacity for optimization of wind farm output. With this goal in mind, the wake of the isolated VAWT is experimentally compared to the wake of the counter-rotating VAWTs. Because of the unsteady aerodynamics, the wake of an isolated VAWT deflected towards the region behind its upwind moving blade. The direction of rotation thus directly influenced the deflection of the wake. This wake deflection can be seen as an advantage for paired configurations. A pair of counter-rotating VAWTs, where the upwind moving blades are at the middle of the pair, display an especially narrow wake.

Darwish et al (2020) [44]. This article reviewed the latest developments in wind energy conversion system technology and discusses future expectations. By 2050, through appropriate investment in renewable energy, the world can achieve 100% clean energy production. Since 2009, the cost of wind turbines has dropped by nearly a third. It is believed that wind has the potential to provide 20% of the world's electricity by 2030, creating 2.4 million new jobs and reducing more than 3.3 billion tons of carbon dioxide each year. In 2019, the global installed capacity of wind power reached 645GW.If the right investment was made and the correct implementation of the renewable energy system is anticipated, renewable energy and energy efficiency can reduced energy-related carbon dioxide emissions by more than 90%.

Trivković et al (2019) [45]. This paper reviewed the possible multi-objective optimization strategies for the design of small VAWT laminated blades from the perspective of main structural parameters (sequence and number of layers). Many structural analyses of composite turbine blades have been carried out by the finite element method (FEM). In view of the total blade mass, the maximum deflection of the blade tip under static load, the calculated natural frequency and the failure index along the blade, multi-criteria constraint optimization is carried out through the evolutionary method-particle swarm optimization (PSO). By combining different input and output parameters (cost functions and constraints), multiple feasible solutions can be realized.

Antar et al (2018) [46]. The purpose of this work is to improve the efficiency of the Savonius Vertical Axis Wind Turbine

(VAWT) by sizing the required rotor guide plate configuration or what is called the turbine housing using the (CFD) technique. Starting with the proposed baseline casing design, a 2-D parametric optimization process is followed where many design parameters pertaining to the geometry of the casing are allocated and optimized. Due to the restrictions of 2-D numerical simulations, optimized casing measurements are extracted and used for 3-D numerical investigations. The turbine with the optimized housing performed better than the caseless turbine, particularly at the lower Tip Speed Ratios (TSR). A maximum relative increase of 27% in the Cp value occurred at a TSR of 0.76. At a higher TSR of 1.19, a maximum of 48% is the relative increase in performance when comparing the optimized to the baseline designs.

Tian et at (2017) [47]. Vertical axis wind turbines (VAWT) have been used to recover energy from vehicle wake on highways, where recovered wind energy in the wake of high-speed mobile vehicles on highways has great potential, but has not been used. So VAWT is designed to be placed on highway intermediaries and generate power from wake up vehicles on both sides. To evaluate VAWT performance and to determine the mechanism of interactions between the moving vehicle and the turbine, 3D computational fluid dynamics simulations based on the Reynolds-Averaged NaviereStokes equations are implements.
Five typical stops, including one car on the traffic lane, one bus on the traffic lane, two moving cars opposite the traffic lane, one car on the main express lane, and one bus on the main express lane, which are taken into consideration and studied. The results showed that VAWT can generate energy from waking up vehicles on a passing lane. Maximum Average Power Factor 0.00464, which corresponds to an average power of 139.60 W.

Vivek et al (2017) [48]. This article concentrated on increasing the reliability of the use of wind energy by generating a significant amount of electricity and reducing the space for installation. This can be achieved by integrating (VAWT) and (HAWT) in a single tower. The integrated vertical and horizontal axis of the wind turbine improved performance and output volume compared to the separate vertical and horizontal axis of the wind turbine.This reduced the area needed for the construction of the wind turbine by fixing the vertical and horizontal wind turbines in a single tower. More wind towers can accumulate in less area than VAWT and HAWT.

Marinić-Kragić (2017) [49]. This paper presents a low-variable framework for generating diverse VAWT shapes. A scalable, precise, and computationally economical CFD-based performanceprediction approach can provide tailored forms for specified places. With short computational time and mesh sensitivity, CFD findings match experimental data. The initial local optimization case studies showed that considering wind speed distribution instead of single-speed optimization can improve Savonius and H-Darrieus designs. Built parameterization adapts to Savonius and H-Darrieus forms and creates new VAWT designs during global optimization. This global optimization represents the second group of case studies where the optimizer has complete freedom of all formvariables in the developed parameterization. The computational methodology may customize VAWT blade design numerically. B-spline surfaces allow the optimizer to create a wide range of shapes and optimize them generically.

ROGOWSKI et al (2017) [50]. The numerical analyes carried out showed that the results of the coefficient of power are obtained with SST k-!, The disturbance model tends to be satisfactory for the entire edge

velocity range. For lower tip speed ratios, the results of the power coefficient correlate very well to the experimental calculation. In addition, tree-dimensional aerodynamic effects of struts, towers, etc. For this range, the tip speed ratio can be ignored. The average velocity field depends significantly on the tip speed ratio. In the case of a rotor operating at lower tip speed ratios, the velocity profile becomes more asymmetric in comparison to higher tip speed ratios. As the tip speed ratio increased, the static pressure differential increases in the area before and after the Darrieus type rotor. The differences in the static pressure at the blade trajectory are ignored for the downwind part of the rotor, particularly forthe lower tip speed ratio. This means that the VAWT blade with a large solidity does not work on this part of the rotor.

Wonga et al (2017) [51]. This paper discusses thoroughly different systems of flow increase and aims to provide researchers with information on existing enhancement techniques and other related studies.The flow increase method is capable of growing the power coefficient, CP, thus enhancing the output power of different types of VAWTs. Some increase systems are able to increase the overall power output by up to 910 per cent. An optimal design, however, is important to ensure that the blockage of the incoming wind stream is minimized and, at the same time, the positive torque is maximized.In depth, the techniques and designs used to increase upwind velocity and reduce the negativetorque generated on the wind turbine were discussed. In addition, this paperalso reports the flow augmentation systems that are incorporated with building structures.

Rezaeiha et al (2017) [52]. As a function of pitch angle using (CFD) calculations, the current study explores the variations in loads and moments on the turbine as well as the experienced angle of attack, shed

vorticity and boundary layer events (leading edge and trailing edge separation, laminar-to-turbulent transition).Using Unsteady Reynolds-Averaged Navier-Stokes (URANS) equations, pitch angles are investigated while turbulence is modeled with the equation transition SST model. The results showed that a 6.6 percent rise in CP can be accomplished by using a pitch angle of-2 at a point rate of 4.In addition, a change in pitch angle is found to transfer instantaneous loads and moments between the upwind and downwind half of the turbine.

Nagare et al (2015) [53]. Darrieus (based on lifted) and Savonius (drag based). Combining all forms into a novel structure solves these issues. To distribute torque evenly, Darrieus blades are helically twisted. The Savonius has half-drum blades in the centre. This peculiar setup lets Savonius self-start the wind turbine that Darrieus cannot. The shaft has 3 circumferential Darrieus blades and 2 couples of Savonius joined perpendicularly. To reduce self-starting motors and test the model's performance. Wind velocity vary throughout model testing. From the data, the combined assembly's power output rose with wind speed and produced greater power at higher wind speeds.

Gang et al (2014) [54]. This paper lays forth the flow field model for the DU93-W-210 airfoil powered vertical axis wind turbine. FLUENT is used with the RNG k- ε turbulence model to solve the two- dimensional unstable incompressible N-S equations. The 2-D unstable flowarea of the wind turbine is simulated with the COUPLE algorithm and sliding mesh. Under the variance of variable blade mounting angle and chord length, the rotor strength coefficient of wind energy and the variation of the overall torque of the wind turbine are studied. As the result showed, the wind energy power coefficient is increased by 2% at the best

installation angle and the wind energy power coefficient is increased by 15 percent at the best strength.

2.4 Wind Power Estimation

Carta et al. [64], examined the probability density functions applied to wind speed data and discovered that the Weibull distribution for two parameters has several advantages, including:
adaptability, the use of only two parameters, simplicity in parameter estimation regardless of the method used, the Weibull distribution may be represented in a closed form, which simplifies its use, and it includes particular tests for adjustment quality, Good estimation when the parameters of the system are approximated using the sample data.

Seguro and Lambert [67], the graphical method is chosensince it required less computation and could be completed by hand.

Arslan et al. [68] stated that the most often used approaches are the moment method, maximum likelihood method, and graphical method. Therefore, the graphical method adopted in this study. Methods for estimating Weibull parameters is dependent on two parameters (c) and (k), and provides generally more precise and superior estimation than other distribution functions.

2.5 Summary of Relevant Research

Table 2.1: The Main Literature review of the related studies

NO. Ref.	Study site	Year	Type of study	Study variables	Conclusion	View of Rotor
31	University of Sfax, Sfax, Tunisia	2015	Experimental	Various external overlaps.	1- Experimental studies were undertaken to research the effect of the external overlap ratios on the efficiency of the Savonius type vertical axis wind rotor. 2- This analysis allowed four mountings characterized by different external overlap ratios to be set up. 3- The overall rotor efficiency estimation was based on the power and dynamic torque coefficients as a function of the air velocity velocity determined in the wind tunnel test vein.	
32	University Technology Petronas, Bandar Seri Iskandar, Perak, Malaysia.	2015	Experimental	1- Number of stage. 2- Number of blades.	1- Model 1, Model 2, and Model 3 have maximum power coefficients of 0.26, 0.17, and 0.21 at TSRs of 0.42, 0.39, and 0.46, respectively. 2- Model 1 refines aspect ratio, increasing power coefficient by 24%. 3- Model 1, Model 2, and Model 3 have maximum dynamic torque coefficients of 0.81, 0.56, and 0.67 at minimal TSR correspondence of 0.28, 0.21, and 0.17.	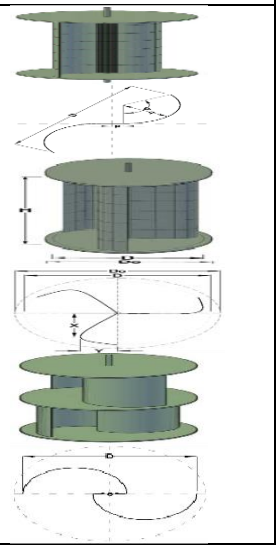

38	Karnataka, India.	2017	Experimental And Numerical	Use magnet rotor to minimize the overall spinning force needed to rotate the blades.	1- The aim of this research is to build a VAWT that can rotate at low velocity i.e. 2 m/s-3 m/s with less drag force. 2- Using a Neodymium permanent magnet rotor with the most powerful blade design to improve the performance of this VAWT.	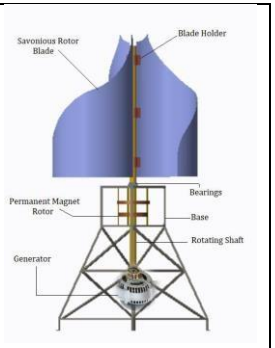
47	Technology, Northwestern Polytechnical University, Xi'an, China	2017	Numerical	Vertical axis wind turbines (VAWT) have been used to recover energy from vehicle wake on highways, where recovered wind energy in the wake of high-speed mobile vehicles on highways has great potential, but has not been used.	1- The results showed that VAWT can generate energy from waking up vehicles on a passing lane. 2- The maximum average power coefficient is 0.00464, which corresponds to an average power of 139.60 W.	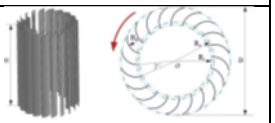 View of the BANKI wind rotor: (a) solid view; (b) section view.
27	University Hussein Onn Malaysia (UTHM)	2019	Experimental	Number of blades, deflector plates and Three different designs to control the wind direction.	This research reviews the most recentand successful power augmentation systems for the Savonius wind rotor. It isnoticed that for the conventional and modified Savonius rotors, the augmentation systems contributed to the power coefficient enhancement. To overcome the negative torque generated on the returning blade, the suggested designs were used.	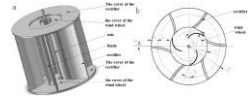 Guide vane  six-bladed rotor

26	Delft University of Technology, Delft, The Netherlands	2020	Experimental	constant incoming wind and an unsteady change in the blade pitch angle	1 - This research proposes an experimental scheme for applying variable loads to the VAWT through a single blade pitch. 2 - The response of the turbine thrust to various pitch plans is consistent with the analysis results of the AC model. When the pitch plan was changed from one to the other, the turbine thrust measurement showed that its response was lagging. 3 - A similar delay is identified in the speed measured in the wake. This phenomenon confirms that variable pitch can be used to display power under low flow conditions. 4 - This study provides an extensive experimental database that can be used to verify the dynamic model of (VAWT).	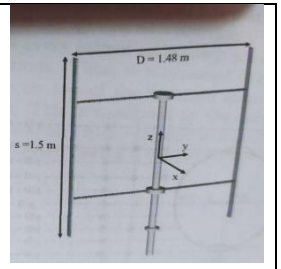 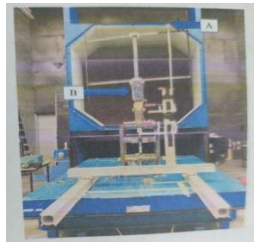
36	Dalian University of Technology, Dalian, China.	2020	Experimental And Numerical	Use of the deflector.	1- It has been found that the deflector has a significant effect on the power output of the two rotors (power increase), which is related to the direction of rotation of the two rotors. 2- Compared with a system without a deflector, the dual VAWT can use up to 38.6% of the wind energy by adding a deflector. 3- It was found that the use of the deflector is a simple and practical method to improve the performance of the dual VAWT system.	

39	Chennai, India	2020	Numerical	1-Used to compare the efficiency of an efficient C-shaped rotor with a low aspect ratio and a proposed involute-type rotor. 2- the WFM model is modified to provide a stack of smaller diameter tubes from the wind inlet to the outlet.	1- The addition of WFM effectively raises the wind turbine's aerodynamic forces at all wind speeds. 2- The WFM model with an involute rotor produces a maximum of 1361 watts at a wind speed of 250 revolutions per minute. 3- Also at low wind speeds, this model's power coefficient is substantially increased to approximately 0.397.Thus, as compared toother configurations, the WFM-based involute rotor VAWT model exhibits superior mechanical and electrical wind energy conversion characteristics.	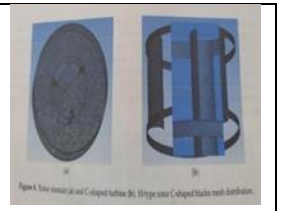
40	Shanghai Jiao Tong University, Shanghai, People's Republic of China.	2020	Numerical	A new VAWT structure with V-shaped blades to increase power output at a medium speed ratio.	1- This study investigated the aerodynamic performance of the new VAWT with V-shaped blades. 2- The SST k-ω model has been used to evaluate the influence of different V-shaped blades on aerodynamic behavior. 3- The results show that, compared with the baseline model, the V-shaped blade has better performance in wind energy conversion.	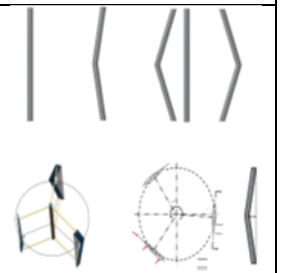
22	Egypt	2021	Experimental	multi-stage rotors with twisted blades **(a)** Single-stage, **(b)** Two-stage, **(c)** Three-stage, and **(d)** Four-stage.	These findings of this research indicate 1 - The new multistage rotor design with twisted blades greatly increases output power. 2 - The highest power coefficient for a two-stage rotor is 0.253; for a four-stage rotor, it is 0.261; and for a single-stage rotor, it is approximately 0.223.	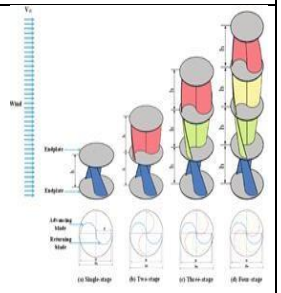

34	Egypt	2021	Experimental And Numerical	Effects of blade attachment angle, radius ratio and number of blades.	1- It is discovered that the radius ratio variation" has a greater effect on the performance of the hybrid rotors tested than the attachment angle variation. 2- Additionally, searching for the optimal blade design at = 0.43 demonstrates that altering the attachment angle and radius ratio can greatly improve hybrid rotor performance. 3- Additionally, it is determined that the suggested hybrid rotor provides C p max. = 0.49 for three-bladed rotors at ϕ= 60 and β= 0.43.	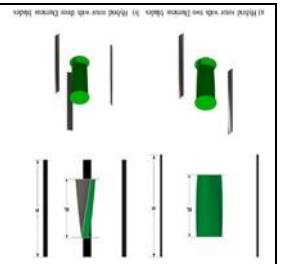

2.6 Work Motivation

From the previous studies which list rated in this chapter,

1- We can suggest new configuration of vertical wind turbine with six arms and sliding of half - cylinder blades (Buckets).

2- The new configuration model give flexibility to change the arm from (10 - 55) cm and angle of blades from (40 - 135) with arm.

3- The aim of this model is to obtain the optimum of blade angle and rotating radius that produce maximum power with optimum power coefficient, and thus obtain the best power generated.

4- The wind speed database collected from Iraqi Metrological Authority is analyzed for Hilla city for the previous 31 years. Using (Weibull Probability Distribution), and obtain the rated velocity (VR), cut-in velocity (VI) and cut-out velocity (VO) for the turbine.

5- The cut -in velocity (VI) of a turbine is minimum wind velocity at which power starts to be produced by the machine. A turbine's rated velocity (VR) is the lowest velocity of the wind corresponding to its rated power. Cut-out velocity (VO) of a turbine is wind velocity at which turbine shut down (no power in the system).

CHAPTER THREE

EXPERIMENTAL WORK

EXPERIMENTAL WORK

3.1. Introduction

All experiments in this study were carried out in the post graduate laboratories of the College of Engineering / University of Babylon, at ambient conditions of 36˚c and a pressure of 100.2 KPa (1 bar).

The study deals with testing a model of a multi-blade vertical axis wind turbine, when exposed to different wind speeds (1.5 m/s, 2.5 m/s, 3 m/s). This chapter deals with the design and manufacture of the test new configuration in a multi-blade vertical axis wind turbine. It also presents the specifications of the turbine required to carry out this study experimentally, and the equations used in the experimental calculations are presented.

3.2. The experimental apparatus

The test model is manufactured from simple materials available in the local markets. The model consists of the following parts, which are shown in Fig. (3.1).

1. Generator.
2. The Blades (Bucket).
3. The arm.
4. The Slider.
5. Stand (base) to install the model on it

Fig. (3.2) shows a schematic diagram of the current study.

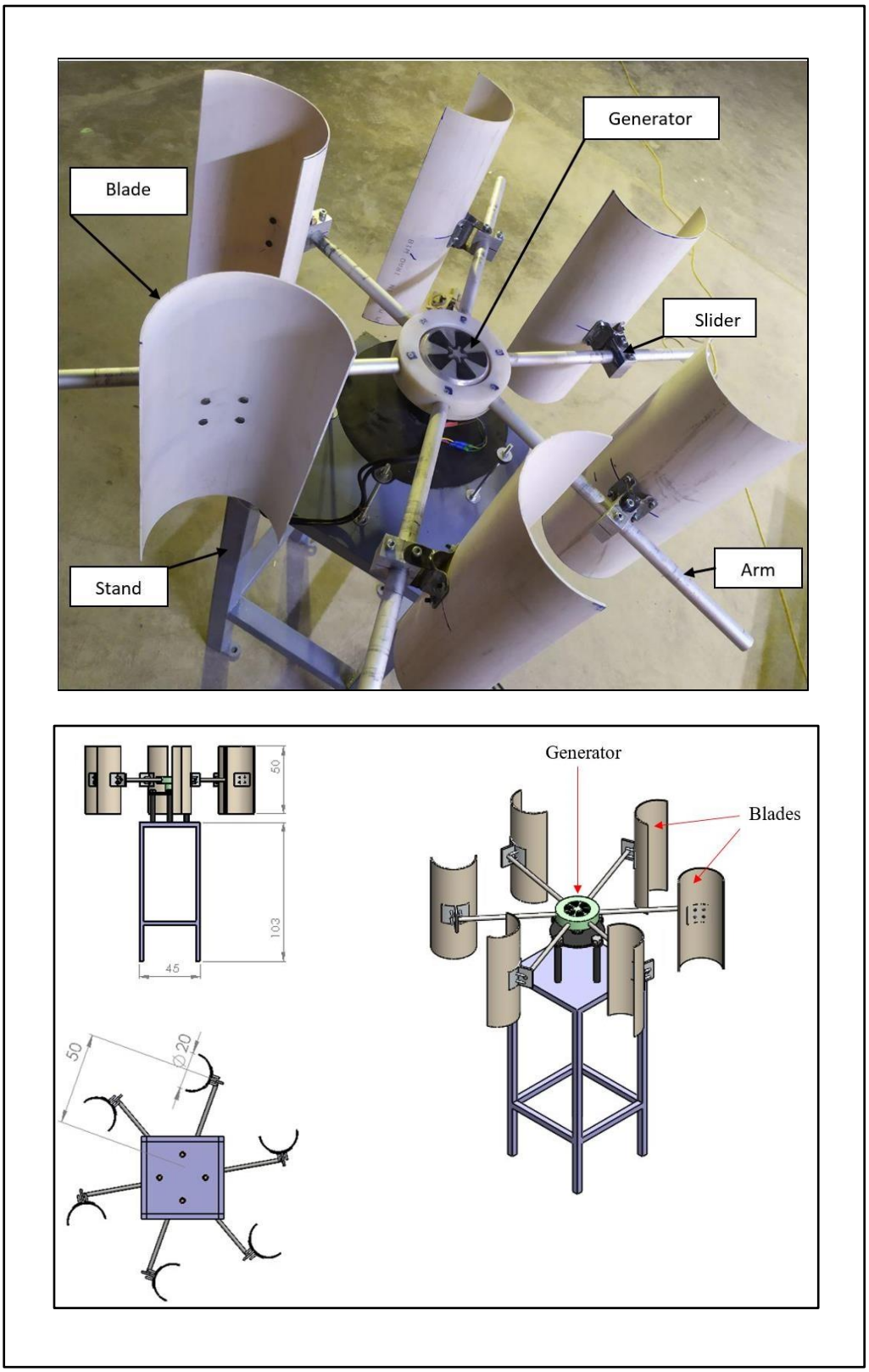

Fig. (3.1) The experimental model (VAWT) with six blades.

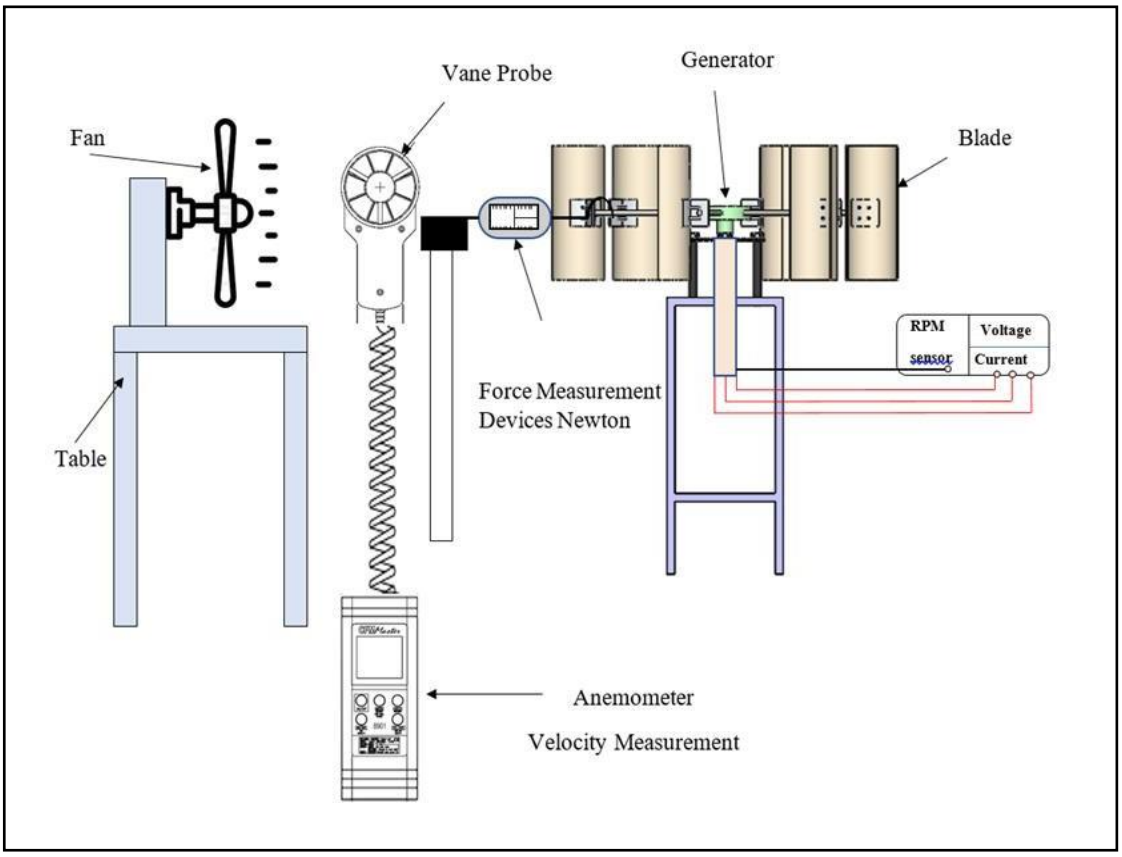

Fig. (3.2) Schematic diagram of the test model.

3.2.1. Generator

Three phase , Max. Power: 250watt , Volt: 12 volt

3.2.2. The Blades

The rotor blades (Bucket) are made of PVC pipe, the shape of the blade is a half-cylinder of 50 cm in high and 20 cm in diameter and their number is 6. The blades are attached to the turbine by several variable length arm. Each blade is connected to the arm by using a slider so that the blade can easily move on the link to change the radius of the rotor.

3.2.3. The arm (linkage)

It is lightweight aluminum tubes, with a diameter of approximately 2.5 cm, connected to the generator on one end and from the other end to the blade by means of the slide.

3.2.4. The Slider

The slider is made of steel and is fixed to the blade, it has a square section that contains in the middle a circular hole whose diameter can be controlled by means of screws. It is used to fix the blade on required arm, to control the required length of the rotor arm.

3.2.5. Stand (base)

The base is made of iron, square in section, its side length is 45 cm, and its height is 103 cm. It is used to support the model during experimental work.

3.3. Measuring Devices

3.3.1. Vane Anemometer

Wind speed is a major factor affecting the mechanical power output of a wind turbine. As a result, wind speed must constantly be measured when evaluating a wind turbine. Vane anemometry is employed in this search to determine the wind speed as illustrated in Fig. (3.3).

Fig. (3.3) Anemometry device

3.3.2. Measuring device

This device is manufactured in a laboratory. It consists of a three-phase bridge rectifier, a resistance of 4 ohms, an L C D 128 * 64 and an Arduino .It used to measure the rotational speed (RPM), the voltage and current generated by the turbine after the model is exposed to a different wind speeds as illustrated in Fig. (3.4).

Fig. (3.4) A device (three in one) for measuring rotational speed, voltage and current

3.3.3. Force meter

Force meter is a type of instrument used to measure the forces. This device are made up of a spring and a metal hook. When a loading is applied to the hook, the spring stretches proportionally. The greater the applied force, the further the spring extend as illustrated in Fig. (3.5).The force measurement device is characterized by a very high precision: maximum deviation ± 0.3 % of load.

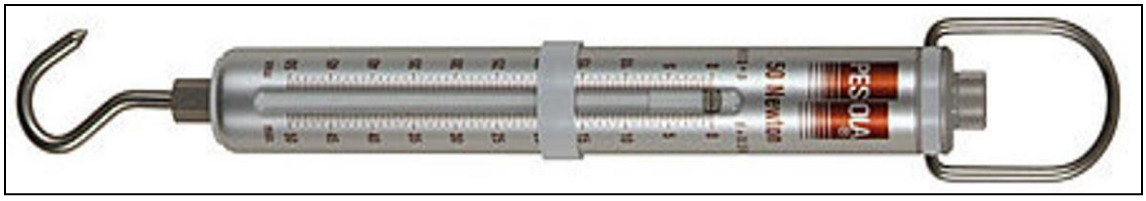

Fig. (3.5) Force meter

3.4. Experiment Procedure

The experimental work is conducted to study a (VAWT) of six blades and three blades, as shown in Fig. (3.1) and Fig. (3.6), as follows:

- The blades of the rotor are made of poly vinyl chloride (PVC) and attached to the turbine by several lightweight aluminum tubes.
- Each blade is connected to the tube by using a suitable slider mechanism, so that the blade can be easily moved along the tube to change the radius of the rotor.
- The shape of the blade is bucket (half-cylinder) of 50 cm in height and 20cm in diameter.
- A specific laboratory fan is used to generate wind for wind turbine experimental testing.
- The wind speed (V) was set to (1.5 m/s, 2.5 m/s, and 3 m/s) as in Table (3.1).
- Anemometry device showed in Fig. (3.3) is used to measure the wind speed.

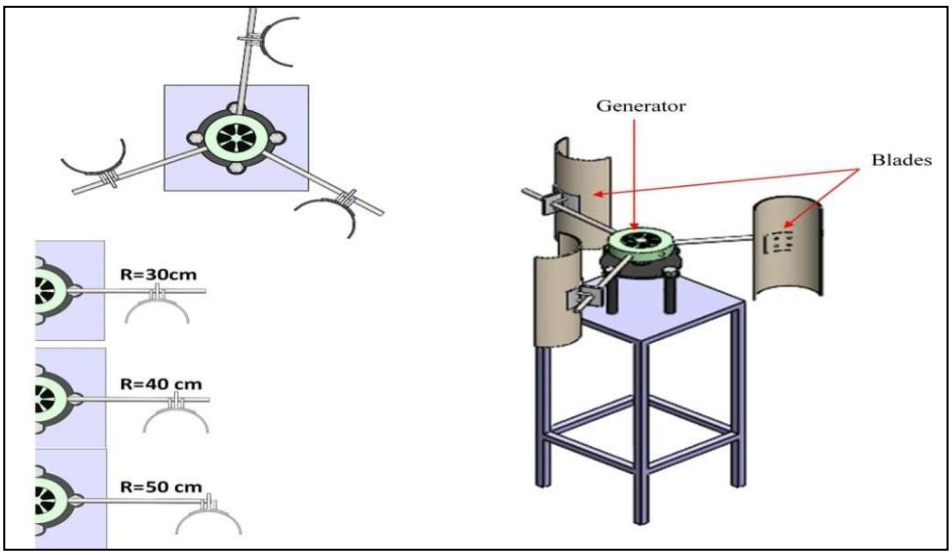

Fig. (3.6) VAWT at Three Blades

Table (3.1) The VAWT model's geometric properties

Property	Symbol	Value	Unit
Blade number	N	3,6	_
Height of the blade	H	50	cm
Diameter of the blade	D	20	cm
Radius of rotor	R	30,40,50,55	Cm
Wind speed	V	1.5,2.5,3	m/s

Testing procedure can be presented by several steps they are:

1- The wind rotor model is placed in the direction of a fan, where the air fan is turned on for variable wind speeds.
2- The wind speed is measured by means of a device (Anemometer) that is placed in front of the rotor blade.
3- Three cases of vertical axis wind turbine are tested.
   a- The first case when the number of blades are six blades (VAWTb6).
   b- The second case when the number of blades are three blades (VAWTb3).
   c- The third case when a multi-blade wind turbine (hybrid) (MBHYWT).
4- Three wind speeds are considered in this work (1.5 m/s, 2.5 m/s and 3 m/s).
5- The experimental work is achieved for different directions of the rotor blades at different angles with each wind speed (40˚, 45˚, 60˚, 90˚, 120˚ and 135˚) with respect to the x-axis as shown in Fig. (3.7).

Fig. (3.7) Changing the direction of the rotor blades at different angles.

6- Three values of the radius of the rotor (30 cm, 40 cm and 50 cm) are considered in the work as well. The rotational speed of the turbine, voltage and the current generated by the turbine are measured by measuring device mentioned previously.

In third case,

7- There are six blades, three blades have a rotor radius constant r = 30 cm .As for the other three blades, the rotor radius has a variable (R = 40 cm, 50 cm and 55 cm).

8- The test is done by changing the angles of the blades at different angles (40, 45, 60, 90, 120, 135) degrees with changing the rotor radius for three blades (R = 40, 50 and 55) cm.

9- Consequently we fix the angles of the blades of variable diameter R at a certain angle and a certain radius with changing the angles of the blades with a fixed diameter r = 30 cm at the angles above and we record the readings for the rotational speed, voltage and current for each time, then we change the angle of the blade with R for another angle with changing the angles of the blades with (r) for the rest of the other angles and so on until we test all the angles, we repeat the above test with the rotor radius changes three times for the above R values, as shown in Fig. (3.8).

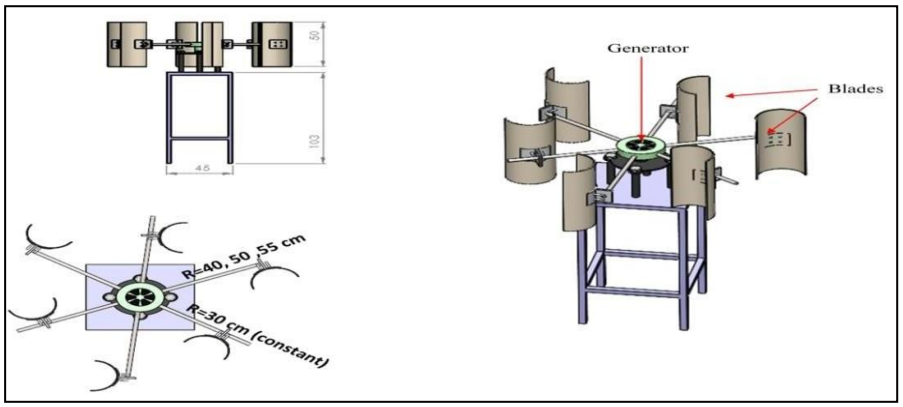

Fig. (3.8) multi-blade hybrid wind turbine

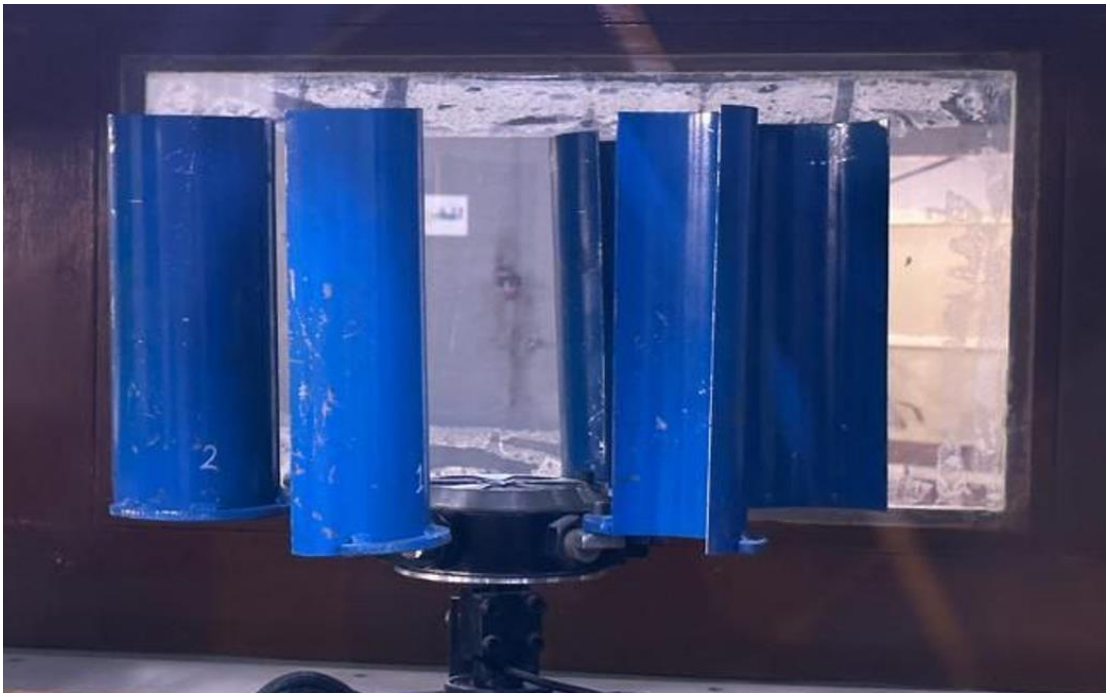

Fig. (3.9) Model in wind tunnel test

3.4.1. Performance Parameters

The wind energy is simply defined by the kinetic energy of vast air masses traveling across the surface of the earth. The kinetic energy is changed into mechanical or electric energies. The efficiency of wind conversion to other usable for mass of energy depends significantly on the efficiency at the interacts of rotor with the wind. In this work, the underlying concepts in the method of conversion of wind energy are discussed. Since air with mass (m) is moving at velocity (V), its kinetic energy equals to [2]:

$$E = \frac{1}{2} mV^2 \quad (3.1)$$

Fig. (3.10) shows a wind rotor with a cross sectional area an exposed to wind stream.

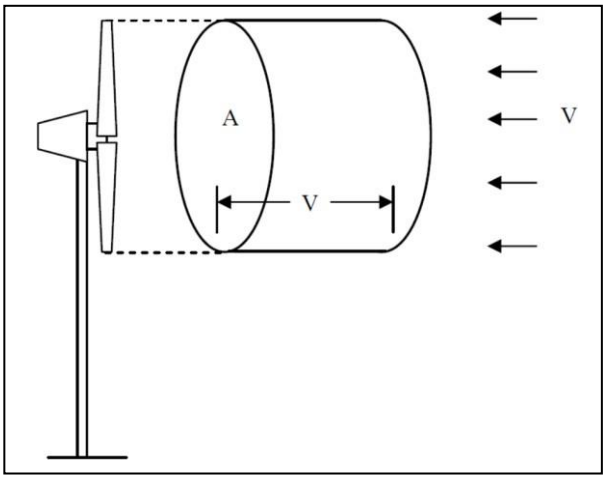

Fig. (3.10) An air parcel moving towards a wind turbine [2].

The expression for the kinetic energy of the air stream available to the turbine is [2]:

$$E = \frac{1}{2} \rho_a v V^2 \quad (3.2)$$

Available to the rotor Per unit time, the air parcel communicating with the rotor has a cross sectional area equal to the rotor (A_T) and a thickness equal to the wind velocity (V). In a wind stream, the theoretical available power (P) is given by, [55]:

$$P = \frac{1}{2} \rho_a A_T V^3 \quad (3.3)$$

However, any turbine cannot completely produce this power from the wind. Thus, the actual power produced by the rotor is affected by the efficiency at which the energy is transferred from the wind to the turbine rotor. This efficiency is often called the power coefficient (Cp), [56], and is given by,

$$C_P = \frac{2P_T}{\rho_a A_T V^3} \quad (3.4)$$

The power coefficient of the turbine depends on important variables, such as the profile of the rotor blades, the configuration and setting of the blade. The designer must attempt to set these parameters at their optimal level in order to reach maximum Cp at a large range of wind velocities. The force of propulsion encountered by the rotor (F) can be expressed as:

$$F = \frac{1}{2}\rho_a A_T V^2 \quad (3.5)$$

while the rotor torque (T) can therefore be expressed as:

$$T = \rho_a A_T V^2 R \quad (3.6)$$

In fact, a rotor shaft only develops a fraction of this torque. The ratio of the actual torque produced by the rotor to the ideal torque is referred as the torque coefficient (C_T) [57] that can be given by,

$$C_T = \frac{2T_T}{\rho_a A_T V^2 R} \quad (3.7)$$

where T_T is the actual torque produced by the rotor. The major non-dimensional parameter is called Tip Speed Ratio (TSR) or (λ) that is used to explain the variables impacting Savonius rotor performance. It is defined as ratio of the rotor's tip speed to the wind velocity (V) as given by Eq. (3.8), [58] :

$$\lambda = \frac{R\omega}{V} = \frac{2\pi NR}{V} \quad (3.8)$$

A rotor's power coefficient and torque coefficient vary with the tip speed ratio. For a given rotor, there is an optimum (λ) at which the energy transfer is most effective and the power coefficient is the maximum (CP max). Thus, to find the relationship between the power coefficient and the tip speed ratio,

Eqn. (3.9) can be used as,

$$C_P = \frac{2P_T}{\rho_a A_T V^3} = \frac{2T_T \omega}{\rho_a A_T V^3} \quad (3.9)$$

By dividing the equation (3.9) and equation (3.7), the tip speed ratio can be given by [59]:

$$\frac{C_P}{C_T} = \frac{R\omega}{V} = \lambda \quad (3.10)$$

3.4.2 Possible Errors in Measuring Devices

There must be errors in most laboratory readings, and in our devices used in measuring torque and rotational speed, and we list below the possible error rate in reading the devices:

a- Speed Measurement

The speed measurement device was calibrated with a type digital device (Hot Wire Anemometer), and the possible error rate was(±1%).

b- Torque measurement

The amount of error in reading the gradients of the ruler with the naked eye is (± 1 mm), since the readings of the radius of the rotor range between (300 mm - 600 mm). The error rate ranges from (0.3% to 0.6%), i.e. an average (± 0.5%). The error rate of the force meter is (± 0.3%). The total accumulated error in reading torque is:

$$\sqrt{0.5^2 + 0.3^2} = \pm 0.58\ \%$$

c- Rotational speed measurement

The rotational speed measuring device is an electronic digital counter, and according to the specifications of the device, the possible error rate is (± 0.2%).

d- power calculation

The cumulative error in measuring power coefficient is the error in measuring torque in addition to the error in measuring rotational speed and wind speed. So the total error will be (± 2%).

CHAPTER FOUR
WIND DATA ANALYSIS

WIND DATA ANALYSIS

Analysis of wind data, which mostly collected from meteorological authority very important requirement for any zone planning to use wind energy. Wind speed, which has a cubic relationship with power, is the most significant parameter to evaluate a candidate site's power potential. It is influenced by the weather system, the topography of the surrounding country, and its elevation above the ground surface. Wind speed changes minute by minute, hour by hour, day by day, season by season, and even year by year. As a result, the annual mean speed must be averaged over a period of at least ten years. Therefore, the wind speed data for Babil Governorate for the period from 1988 to 2018, was analyzed in this work. These data are obtained from the Iraqi Meteorological Authority as shown in table (4.1). Several methods for data analysis are used that will be presented later in this chapter.

Table (4.1) Presents wind database for Babylon city. (velocity m/s)

STATION: HILLA	MEAN WIND SPEED											
YEAR	JAN	FEB	MAR	APR	MAY	JUN	JUL	AUG	SEP	OCT	NOV	DEC
1988	1.4	1.6	2.8	2.6	2.4	2.2	2.7	1.7	1.5	1.5	1.5	1.3
1989	1.5	1.5	2.4	1.6	2.5	3.7	3.5	2.3	1.9	2.0	1.5	1.4
1990	1.3	2.4	2.9	2.4	2.7	3.7	3.7	3.1	2.4	1.3	1.3	1.7
1991	MISS	MISS	MISS	1.0	3.8	2.8	4.3	2.8	2.5	1.1	1.5	1.4
1992	1.7	2.7	1.9	1.9	2.1	2.2	3.8	2.1	1.1	1.1	1.2	1.3
1993	1.3	1.7	2.8	2.0	2.6	2.4	3.0	1.4	1.2	0.9	1.4	0.9
1994	1.4	1.9	2.2	2.5	2.2	3.0	3.3	2.4	1.1	1.4	1.4	1.8
1995	0.7	2.0	2.1	2.5	2.1	2.3	3.0	2.4	1.7	1.1	1.2	0.7
1996	1.2	1.7	1.9	2.4	1.4	1.9	2.0	1.5	1.6	1.6	0.8	1.3
1997	1.0	1.4	1.8	1.4	1.2	1.2	2.9	2.7	0.6	0.5	0.8	0.6
1998	1.3	1.0	1.7	1.3	1.2	1.7	1.3	0.7	1.2	0.7	0.4	0.6
1999	0.6	0.7	1.7	1.6	1.5	1.3	2.0	1.7	0.8	0.8	0.9	0.7
2000	1.1	1.6	1.9	1.6	1.1	2.5	1.5	1.5	1.3	0.9	0.5	1.1
2001	1.2	1.7	1.5	2.4	2.8	4.1	2.7	2.2	1.8	1.7	1.7	1.6
2002	1.8	2.1	2.5	2.8	2.0	2.5	2.0	2.5	2.0	1.2	1.4	MISS
2003	MISS	MISS	2.9	2.2	1.7	2.0	2.4	1.4	1.3	1.1	1.1	1.1
2004	1.2	2.3	2.2	2.4	4.7	2.5	2.4	1.6	1.3	0.6	1.0	1.2
2005	1.6	1.1	1.7	1.9	1.8	2.3	2.1	1.8	1.4	1.1	0.9	1.1
2006	1.6	1.7	2.5	1.8	1.5	2.1	2.3	1.5	1.5	1.3	1.0	1.5
2007	1.3	1.6	1.8	1.9	1.4	2.0	1.9	1.6	1.6	0.8	0.8	1.2
2008	1.4	2.2	1.5	1.8	1.6	3.1	2.2	1.4	1.3	1.0	1.0	1.7
2009	1.3	1.7	2.2	1.4	1.2	1.6	2.6	1.1	1.0	0.9	1.0	0.6
2010	1.7	1.7	1.6	1.6	1.6	2.0	2.1	1.1	1.2	1.0	1.0	1.2
2011	0.8	1.3	2.3	1.9	1.4	2.5	1.8	1.6	1.2	1.5	0.9	1.2
2012	1.3	1.9	1.7	1.5	1.4	2.2	2.3	1.6	1.2	0.9	0.9	1.4
2013	2.2	2.1	2.2	2.9	2.9	3.6	3.8	3.0	2.2	2.0	1.4	2.0
2014	2.1	2.0	2.3	2.2	2.6	2.8	3.1	2.3	1.6	1.7	2.1	1.5
2015	2.1	2.4	2.1	2.4	2.4	3.0	2.8	2.1	1.4	1.6	1.2	1.7
2016	1.5	1.5	2.1	1.5	2.4	2.1	2.2	1.4	1.7	1.1	1.5	2.1
2017	1.2	1.6	1.8	2.1	1.9	2.4	2.1	2.0	1.4	1.1	1.3	1.3
2018	2.1	1.7	2.0	1.8	1.7	2.3	2.9	2.3	1.0	1.7	0.9	1.0
2019	1.3	1.5	2.4	1.9	1.3	1.8						
2020												

4.1. Wind Power Density Estimation

The data presented in table (4.1) will be used to calculate wind power density. In general there are three methods used to analyze wind speed rates and thus wind power:

4.1.1. Arithmetic Mean Method

The arithmetic mean value can be calculate by, [60]:-

$$\bar{V} = \frac{\sum_{i=1}^{i=n} f_i v_i}{\sum_{i=1}^{i=n} f_i} = \frac{1}{n}\left[\sum_{i=1}^{i=n} f_{i.} v_i\right] \quad (4.1)$$

To calculate the power density, the arithmetic rate of velocity in Eqn. (4.1) used to obtain wind power density by:

$$P_w = \frac{1}{2}\rho\bar{V}^3 \quad (W/m^{2)} \quad (4.2)$$

4.1.2. Mean Cubic Method

This method is more accurate than the previous method [60].

$$\bar{V}^3 = \frac{\sum_{i=1}^{i=n} f_i V^3}{\sum_{i=1}^{i=n} f_i} \quad (4.3)$$

This equation is used with Eqn. (4.2) to obtain power density.

4.1.3. Weibull Method

The two - parameters Weibull distribution is universally accepted as a suitable model. This method is the most extensively employed in the wind business [61, 62]. Jung and Schindler [63] examined the goodness-of-fit of various theoretical parametric distributions in 46 research published between 2010 and 2018. According to the authors, the most often examined distribution is the two-parameter Weibull distribution.

The probability density function Eqn. (4.4) and cumulative distribution function Eqn. (4.5) can be used to depict the Weibull distribution that is used in this work [60, 65].

$$f(v) = \left(\frac{k}{c}\right)\left(\frac{v}{c}\right)^{k-1} exp\ \left[-\left(\frac{v}{c}\right)^{k}\right] \quad (4.4)$$

$$F(v) = 1 - exp\ \left[-\left(\frac{v}{c}\right)^{k}\right] \quad (4.5)$$

4.1.3.1 Estimation Methods for Weibull Parameters

Additionally, numerous approaches for estimating the Weibull parameters have been developed. Several of these techniques include the following [66]:

(1) Moment method
(2) Graphical method
(3) Energy pattern factor method
(4) Power density method
(5) Maximum likelihood method
(6) Standard deviation method

The graphical method requires the twice logarithm to be applied to equation (4.5), resulting in equation (4.6) after some mathematical manipulations [60]:

$F(v) = 1 - exp\ \left[-\left(\frac{v}{c}\right)^{k}\right]$ Cumulative distribution function (4.5)

$$\ln(1 - F(v)) = -\left(\frac{v}{c}\right)^{k}$$

$$\ln[\ln(1 - F(v))] = \ln\left[-\left(\frac{v}{c}\right)^{k}\right] \quad (4.6)$$

$$\ln[-\ln(1 - F(v))] = k\ln(v) - k\ln(c)$$

Equation (4.6) can be thought of as a line equation, y = ax + b.

Where: $y_i = \ln[-\ln(1 - F(v))]$

$x_i = \ln(v)$

i=1, 2, 3……

Thus Weibull parameters are obtained as

$$k = a \tag{4.7}$$

Scale parameter is

$$b = -\ln(c)$$

$$c = exp^{\frac{-b}{a}} \tag{4.8}$$

According to Akdag and Dinler [69], this approach is implemented in three stages:

(i) Calculate cumulative frequency distribution using wind speed data, or evaluate frequency distribution first, which requires sorting wind speed data into bins and then calculating cumulative frequency distribution using frequency distribution,

(ii) Compute { $\ln(v)$, $\ln[-\ln(1-F(v))]$ } pairs and

(iii) Solve the linear least squares problem and calculate the scale and shape parameters by using equations (4.7) and (4.8).Table (4.2) presents these accounts.

Table (4.2)

	Bin	No.V	Frg.	Frg.%	F(v)	1-F(V)	Ln(1-F(V))	Ln(V)	Ln[-Ln(1-F(V)]
0	0	0	0	0	0	0	0		
1	0.8	22	0.05914	5.913978	0.05914	0.94086	-0.060960928	-0.223143551	-2.79752214
2	1.3	86	0.231183	23.11828	0.290323	0.709677204	-0.342945054	0.262364264	-1.07018504
3	1.8	114	0.306452	30.64516	0.596774	0.403225591	-0.908259094	0.587786665	-0.0962256
4	2.3	77	0.206989	20.69892	0.803764	0.196236344	-1.628435509	0.832909123	0.487619743
5	2.8	47	0.126344	12.63441	0.930108	0.069892258	-2.660800393	1.029619417	0.978626977
6	3.3	15	0.040323	4.032258	0.97043	0.029569677	-3.521005854	1.193922468	1.258746703
7	3.8	8	0.021505	2.150538	0.991936	0.008064301	-4.820308233	1.335001067	1.572837875
8	4.3	2	0.005376	0.537634	0.997312	0.002687957	-5.918973857	1.458615023	1.778163099
9	4.8	1	0.002688	0.268817	1	-2.15054E-07			
10	5.3	0							
		372							

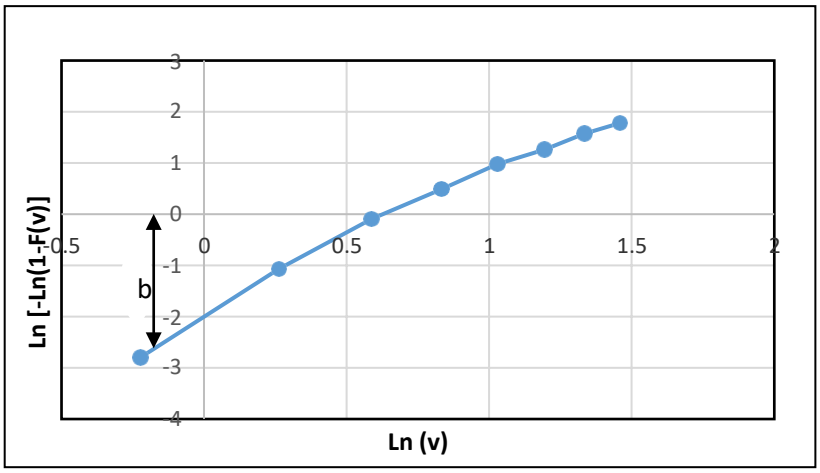

Fig. (4.1) Representation straight line.

After calculating x and y values for all velocities, we plot all the x_i and y_i values, and note that the graph is a straight line as shown in Fig. (4.1).

By using the Excel program, the slope of the straight line is calculated, which represents the value of k and the intercept, which represents the value of b, and thus the Weibull parameters is calculated. As for the slope of the straight line, it can be calculated from a function in the Excel program, which is:

Slop (known –y's , known –x's)

After entering the values of x and y we get the slope value (k), k= 2.6793

The intercept is also a function in Excel, we get

Intercept (b) = - 1.9051

Substituting these values into Eqn. (4.8), we get

c = 2.0361 m/s

Now, Weibull distribution can be drawn using a function in Excel, which is:

WEIBULL DIST (x- alpha, beta, cumulative)

Where: x=Bin , alpha = k , beta = c , cumulative = F (v)

Table (4.3) Weibull distribution with bin (velocity value)

Bin	Weibull Dist.
0	0
0.8	0.252563619
1.3	0.45863996
1.8	0.521410628
2.3	0.403743716
2.8	0.214698273
3.3	0.077213826
3.8	0.018327797
4.3	0.002791326

4.2. Theoretical available wind energy

The theoretically available energy is determined by three methods:

1- Power Duration Curve

2- Energy Distribution Curve

3- The Energy Rose

In the present work we used first method (power-duration curves) is used.

4.2.1. Power Duration Curve

This curve is determined based on the velocity duration curve, which is drawn between the velocity and time percentage values. Once the velocity axis is cubed, get a power curve, will be created so that the area under this curve is proportional to the amount of energy available annually, as follows:

$$\int_0^t P \, d\, t \tag{4.9}$$

where: P is a power , t is the time.

$$P = \frac{1}{2} \rho \times the\ area\ under\ thr\ curve \tag{4.10}$$

4.2.2. Actual Available Wind Energy

In fact, any wind machine cannot take advantage of all the energy available theoretically in the wind due to a number of factors related to the speed at which the turbine is designed, which are as follows [2]:

- Cut in speed (V_I) : It is the speed at which the available power from the machine shaft is equal to the amount of power absorbed by all parts of the system in the event of no load (meaning the power needed to overcome the frictional forces in the parts of the system).
- Rated speed (V_R): When the wind speed increases to a value (V_R), this speed will equip the machine with the power that must be obtained naturally, which remains constant at this rate according to the existing control system to regulate the work of the particular system.
- Cut off speed (V_O): When the wind speed decreases to a certain value of (V_O), this speed is known as the stopping speed, at which the machine stops rotating, and thus the power supply by the machine becomes equal to zero, for matters related to the safety of the system.

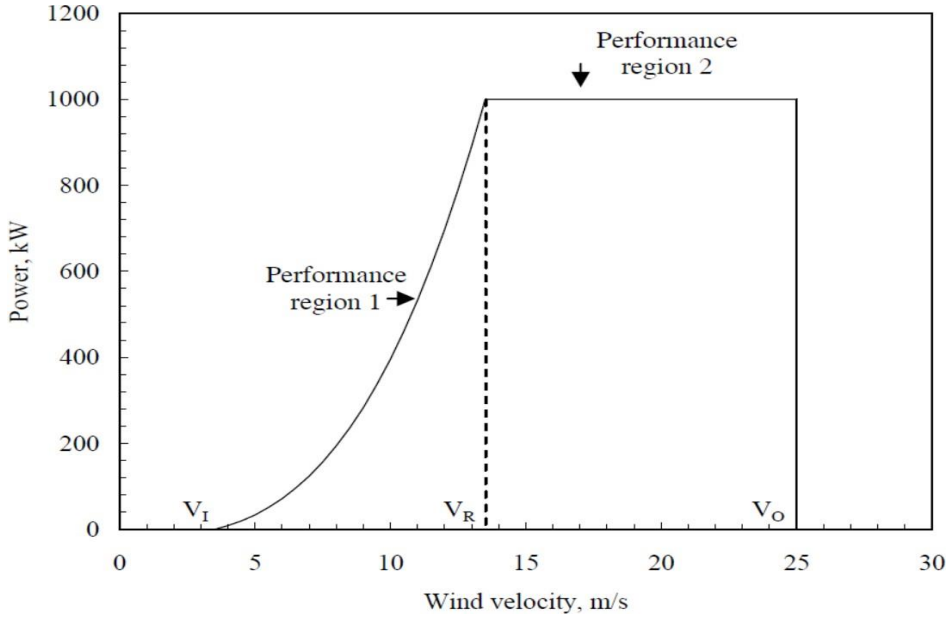

Fig. (4.4) Ideal power curve of a pitch controlled wind turbine [1]

Table (4.4). Performance regions of a wind turbine [1]

Velocity range	**Power**
0 to V_I	No power as the system is side
V_I to V_R	Power increases with V
V_R to V_O	Constant power P_R
Greater than V_O	No power as the system is shut down

Fig. (4.4) displays the standard power curve of a wind turbine with pitch function. It can be seen that the cut-in velocity (V_I), rated velocity (V_R) and the cut-out velocity (V_O) are the major characteristic velocities of the turbine. The cut-in velocity of a turbine is the minimum wind velocity at which power starts to be produced by the machine. Therefore, as shown in the table (4. 4), the turbine has four distinct output regions. Effectively, the power produced by the device is extracted from output region corresponding to VI to VR and VR to VO. Let us label these as regions 1 and 2, respectively in fig. (4.4).

4.3. The Calm Speed

It is the wind speed whose values are between (0-1), and it is unable to drive wind turbines, so the output power is considered zero. These speeds are usually represented with percentage Formula, as follows.

$$\emptyset = \frac{Number\ of\ calm\ speed}{total\ \ speed} \times 100\% \qquad (4.11)$$

where: $\emptyset$ is percentage to Calm speed.

In the current work, the wind data for Babylon city are analyzed for the previous four years (1988, 1998, 2008, 2018), respectively, using diagrams velocity duration curve and power duration curve, and depending on Weibull

distribution in Fig. (4.2) and the frequency diagram in Fig. (4.3), it is found that the highest frequency of wind speed at 1.8 m/s with a frequency of 30%, and a speed of 1.3 m/s with a frequency of 23%.

It is fount that which is 1.8 m/s, will be considered as the velocity of (V_R), cut in speed (V_I) is 0.75 m/s and cut off speed (V_O) is 2.5 m/s. From velocity duration curve diagrams power duration curve are drawn, where the areas under the curve represent the power, and using equation (4.10), we find the resulting power from the use of wind energy for the previous years. Also the percentage of calm speeds for those years is also calculated.

CHAPTER FIVE
RESULTS AND DISCUSSION

Results and Discussion

In this chapter, the experimental results and analysis of wind speed data for the city of Babylon for the previous thirty years are presented and discussed.

5.1. Experimental Results

5.1.1 Effect of Drag Force

As mentioned previously, drag force generated in vertical axis wind turbine is one of main disadvantages that may reduce turbine performance. Thus, one case of VAWT with six bucket of constant diameter is achieved to showdrag force effect.

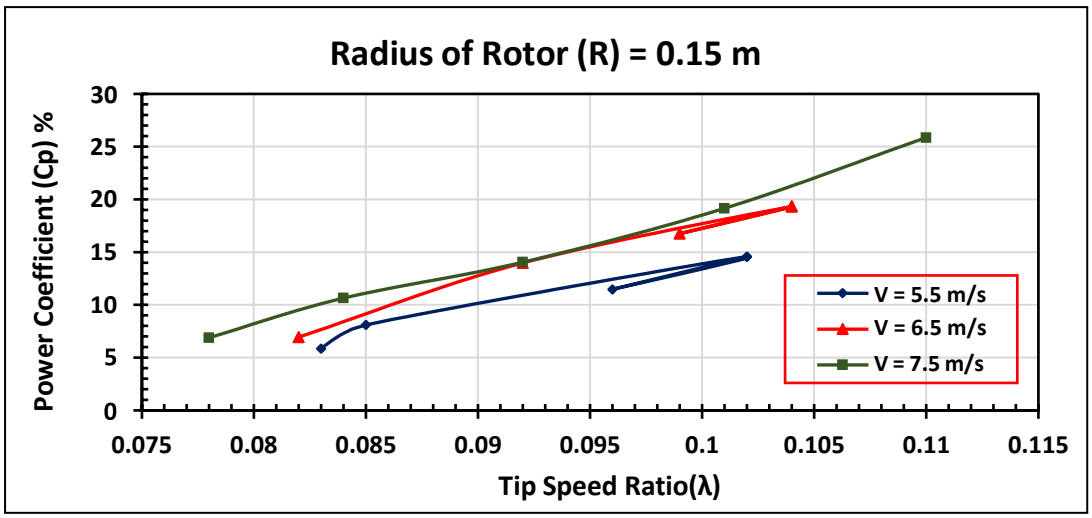

Fig. (5.1) Power coefficient of the wind turbine for radius is 0.15 m, and different wind speeds, at number of blades = six.

Fig. (5.1) and (5.2) show the results of a test inside the wind tunnel of the model shown in Fig. (3.9), and it was found that the results are incorrect due to the factors affecting the model blades (boundary layer) that create on the walls of the wind tunnel.

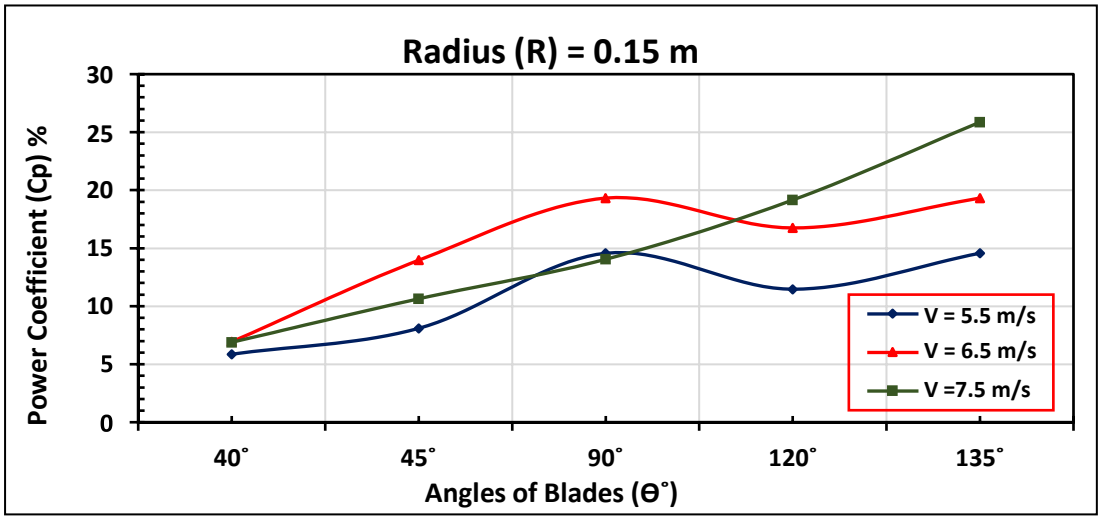

Fig. (5.2) Power coefficient versus the angle of blades for a radius of the rotor (R) is 0.15 m, and different wind speed (V), number of blades =6.

These results showed the opposite effect of drag force on the power coefficient. Based on that, the other case studies are achieved out of the wind tunnel to magnify the effect of other parameters (diameter, bucket number, angles and turbine configuration).

5.1.2. Effect of Tip Speed Ratio on the Turbine Performance

Three cases of vertical axis wind turbine are tested.

5.1.2.1. First case (VAWTb-6).

The power coefficients and tip speed ratios of turbine are determined at three wind speeds. Fig. (5.3) shows the variations of the power coefficients due to variations of the tip speed ratio for different values of radius and wind speeds. Fig. (5.3-a) shows power coefficients when the radius (R) = 30 cm. The main characteristics of the subfigures is the nonlinear behavior of the power coefficients due to changes in TSR. In other words, a critical value for a specific wind speed is noticed. This behavior is noticed for all values of radius and wind velocities. On the other hand, it is noted that a turbine that operates at the lower values of the tip speed ratio (corresponding to higher wind speed) shows smaller values of the power coefficients.

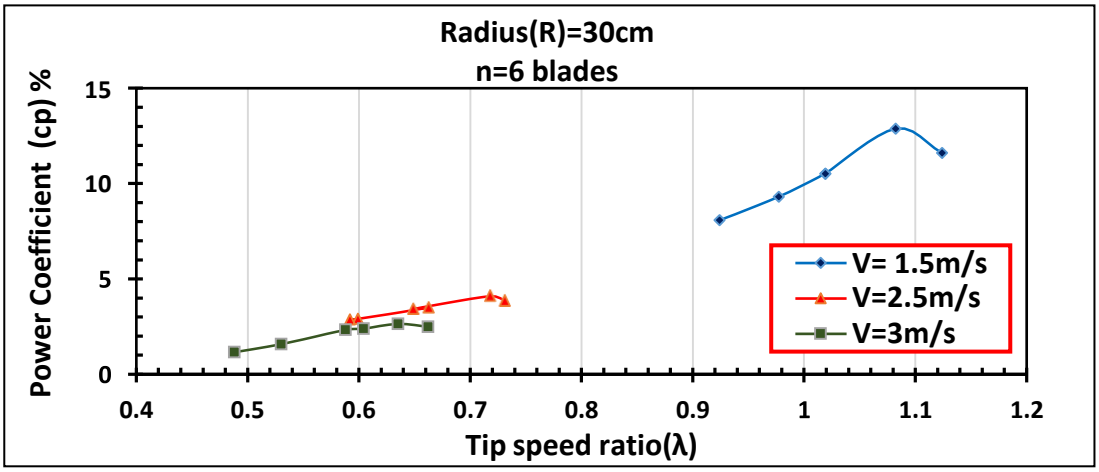

(a)

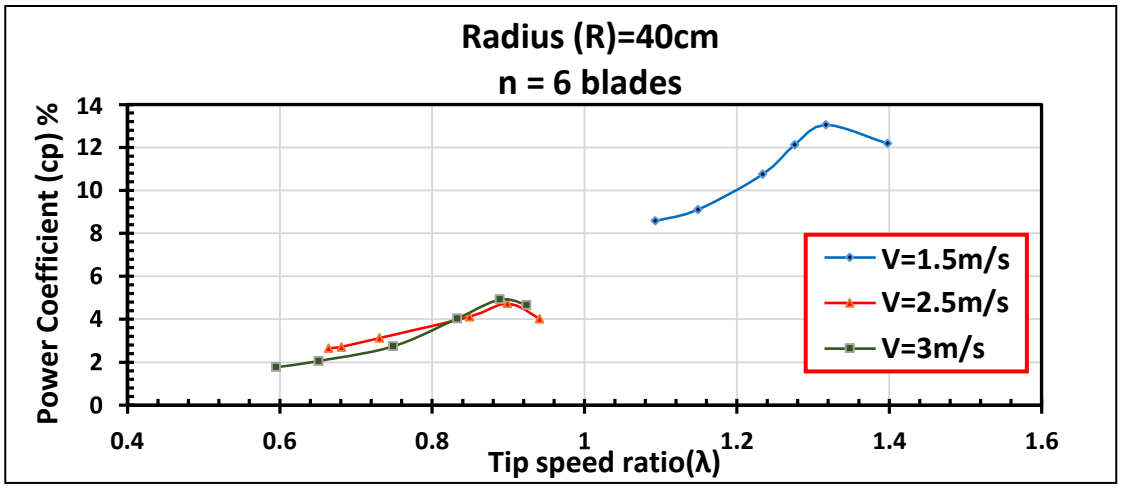

(b)

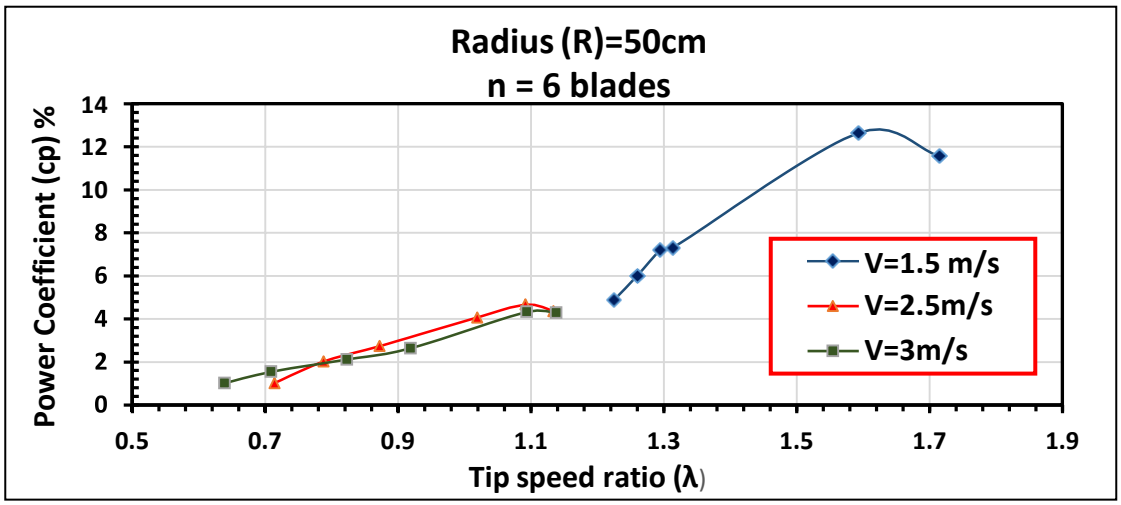

(c)

Fig. (5.3) Power coefficient of the wind turbine for different radius and wind speeds, at number of blades are six.

That means the turbine operate under what called by stall mode condition during turbine blades rotation, leading in reducing the power generated by the turbine. In addition, at higher tip speed ratio, the turbine spins faster. However, the fast spinning modifies the aerodynamic behavior of the stream around the blades and enhances incoming flow blockage. This blockage might enforce the streamlines for bypassing the rotors. Similar behavior can be noticed for the other values of the blades location (the radius increases). The main behavior of plots in Fig. (5.3) is attributed to the inverse relationship between the wind speed and power coefficients as noticed by Eqn.s (3.4) and (3.9), respectively. It is worthy to mention that the highest value of power coefficient is (Cp=13.05 at TSR=1.3) for wind speed V= 1.5 m/s and the rotor radius R=40 cm.

For more convenient, the relationship between power coefficient and the tip speed ratio, when the wind speed is fixed while the blade locations or blade radius is variable, is presented in Fig. (5.4) the critical value of the tip speed ratio is higher when the turbine blades are the farthest in the design (R=50 cm). Similar behavior for the subfigures of the turbine in this figure is noticed. However, the maximum value of the power coefficients is noticed in Fig. (5.4-a) at the smaller wind speed (V= 1.5 m/s) and blade radius (R= 40 cm).

To sum up with, when the value of the rotor radius is constant with the change in wind speed, or the rotor radius changes with the wind speed remaining constant, and according to equation (3.8), the TSR depends on the rotor radius and wind speed, as it is directly proportional to the rotor radius and inversely with wind speed. When the radius of the rotor is increased for same wind speed, TSR increases, and when the wind speed increases with the radius of the rotor held constant, the TSR decreases.

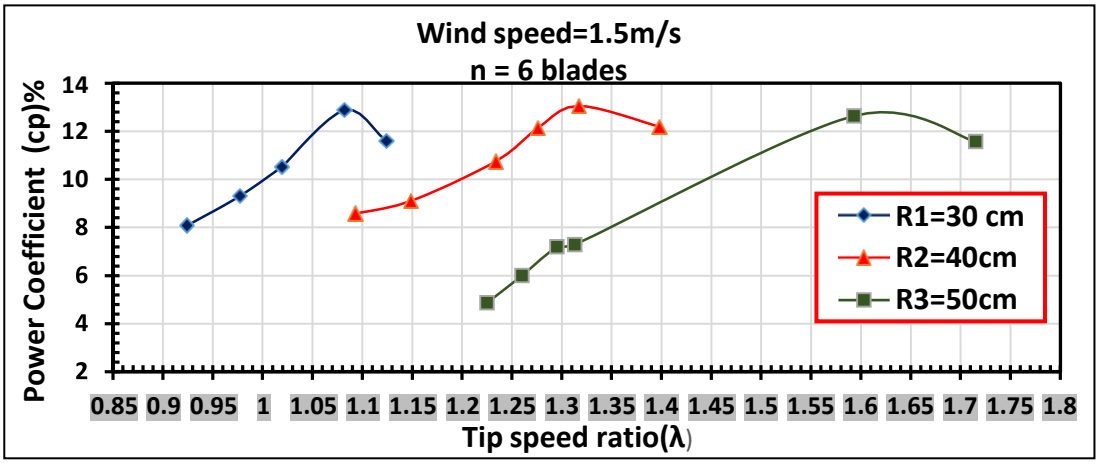

(a)

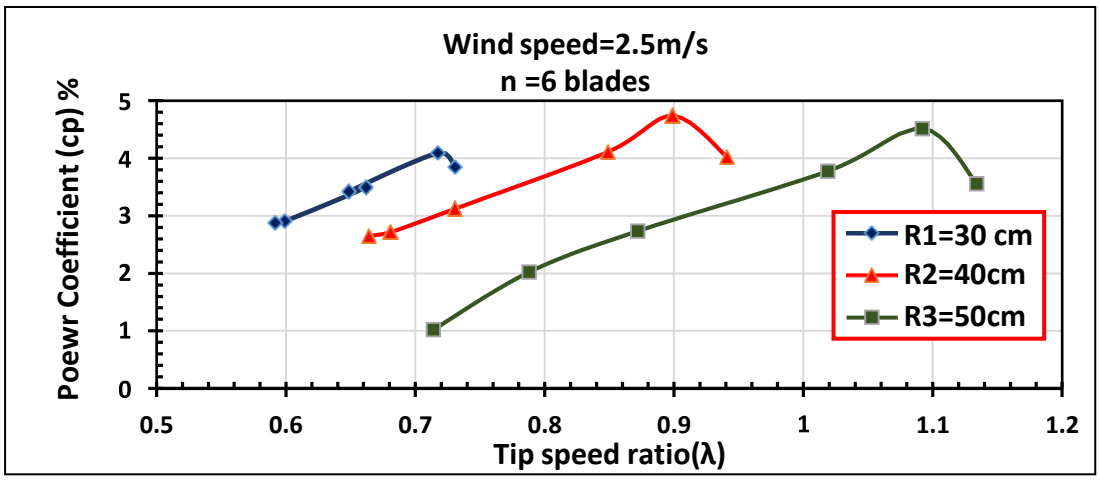

(b)

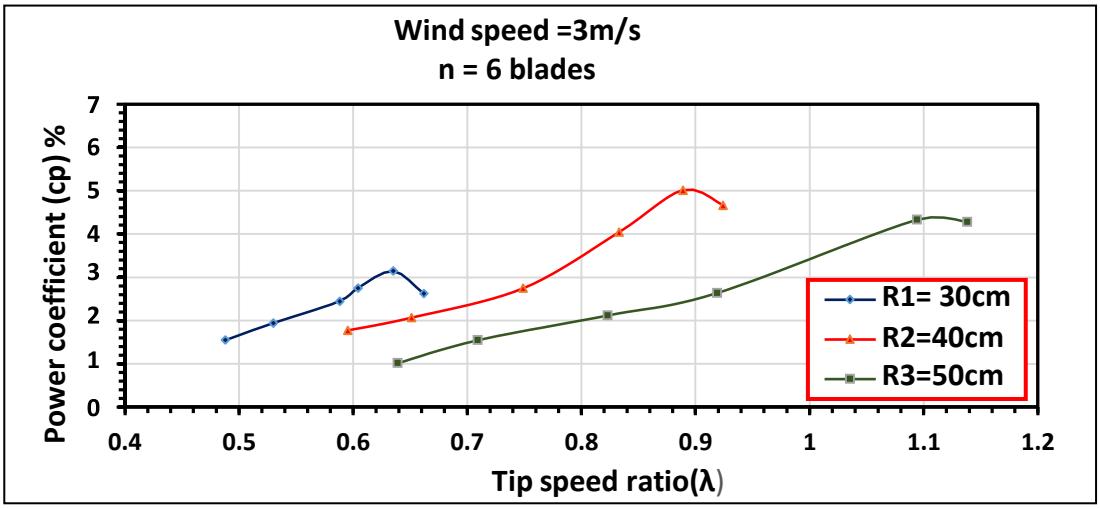

(c)

Fig. (5.4) Power Coefficient versus (TSR) for different radius of the rotor (R) when three wind speed (V), at number of blades = six.

5.1.2.2. Second case (VAWTb-3).

The power coefficients and tip speed ratios are presented by Fig. (5.5) and Fig. (5.6), respectively. Fig. (5.5) shows the variations of the power coefficients due to variations of the tip speed ratio for different values of radius and wind speed. It is worthy to mention that the highest value of power coefficient is (Cp=9.567 at TSR=1.148) for wind speed V= 1.5 m/s and the rotor radius R=40 cm as shown in Fig. (5.5-b). Power coefficient of Fig. (5.3) and Fig. (5.5) for 6 blades and 3 blades show similar trend of increasing with tip speed ratio. However, their value are not comparable due to very wind speed when n = 3 as compared with the case when n = 6.

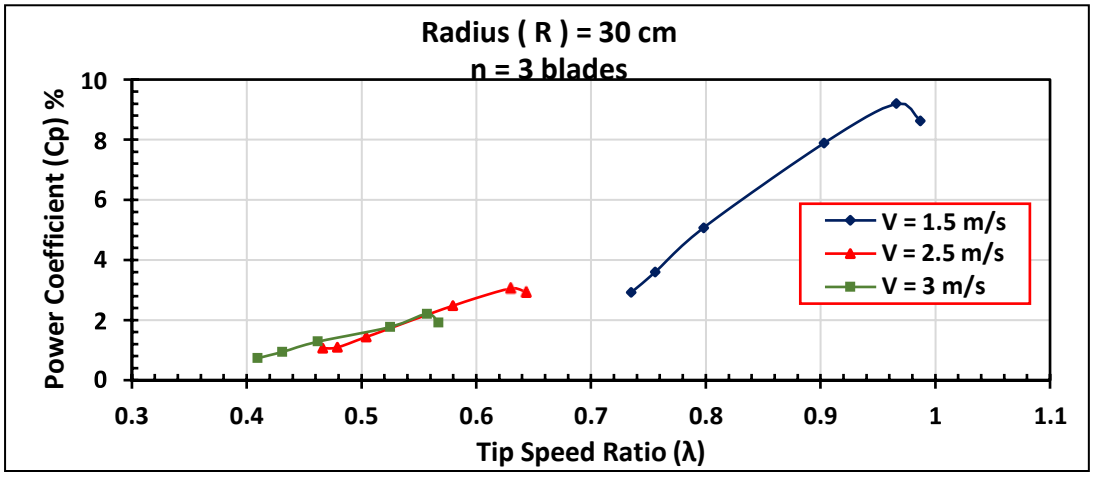

(a)

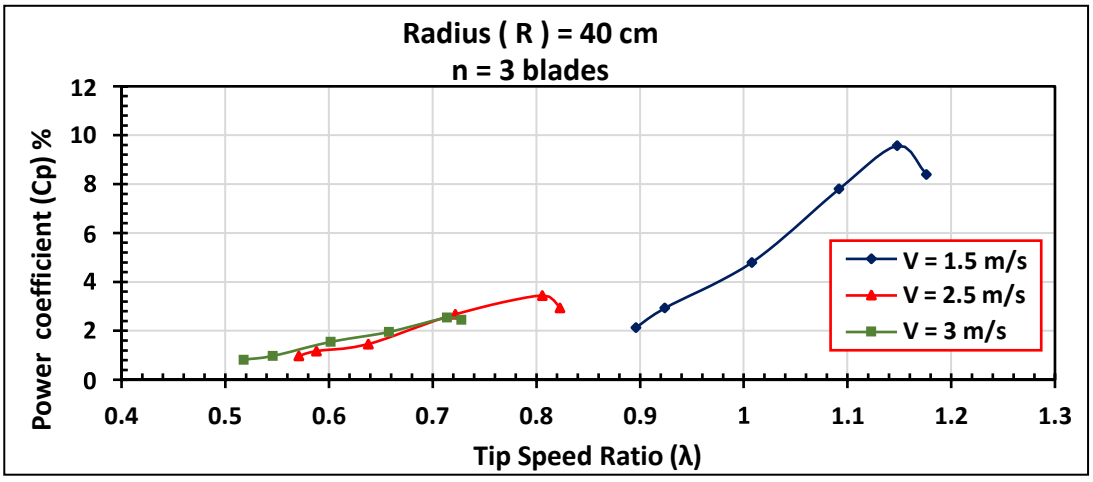

(b)

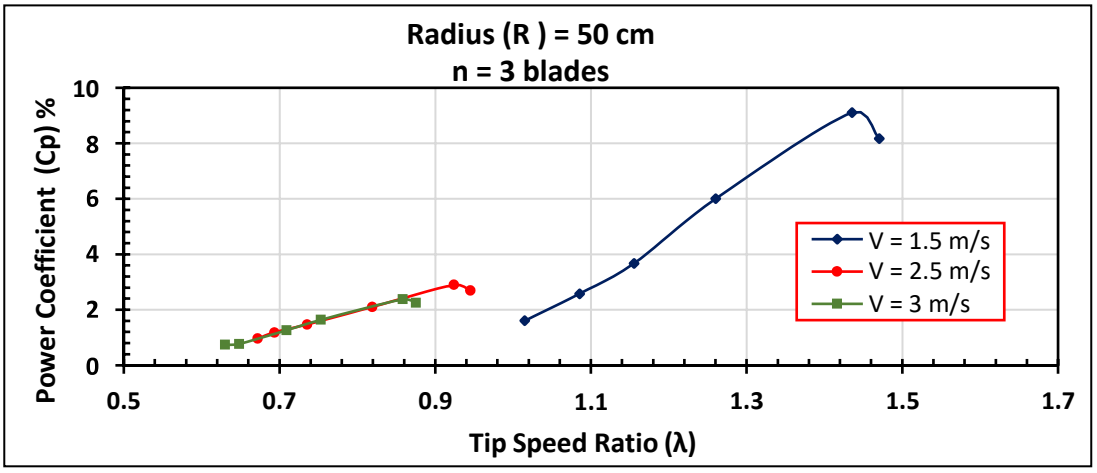

(c)

Fig. (5.5) Power coefficient of the wind turbine versus (TSR) for different radius of the rotor (R) when three wind speed (V), (n =3).

Fig. (5.6) shows effect of blade radius on Cp for three constant , wind speed of 1.5 m/s, 2.5 m/s, and 3 m/s, respectively, and with different diameters for the rotor. The highest value of the power coefficient (Cp =9.567%) is noticed at (R= 40 cm) as shown in Fig. (5.6-a).

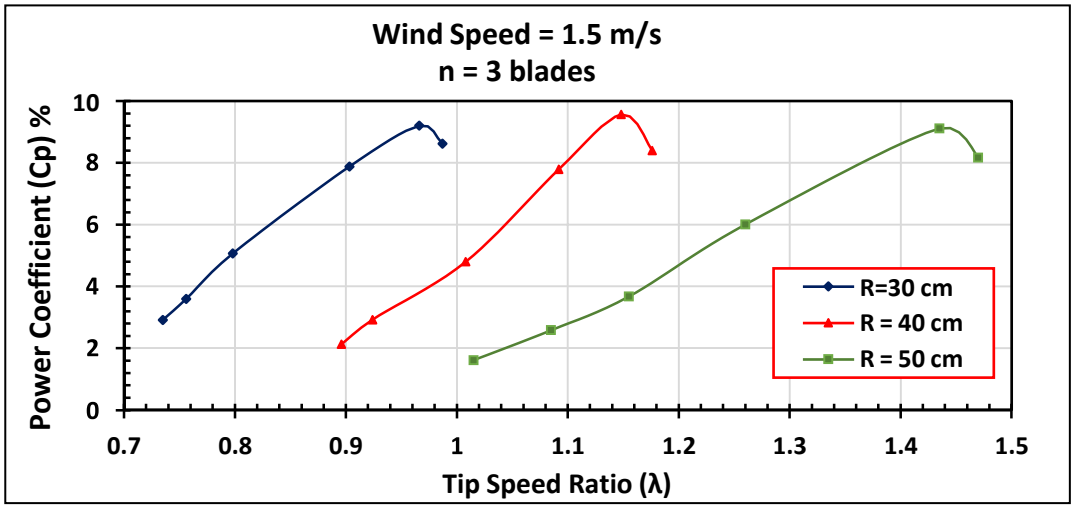

(a)

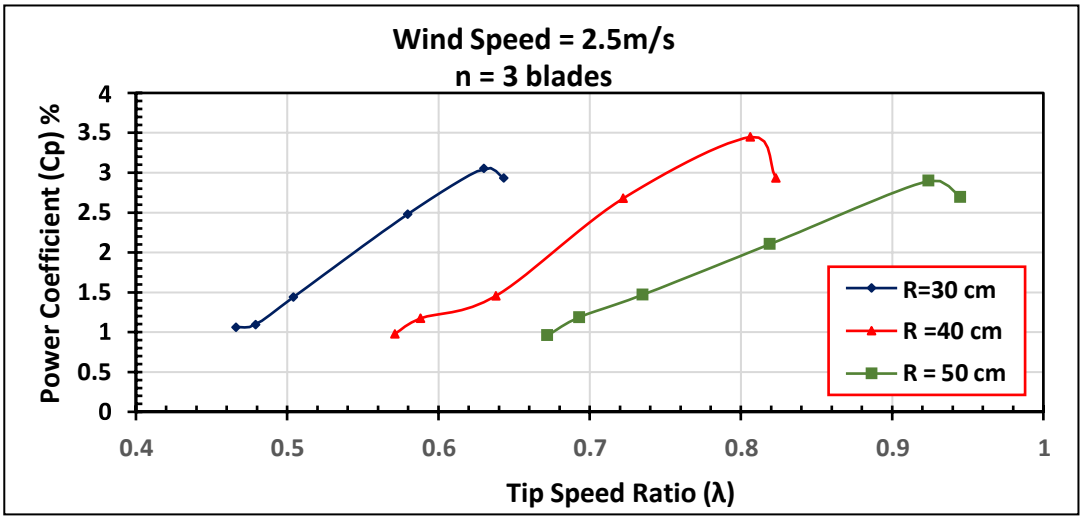

(b)

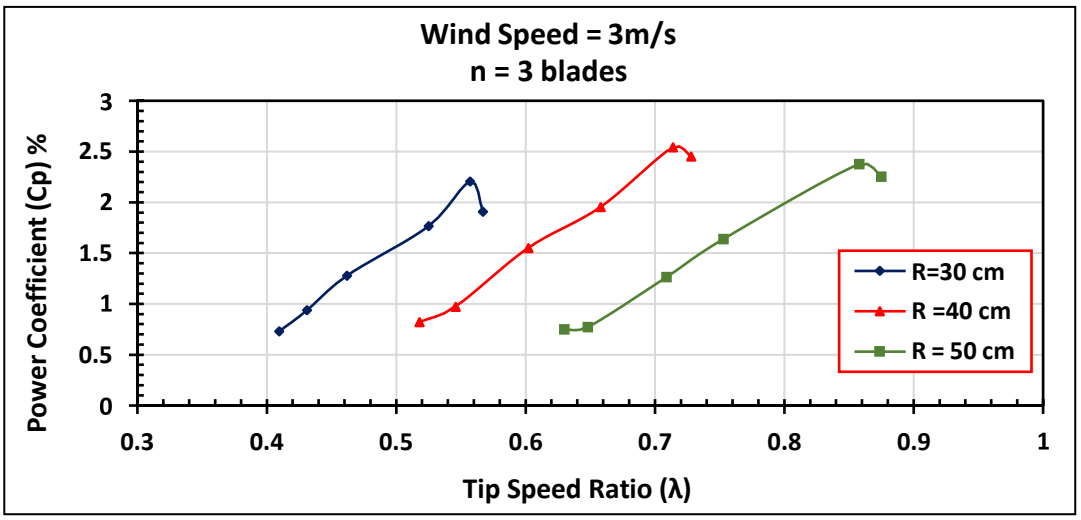

(c)

Fig. (5.6) Power coefficient versus (TSR) for different radius of the rotor (R) when three wind speed (V), at number of blades = 3.

5.1.2.3. Case three (MBHYWT)

The power coefficients and tip speed ratio turbine are determined for three wind speeds and presented in Fig. (5.7) to Fig. (5.12). Fig. (5.7) shows power coefficient versus (TSR) for a different rotating radius (R=40cm, 50cm and55cm) for three blades at different angles (ϴ = 45˚, 60˚, 90˚, 120˚and 135˚), and a fixed rotating radius (r =30 cm) for the other three

blades of the hybrid multi-blade wind turbine, when the wind speed (V) = 1.5 m / s.

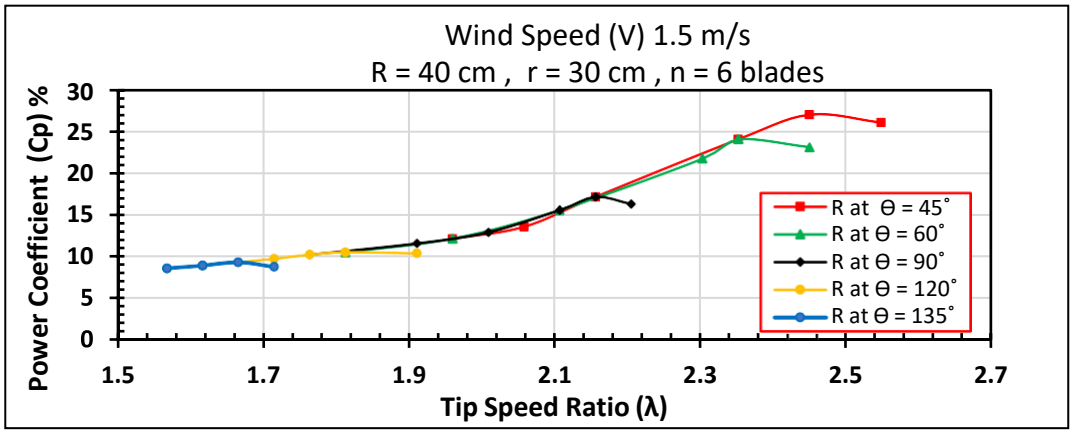

(a)

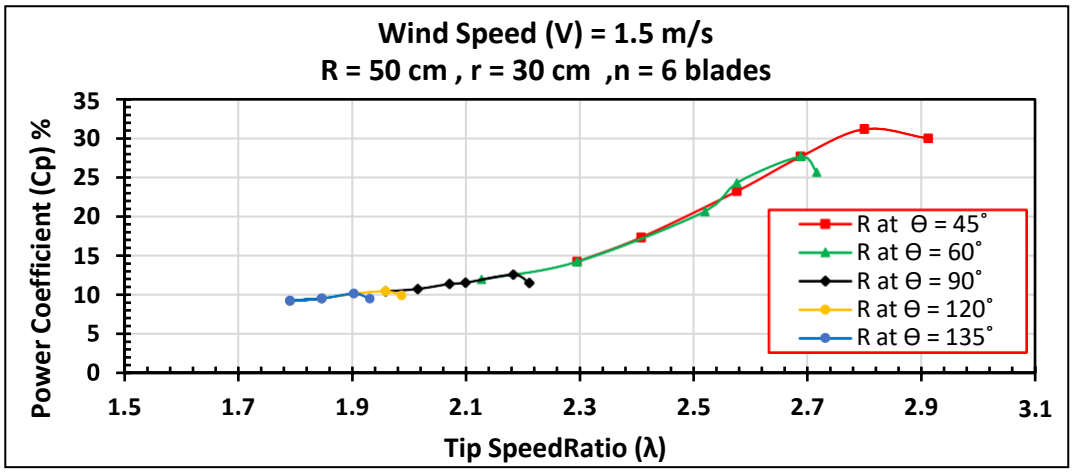

(b)

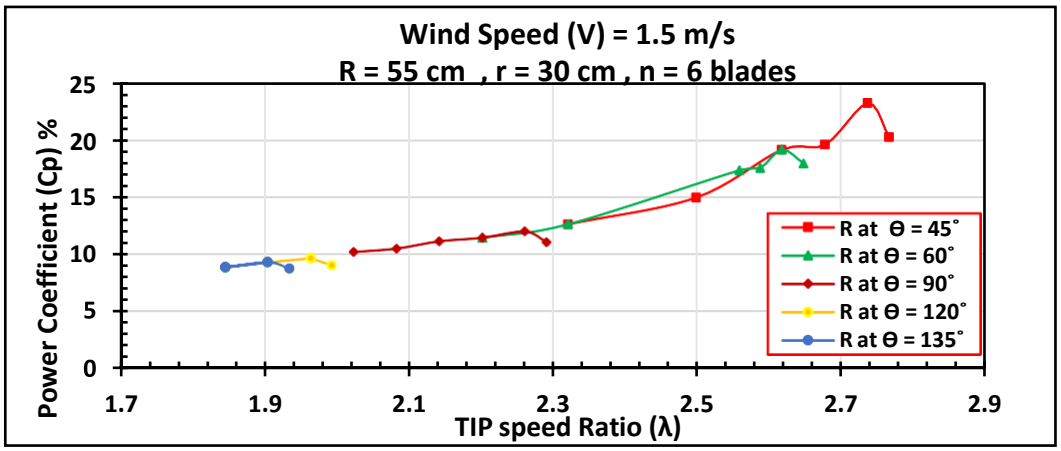

(c)

Fig. (5.7) Power coefficient versus (TSR) for different rotor radius (R) of a multi-blade hybrid wind turbine, when wind speeds (V) =1.5m/s, number of blades = 6.

The maximum value of the power coefficient (Cp) is noticed at angle (Θ = 45˚) as in Fig.s (5.7-a), (5.7-b) and (5.7-c). Fig. (5.8) shows a comparison of the highest value of (Cp) at (V = 1.5 m/s), (R = 40 cm, 50 cm and 55 cm) at Θ= 45˚, so the maximum value of (Cp=31.11%) at R = 50 cm.

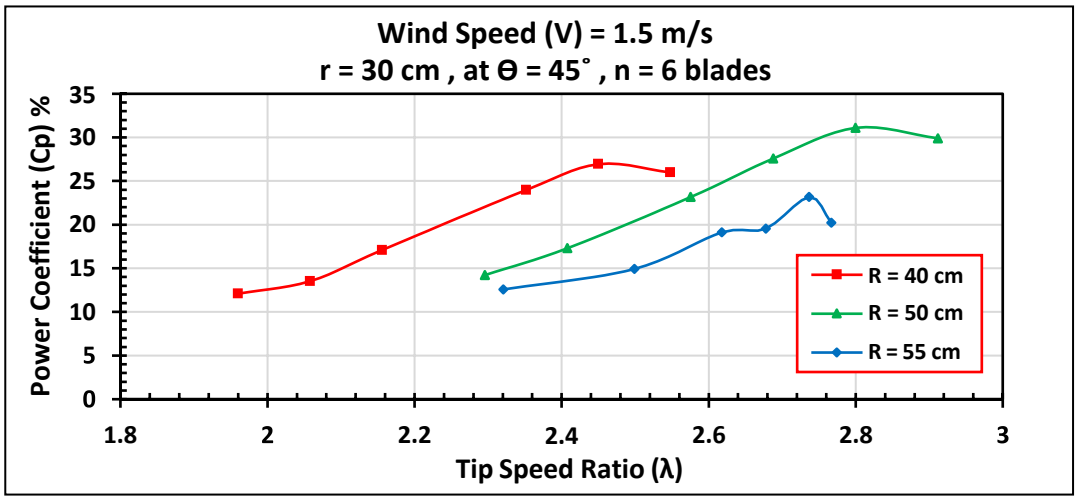

Fig. (5.8) Comparing power coefficient versus (TSR) for different radius of the rotor (R) of (MBHYWT), when wind speed (V) = 1.5 m/s, number of blades = 6.

Fig. (5.9) shows power coefficient versus (TSR) for a different rotating radius (R=40cm, 50cm and55cm) for three blades at different angles (Θ = 45˚, 60˚, 90˚, 120˚and 135˚), and a fixed rotating radius (r =30 cm) for the other three blades of the hybrid multi-blade wind turbine, when the wind speed (V) = 2.5 m / s. The maximum value of the power coefficient (Cp) is noticed at angle (Θ = 45˚) as in Fig.s (5.9-a), (5.9-b) and (5.9-c). Fig. (5.10) shows a comparison of the highest value of (Cp) at (V = 2.5 m/s), (R = 40 cm, 50 cm and 55 cm) at Θ= 45˚, so the maximum value of (Cp=6.839%) at R = 50 cm.

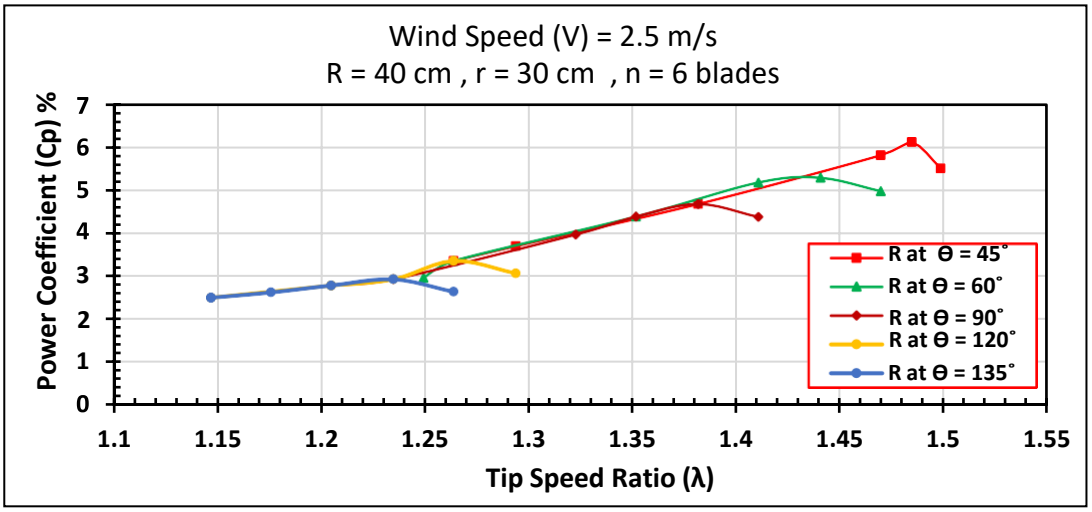

(a)

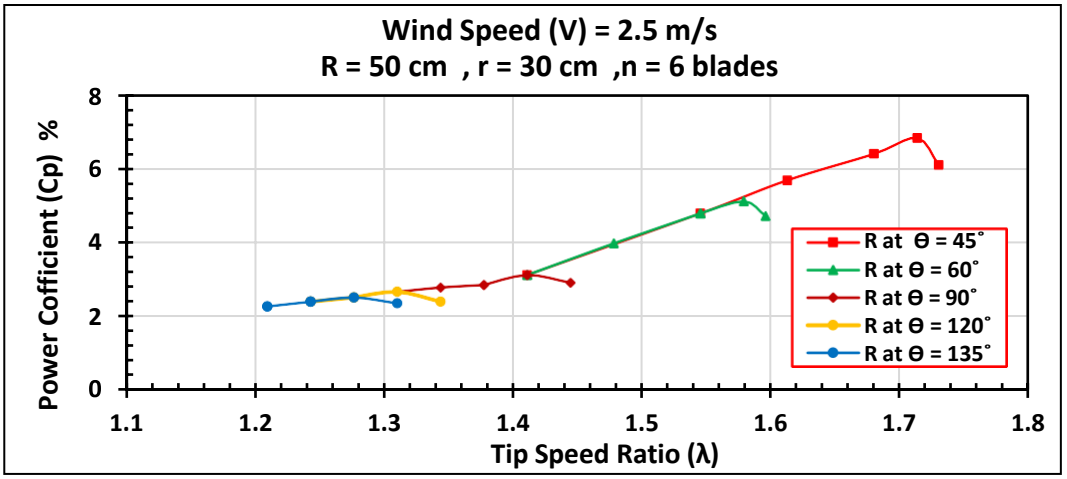

(b)

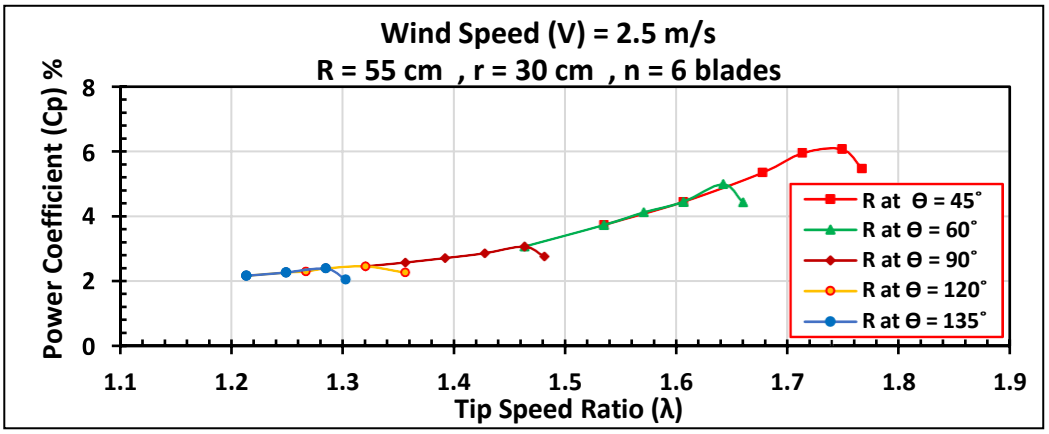

(c)

Fig. (5.9) Power coefficient versus (TSR) for different rotor radius (R) of (MBHYWT), when wind speeds (V) =2.5m/s, number of blades = 6.

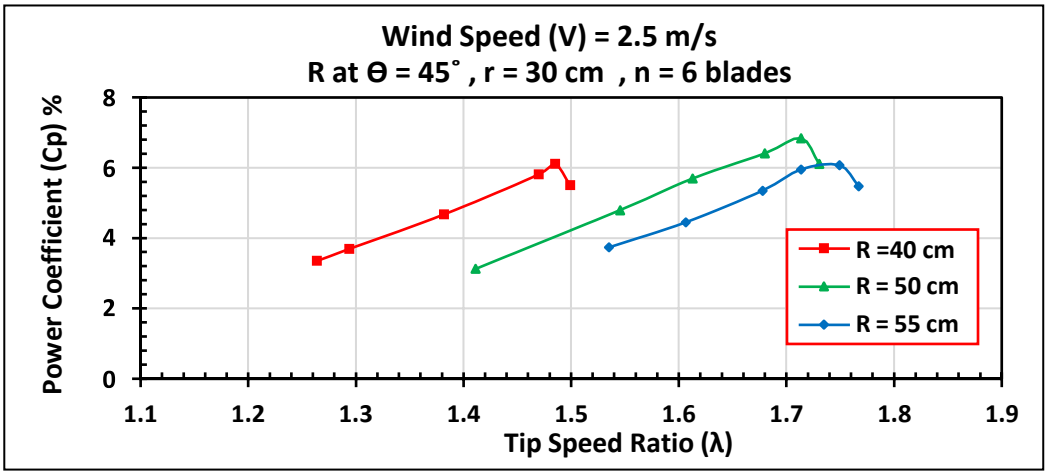

Fig. (5.10) Comparing power coefficient versus (TSR) for different radius of the rotor (R) of (MBHYWT), when wind speed (V) = 2.5 m/s, number of blades = 6.

Fig.(5.11) shows power coefficient versus (TSR) for a different rotating radius (R=40cm, 50cm and55cm) for three blades at different angles (Θ = 45˚, 60˚, 90˚, 120˚and 135˚), and a fixed rotating radius (r =30 cm) for the other three blades of the hybrid multi-blade wind turbine, when the wind speed (V) = 3m / s. The maximum value of the power coefficient (Cp) is noticed at angle (Θ = 45˚) as in Fig.s (5.11-a), (5.11-b) and (5.11-c). Fig. (5.12) shows a comparison of the highest value of (Cp) at (V = 3 m/s), (R = 40 cm, 50 cm and 55 cm) at Θ= 45˚, so the maximum value of (Cp=6.606%) at R = 50 cm.

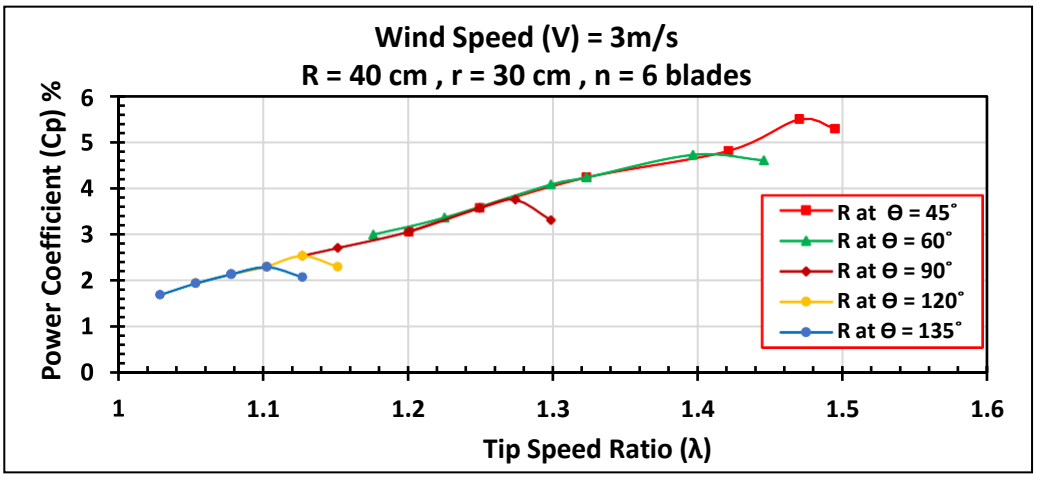

(a)

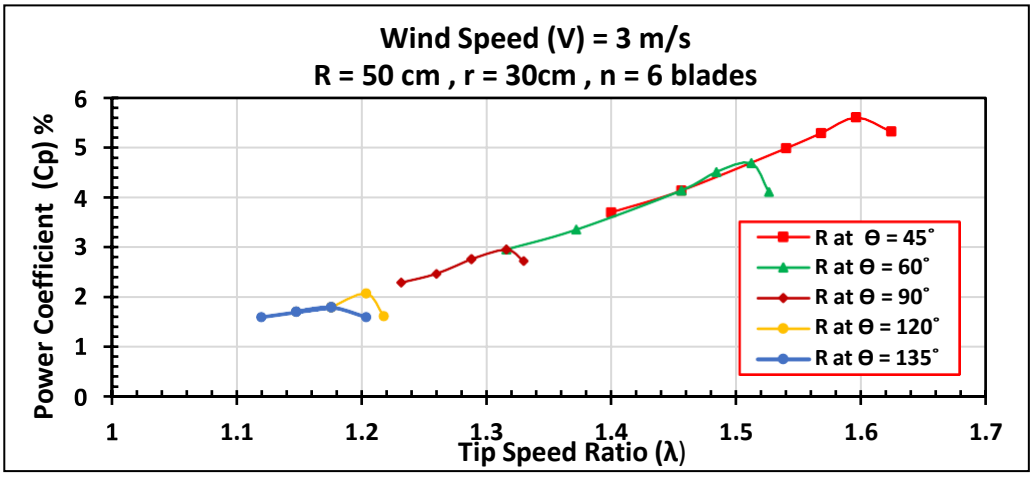

(b)

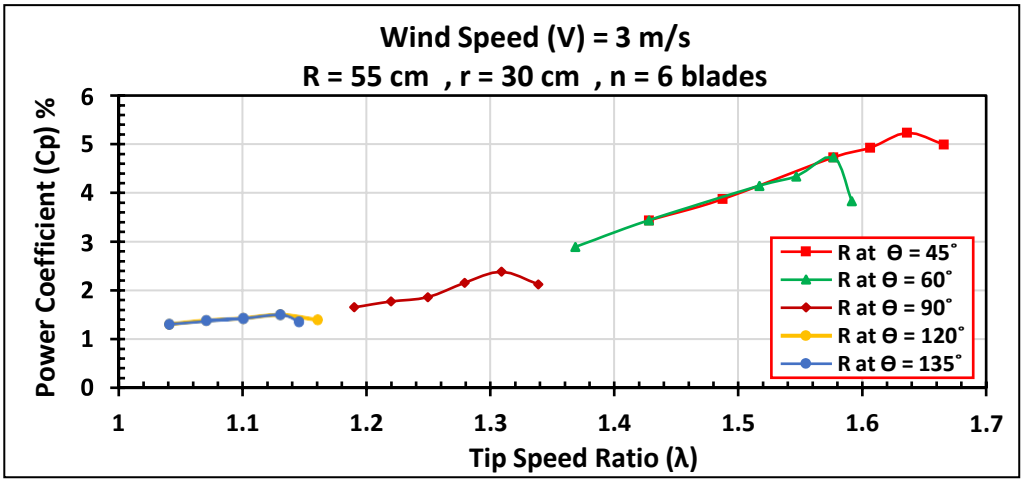

(c)

Fig. (5.11) Power coefficient versus (TSR) for different rotor radius (R) of (MBHYWT), at wind speeds (V) =3m/s, number of blades = 6.

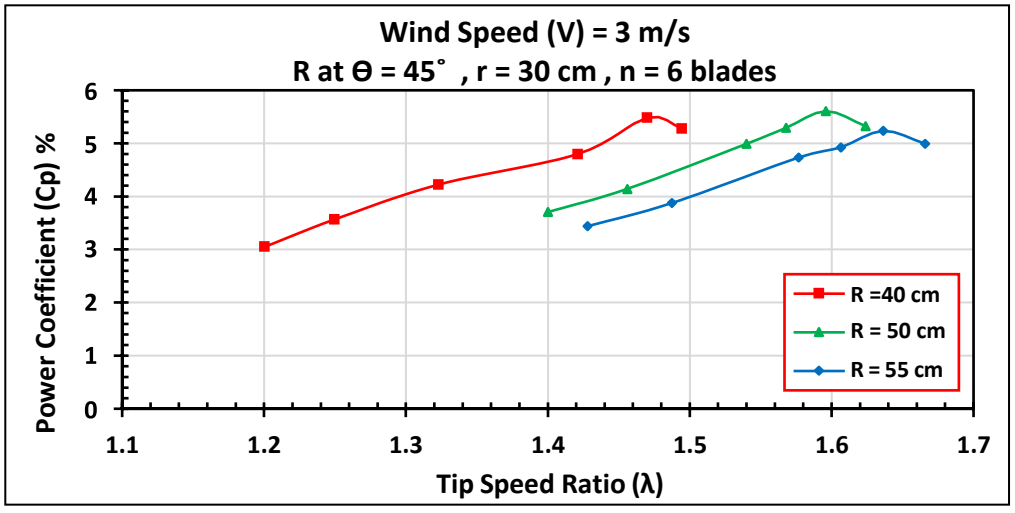

Fig. (5.12) Comparing of power coefficient versus (TSR) for different radius of the rotor (R) of (MBHYWT), when wind speed (V) = 3 m/s, number of blades = 6.

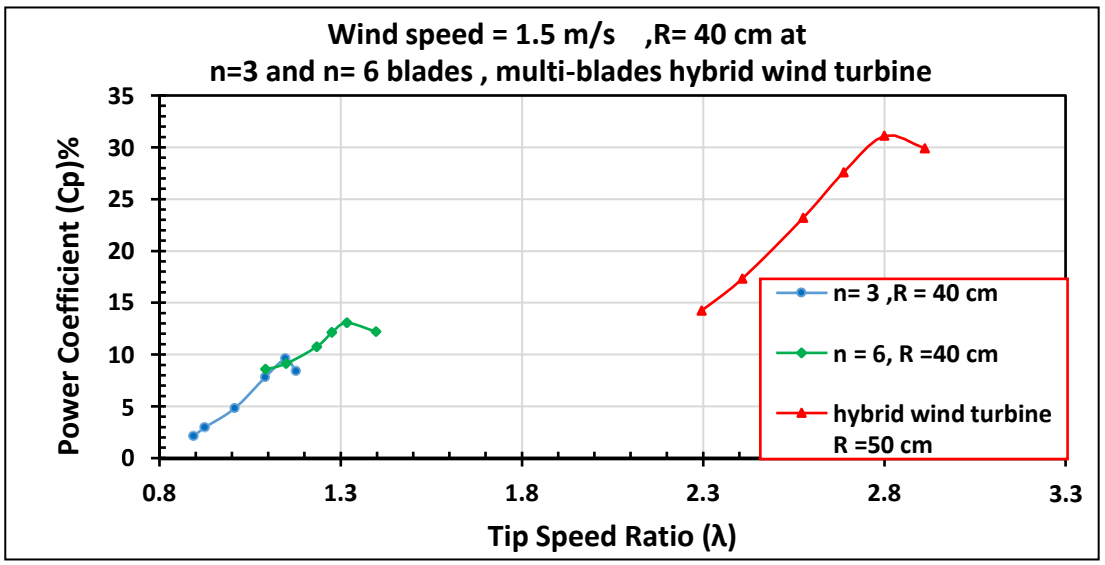

Fig. (5.13) Comparing of power coefficient versus (TSR) for radius of the rotor (R), when wind speed (V) = 1.5 m/s, number of blades = 3 and 6, (MBHYWT).

Fig. (5.13) shows the maximum power coefficient returns to multi-blade hybrid wind turbine (MBHYWT) compared to the three-blade and six-blade turbines. Addition of another group of blades (three extra blades) have increased the active force resulted in the generated torque and reduce effect of air stream blockage.

5.1.3. Effect of Blade Angle on the Wind Performance.

Power coefficient are calculated for the different values of blade angle, blade position, and wind speed for three cases of the vertical axis wind turbine.

5.1.3.1. First case, (VAWTb-6).

The power coefficients and angles of blades to turbine are calculated for three wind speeds and presented in Fig. (5.14), in order to investigate effect of all of these parameters on the turbine performance. Several values of blade locations (R=30, 40 and 50) cm and wind speeds (V=1.5, 2.5, 3) m/s are used. It is noticed that the critical values (maximum value) of the power

coefficients for all subfigures of Fig. (5.14) are located at 45º blades angles. However, their values vary with both of blade location and wind speed. Effect of blade angles is significant when the blade located at the critical distance from the rotational center with smaller values of the wind speed as shown in Fig. (5.14c).This explains how power coefficients is sensitive to wind speed and blade locations. The maximum value of (Cp=13.055%) at speed (1.5 m/s), radius (40 cm), and angle (45˚) as shown Fig. (5.15).

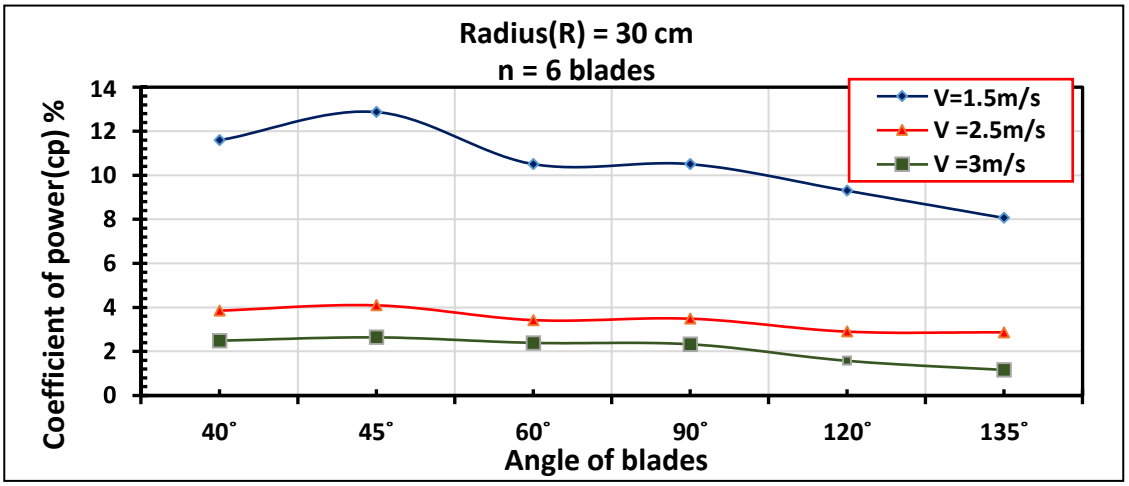

(a)

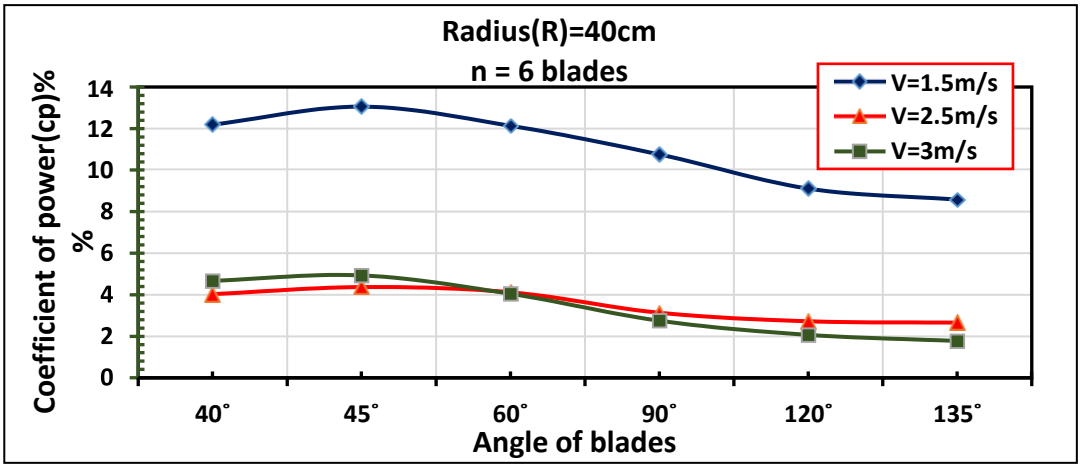

(b)

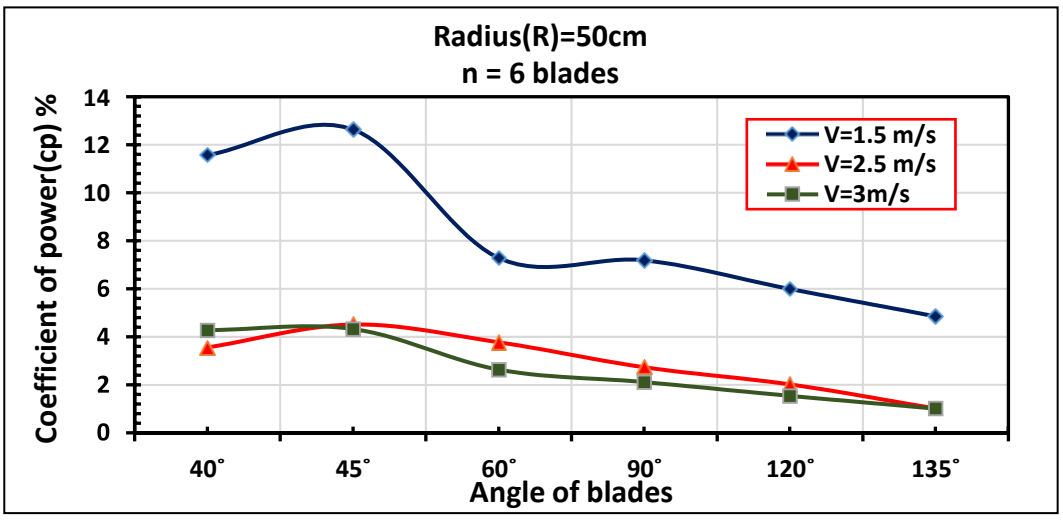

(c)

Fig. (5.14) Power coefficient versus the angle of blades for a different rotor radius (R) and wind speed (V), number of blades =6.

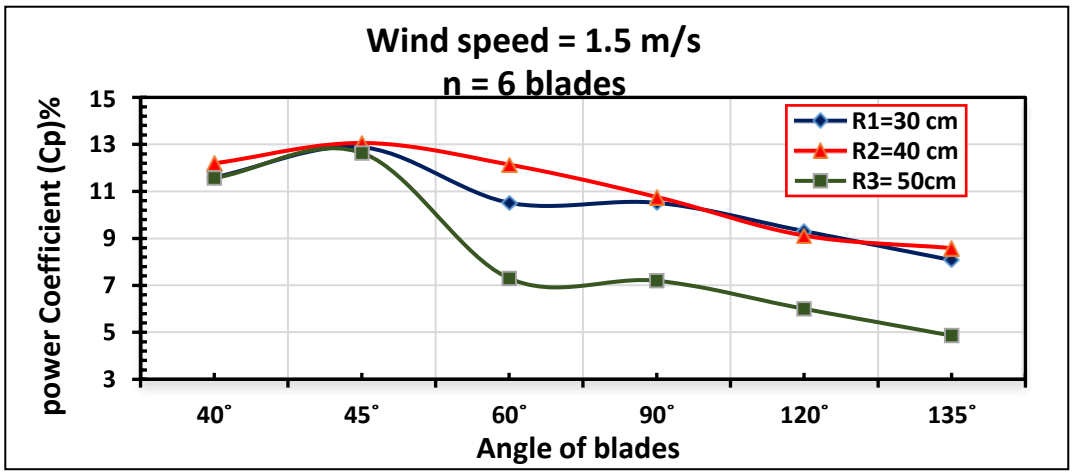

Fig. (5.15) Comparing of power coefficient versus angle of blades for different rotor radius (R) when wind speed (V) = 1.5 m/s, number of blades = 6.

5.1.3.2. Second Case, (VAWTb-3)

The power coefficients and angle of blades are calculated for three wind speeds and different radius of the rotor (R) as shown in Fig. (5.16) and Fig. (5.17) respectively. The maximum value of (Cp=9.567%) at speed (1.5 m/s) and radius (40 cm) and angle (45˚) as shown in Fig. (5.16-b).

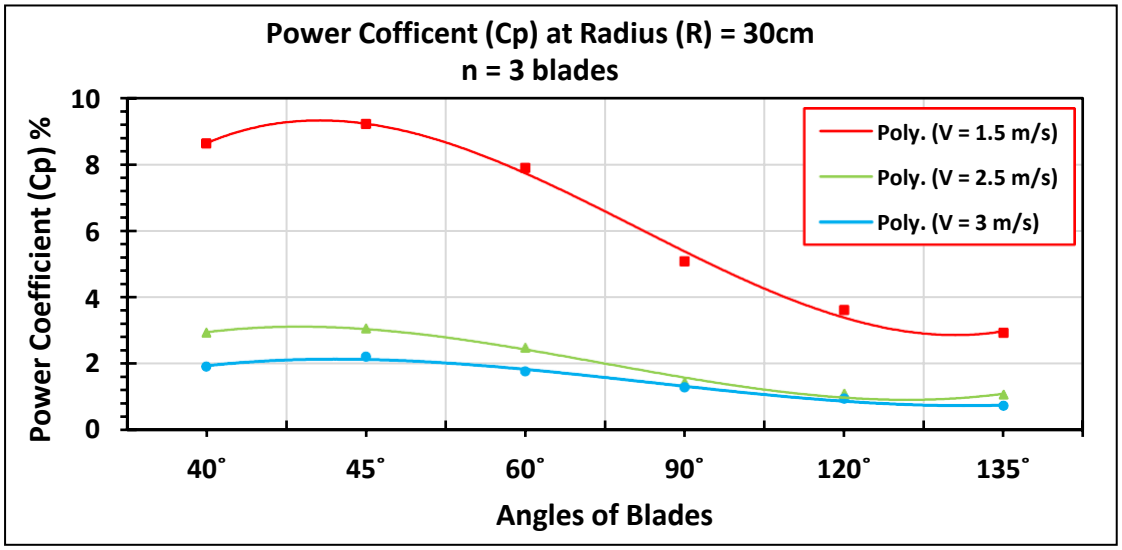

(a)

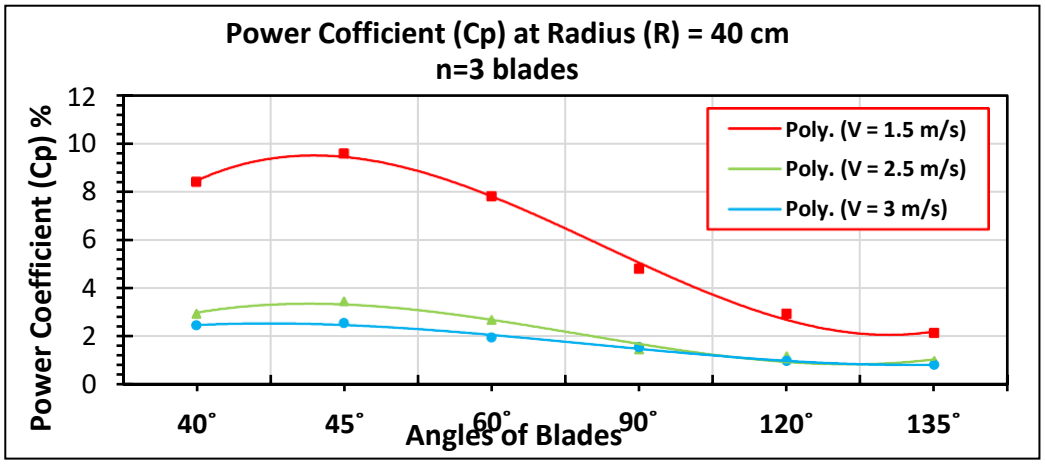

(b)

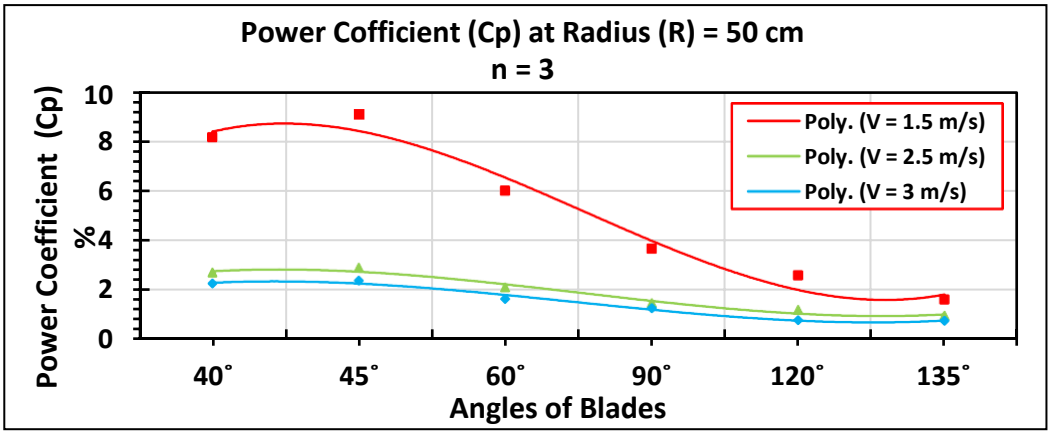

(c)

Fig. (5.16) Power coefficient versus the angle of blades for a different radius of the rotor (R) and wind speed (V), number of blades = 3.

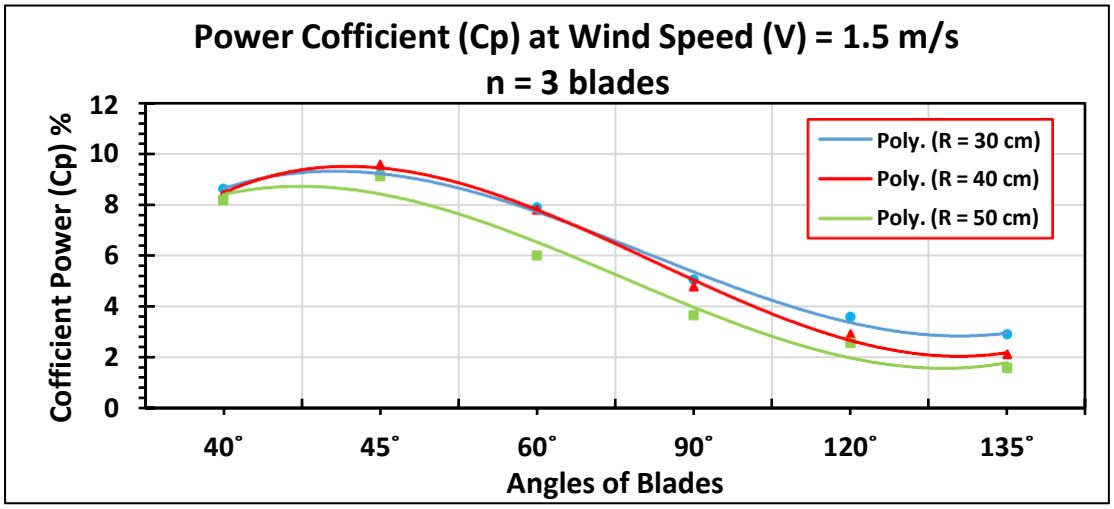

Fig. (5.17) Comparing of power coefficient versus angle of blades for different radius of the rotor (R) when wind speed (V) = 1.5 m/s, number of blades = 3.

5.1.3.3. Case three (MBHYWT).

The power coefficients and angle of blades were calculated at three wind speeds and different radius of the rotor (R) as shown in Fig. (5.18) to Fig. (5.24).

In this case, the maximum value of (Cp=31.111%) at speed (1.5 m/s) and radius (50 cm) and angle (45) as Fig.s (5.18-b) and (5.19).

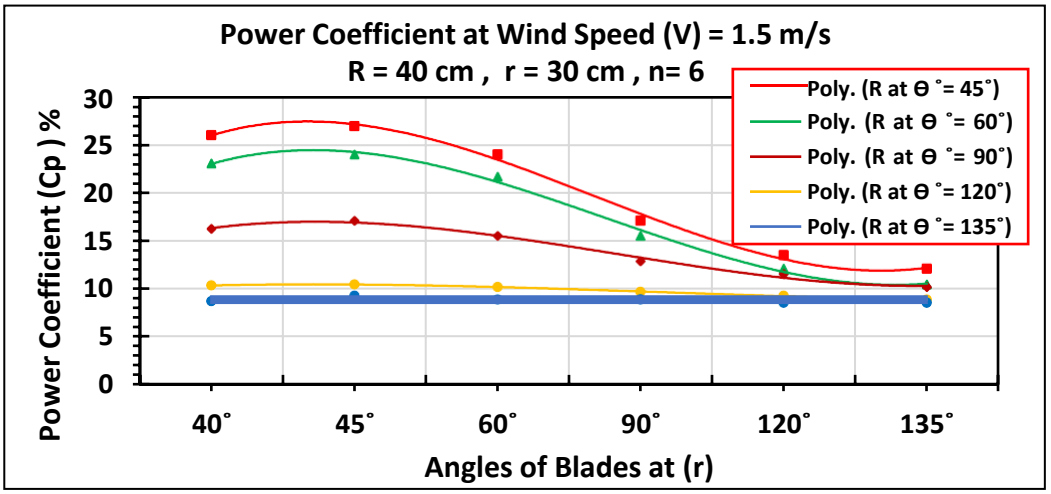

(a)

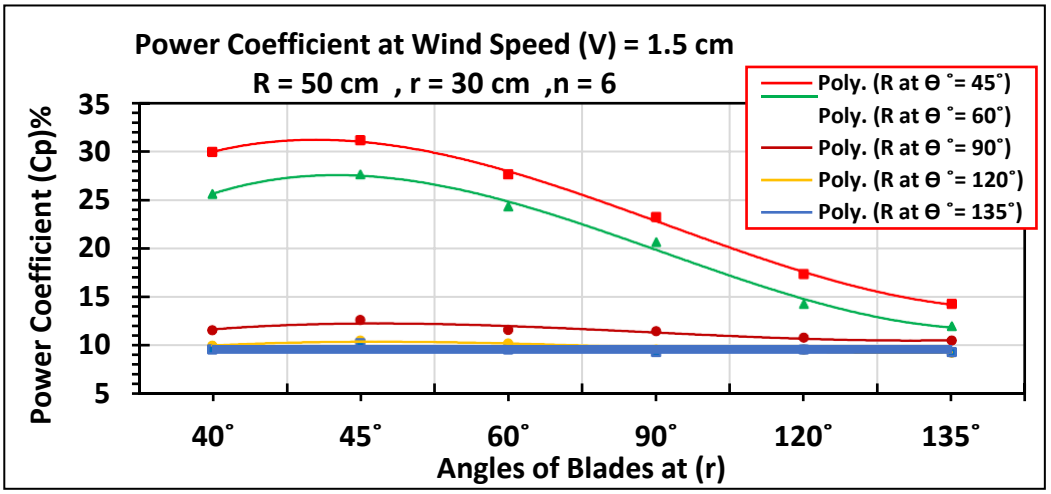

(b)

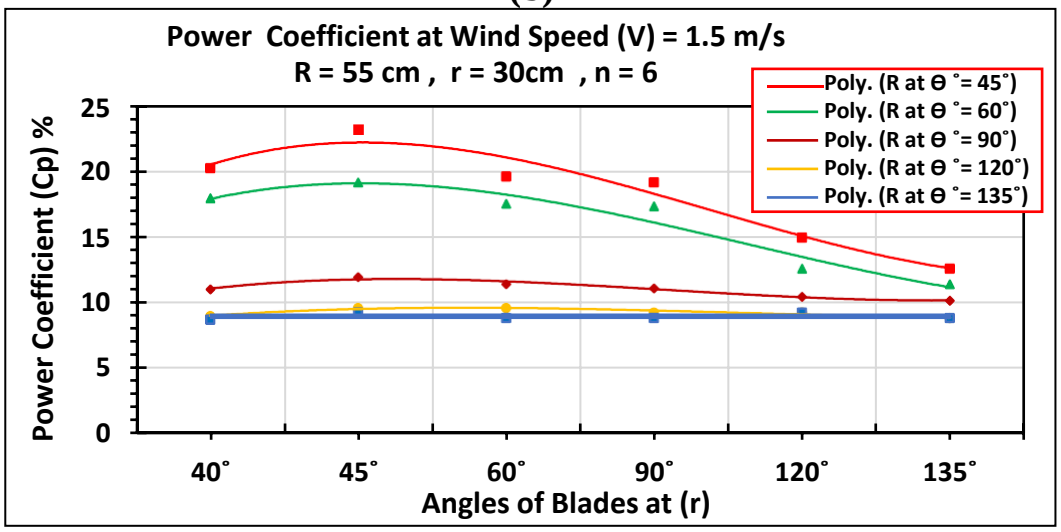

(c)

Fig. (5.18) Power coefficient versus angle of blades for different rotor radius (R) of (MBHYWT), when wind speeds (V) =1.5m/s, number of blades = 6.

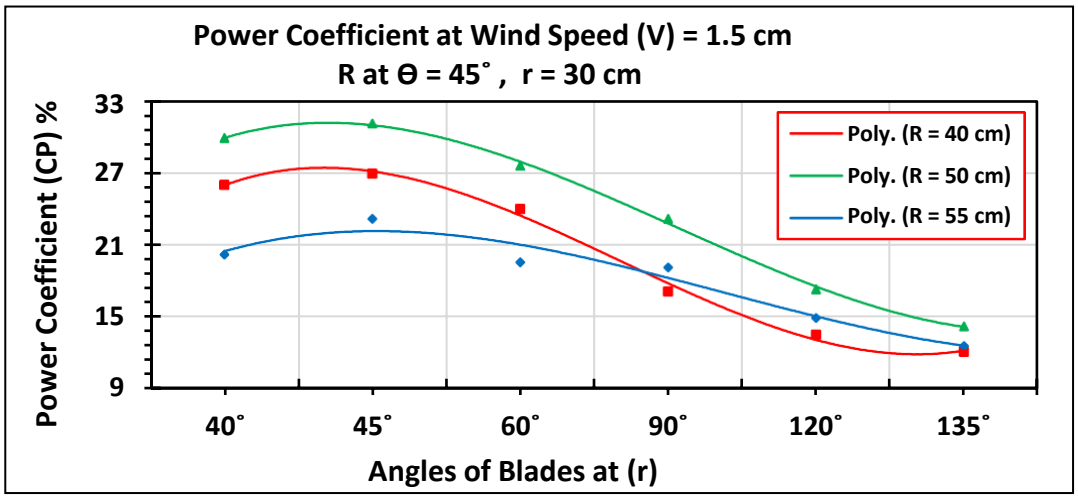

Fig. (5.19) Comparing of power coefficient versus angle of blades for different radius of the rotor (R) of (MBHYWT), when wind speed (V) = 1.5 m/s, number of blades = 6.

At wind speed = 2.5 m/s, the maximum value of (Cp=6.839 %) at speed (2.5 m/s) and radius (50 cm) and angle (45) as Fig.s (5.20-b) and (5.21).

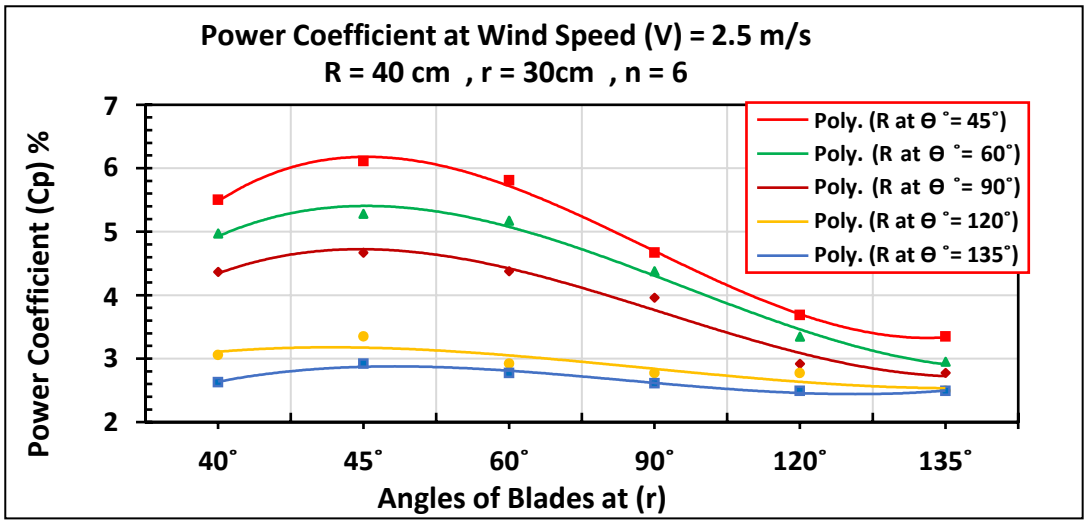

(a)

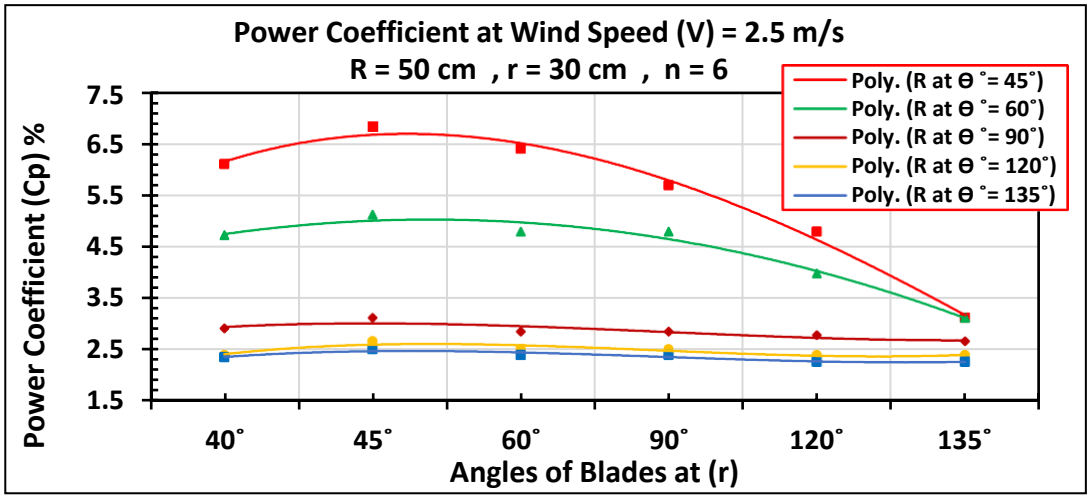

(b)

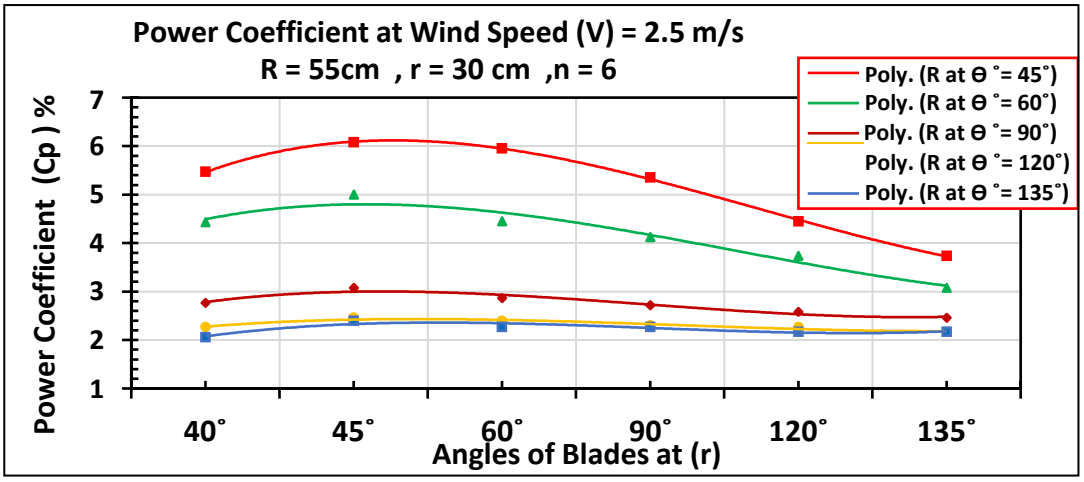

(c)

Fig. (5.20) Power coefficient versus angle of blades for different rotor radius (R) of (MBHYWT), when wind speeds (V) =2.5m/s, number of blades = 6.

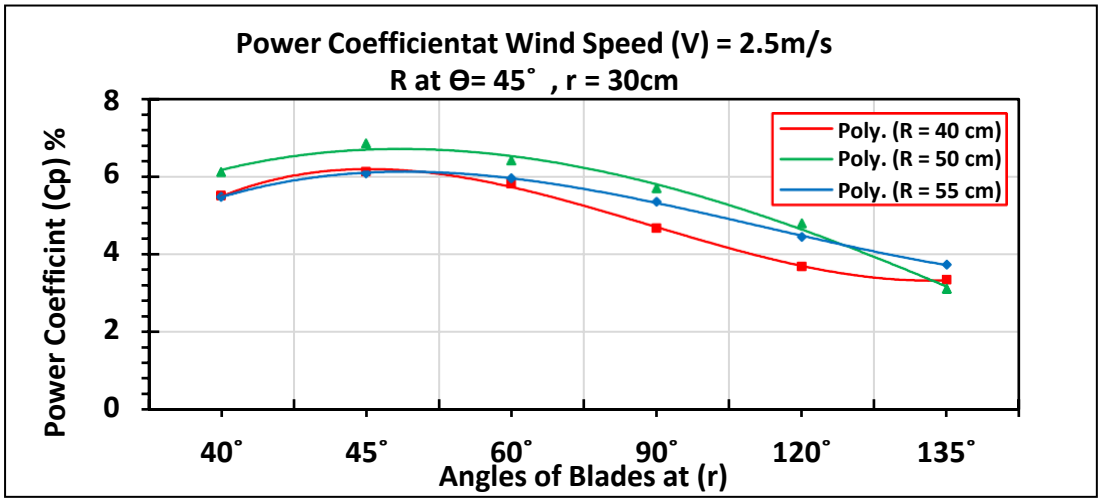

Fig. (5.21) Comparing of power coefficient versus angle of blades for different rotor radius (R) of (MBHYWT), when wind speed (V) = 2.5 m/s, number of blades = 6.

At wind speed = 3 m/s, the maximum value of (Cp=6.606%) at speed (1.5 m/s) and radius (50 cm) and angle (45) as Fig.s (5.22-b) and (5.23).

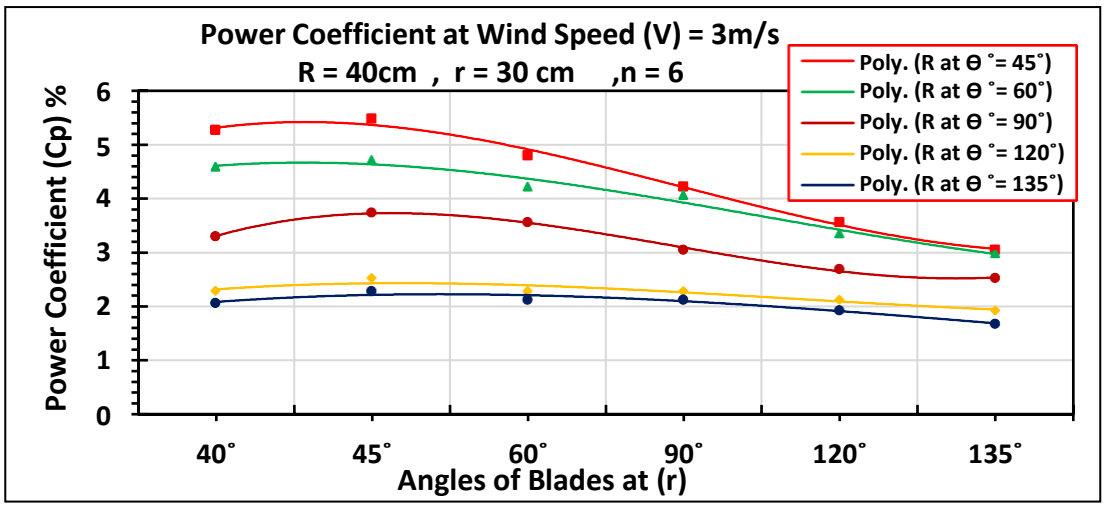

(a)

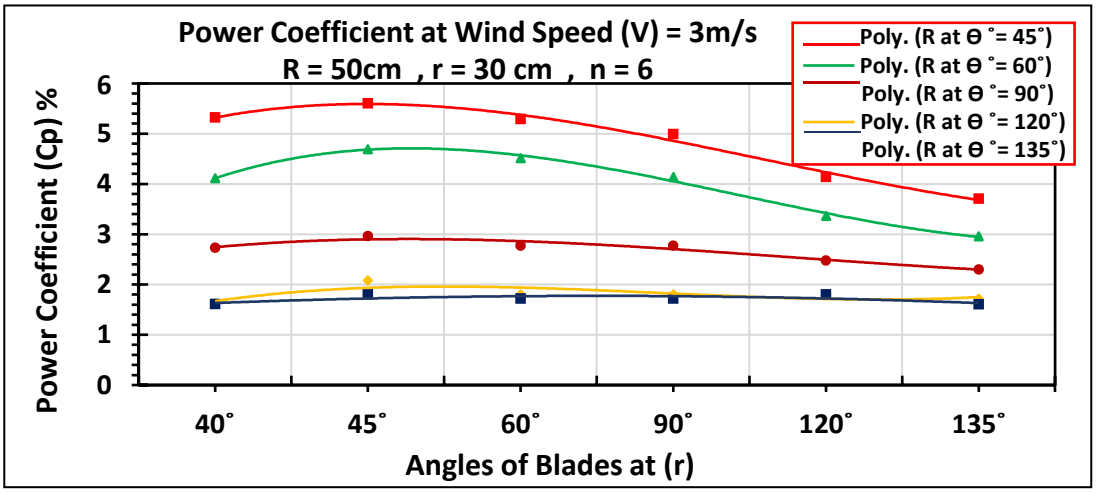

(b)

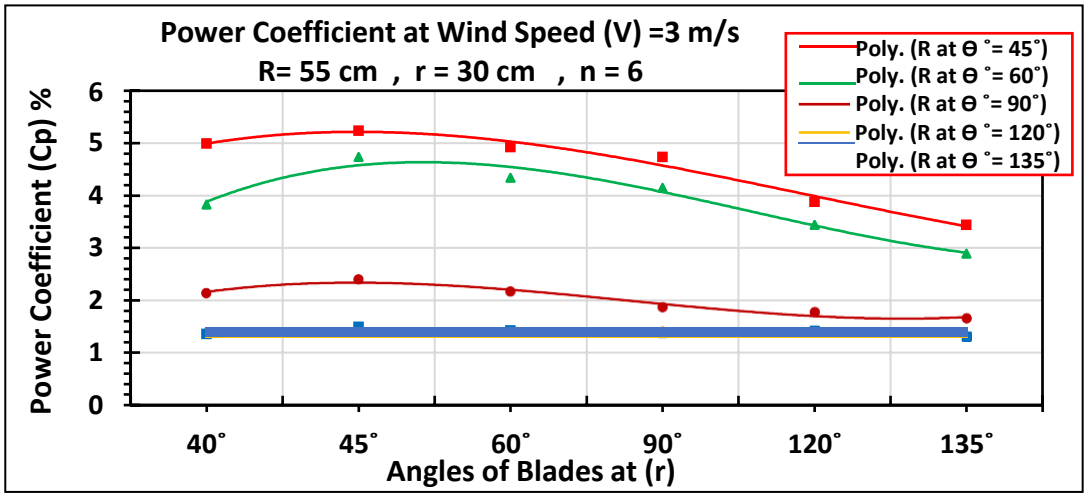

(c)

Fig. (5.22) Power coefficient versus angle of blades for different rotor radius (R) of (MBHYWT), when wind speeds (V) =3m/s, number of blades = 6.

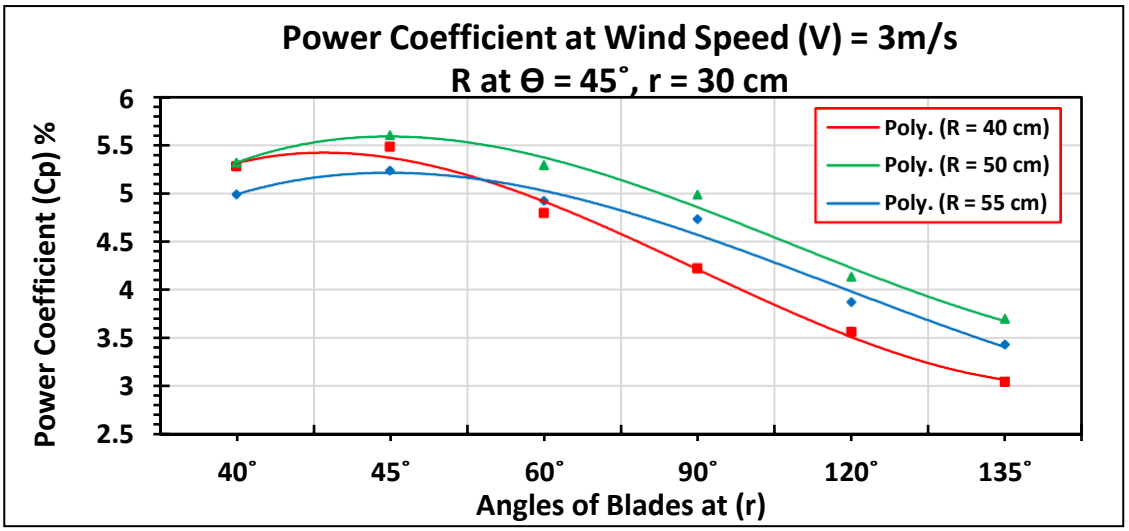

Fig. (5.23) Comparing of power coefficient versus angle of blades for different radius of the rotor (R) of (MBHYWT), when wind speed (V) = 3 m/s, number of blades = 6.

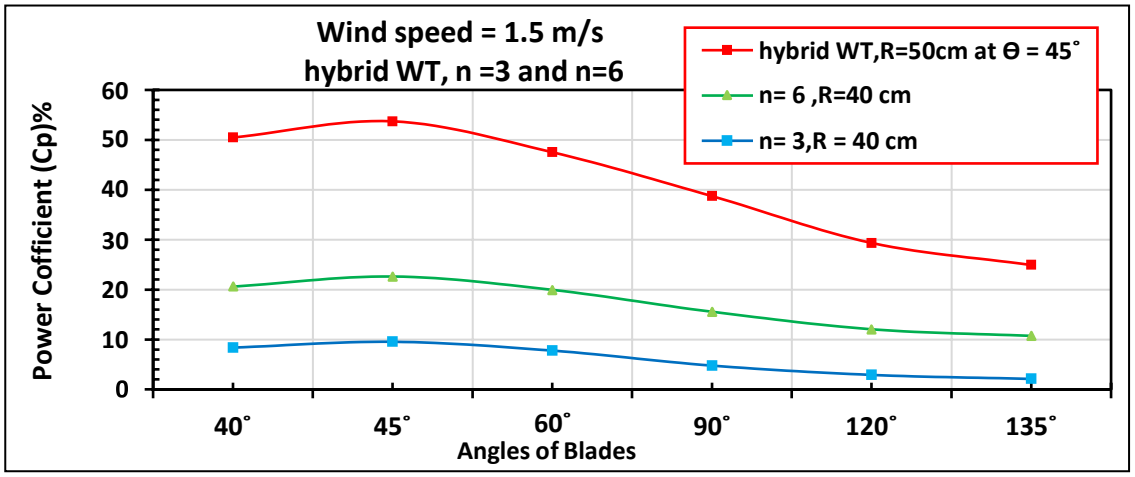

Fig. (5.24) Comparing of power coefficient versus angle for radius of the rotor (R), when wind speed (V) = 1.5 m/s, number of blades = 6 and 3 blades and (MBHYWT)

Fig. (5.24) shows the highest power coefficient to multi-blade hybrid wind turbine compared to the three-blade and six-blade turbines.

The torque is calculated for the different values of blade angle, blade position and wind speed for three cases of the vertical axis wind turbine.

5.1.3.4. First case, (VAWTb-6)

The torque at different angles of blades to turbine are recorded for three wind speeds and presented in the Fig. (5.25), in order to investigate effect of all of these parameters on the turbine performance. It is noted that torque is slightly decreased with increasing blade angle for all values of blade radius and its values are comparable when the wind speed are 1.5 m/s and 2.5 m/s. However, the response change when wind speed increases to 3 m/s as shown in Fig. (5.25- c). The maximum torque achieved at wind speeds of (1.5, 2.5, 3) m/s is (0.5, 0.75, 1.12) N.m, respectively at rotor radius(R= 40 cm) as shown in Fig.s (5.25- a, b, c). The maximum torque at wind speed (V= 3m/s) at R= 40 cm is (1.12 N.m) as shown in Fig. (5.26). It is noted that the maximum torque increases with the increasing in wind speed.

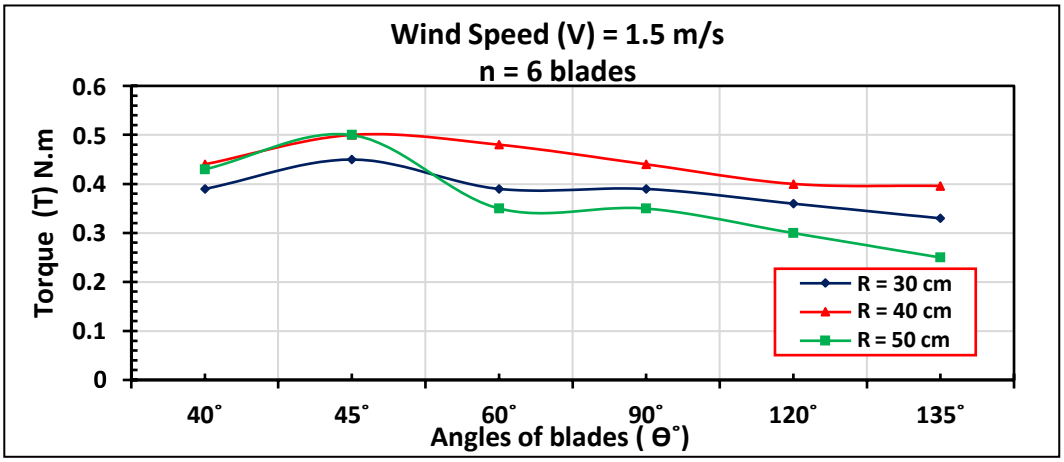

(a)

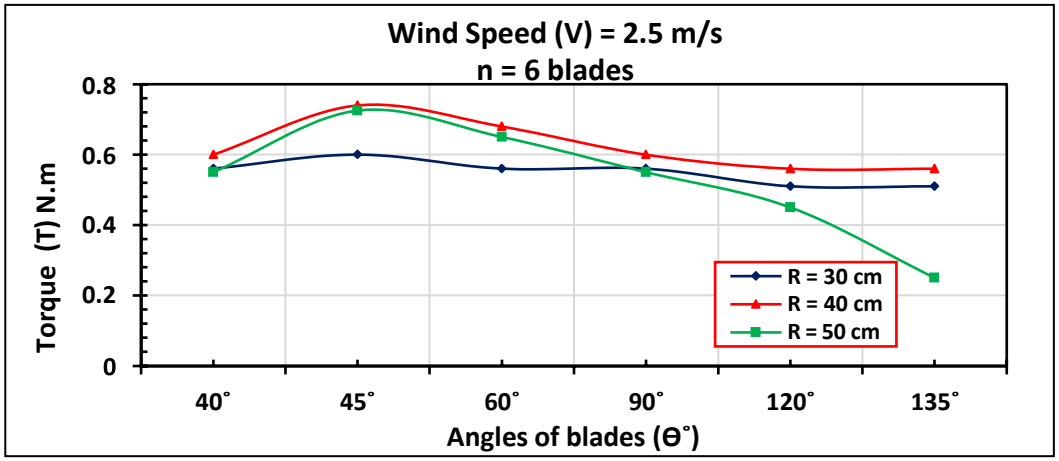

(b)

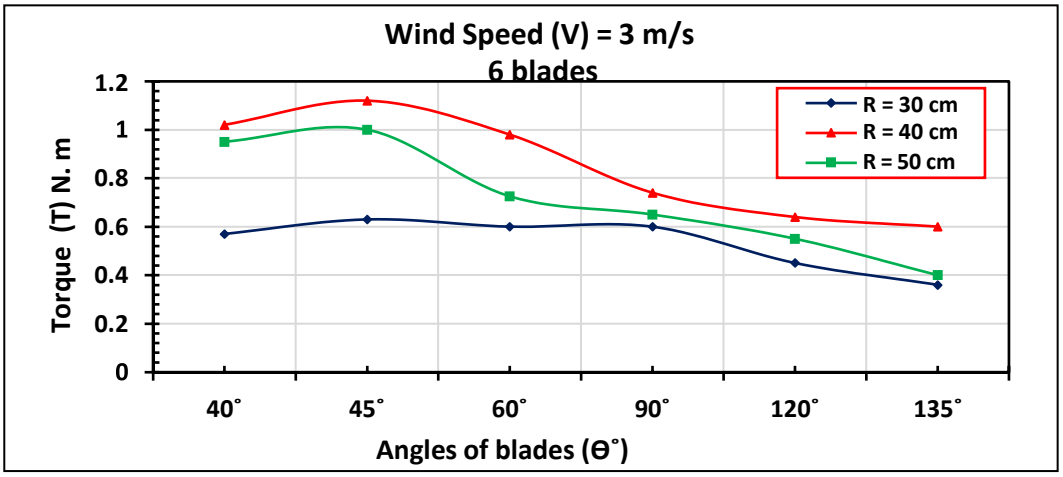

(c)

Fig. (5.25) The torque versus the angle of blades for a different radius of the rotor (R) and three wind speed (V), number of blades = 6.

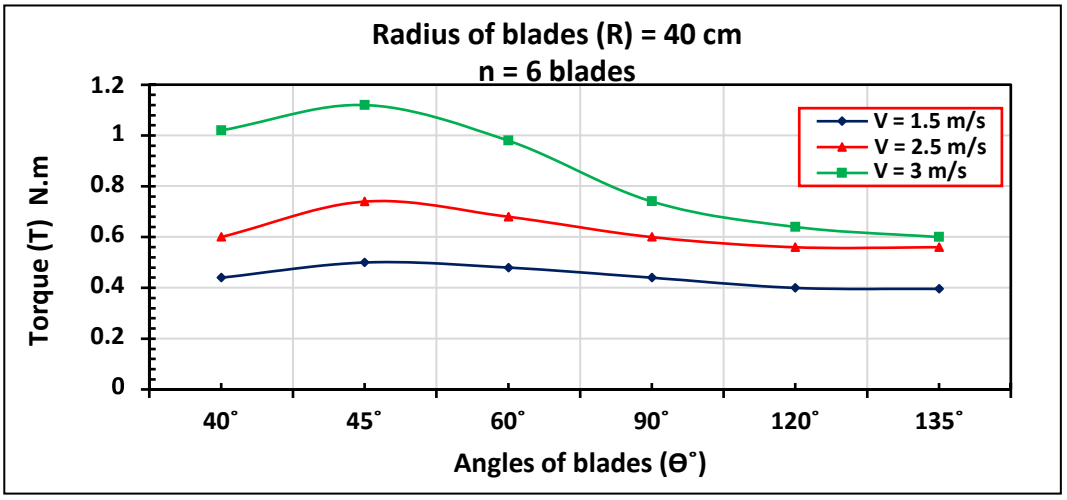

Fig. (5.26) Comparing of torque versus angle of blades for different wind speed (V) when radius of the rotor (R) = 40 cm, number of blades = 6.

5.1.3.5. Second case, (VAWTb-3).

The torque at different angle of blades was recorded for three wind speeds and different radius of the rotor (R) and presented in Fig. (5.27) and Fig. (5.28). The maximum torque at wind speed (V= 3m/s) at R= 40 cm is (0.72 N. m) as shown in Fig.s (5.27 –a, b, c) and (5.28).

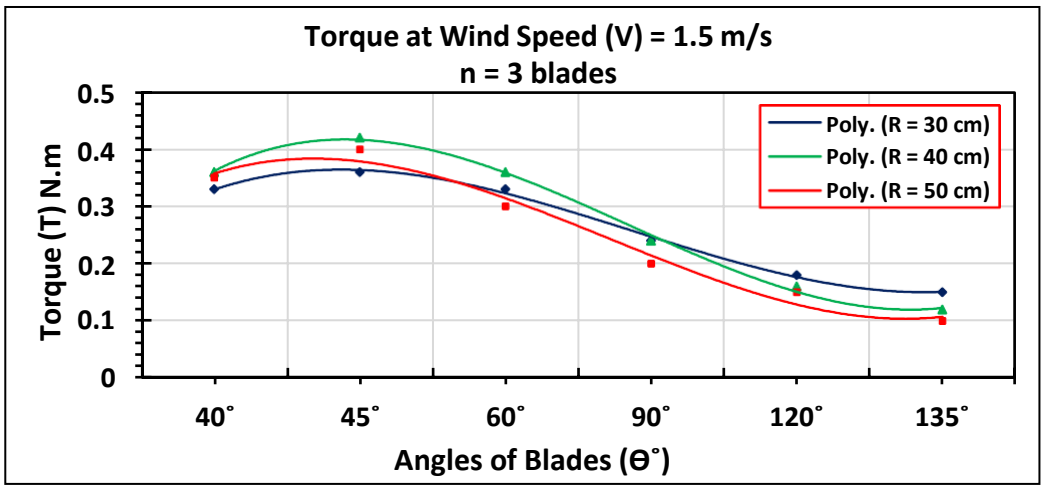

(a)

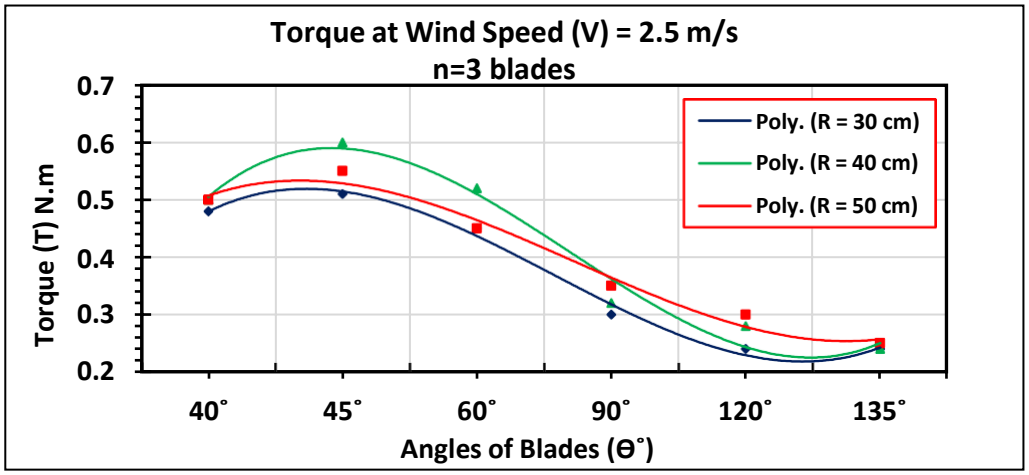

(b)

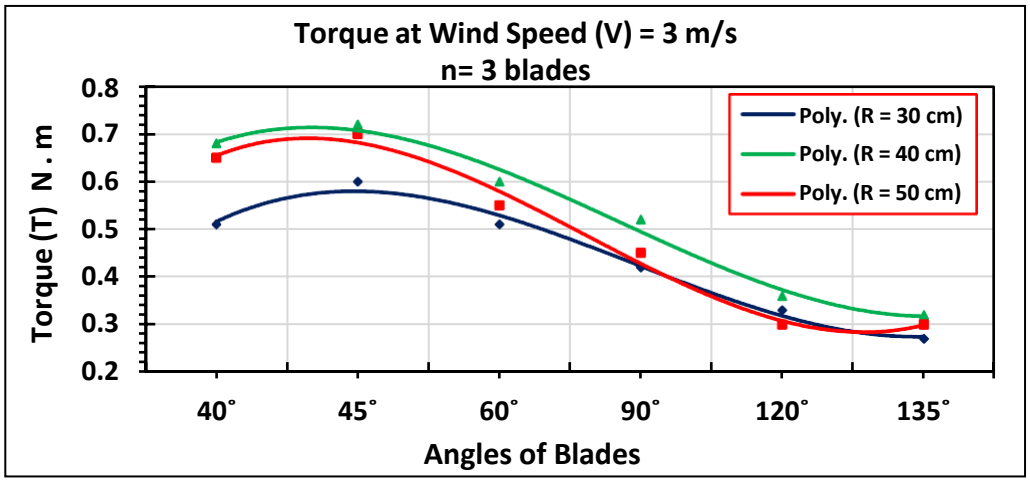

(c)

Fig. (5.27) the torque versus the angle of blades for a different radius of the rotor (R) and three wind speed (V), number of blades = 3.

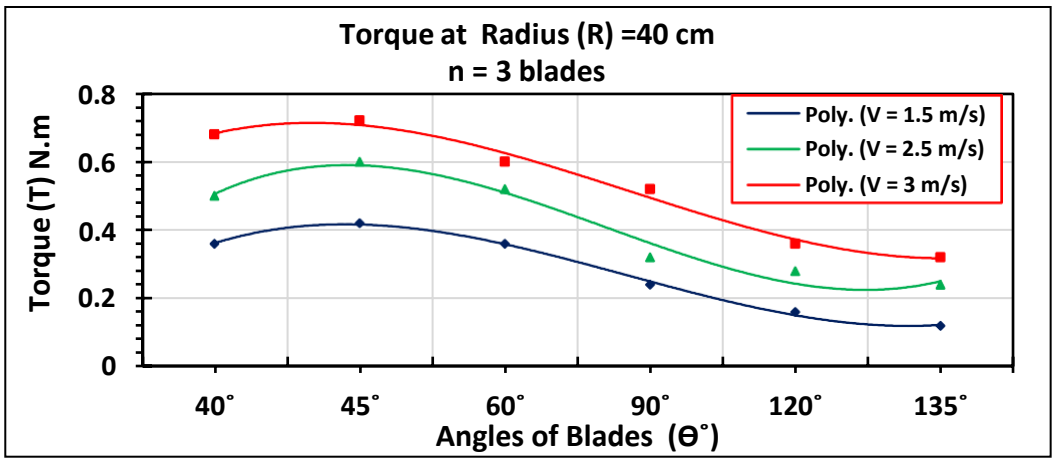

Fig. (5.28) Comparing of torque versus angle of blades for different wind speed (V) when radius of the rotor (R) = 40 cm, number of blades = 3.

5.1.3.6. The third case, (MBHYWT).

The torque and angle of blades to turbine was recorded for three wind speeds and different radius of the rotor (R) as shown in Fig. (5.29) to Fig. (5.35). The maximum torque at wind speed is noticed at (V= 3m/s) and R= 50 cm is (1.42 N. m) as shown in Fig.s (5.34).

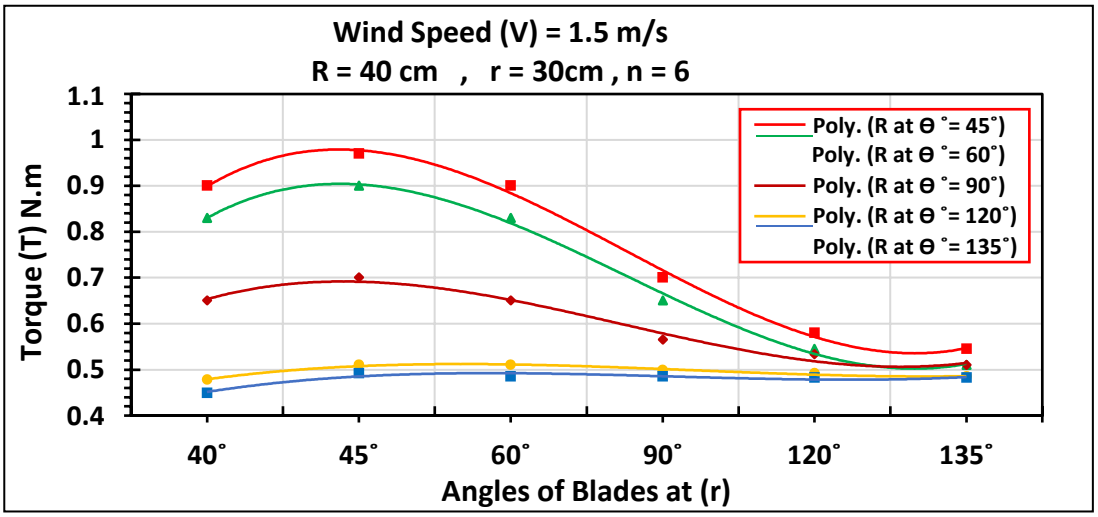

(a)

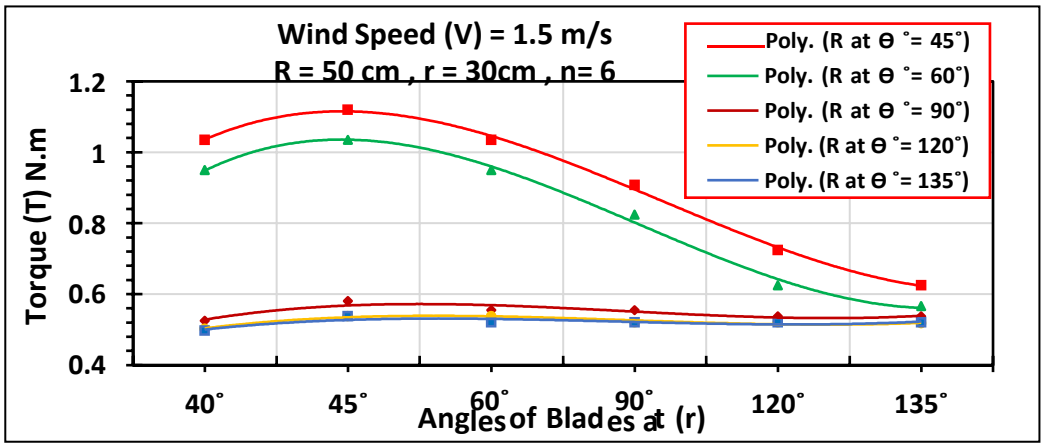

(b)

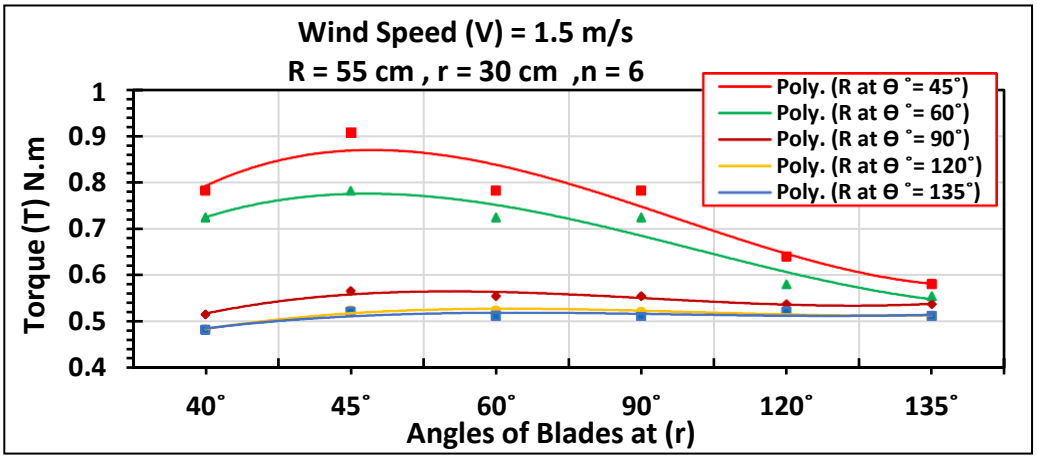

(c)

Fig. (5.29) Effect of angle of blades on the torque at several value of rotor radius (R) for (MBHYWT), when wind speeds (V) =1.5 m/s, number of blades=6.

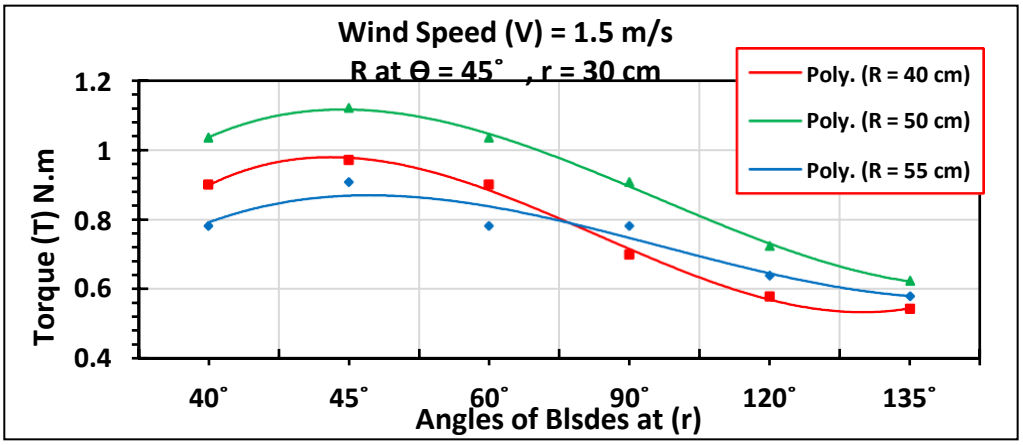

Fig. (5.30) Comparing effect of angle of blades on the torque at several value of rotor radius (R) for (MBHYWT), when wind speeds (V) =1.5 m/s, number of blades=6.

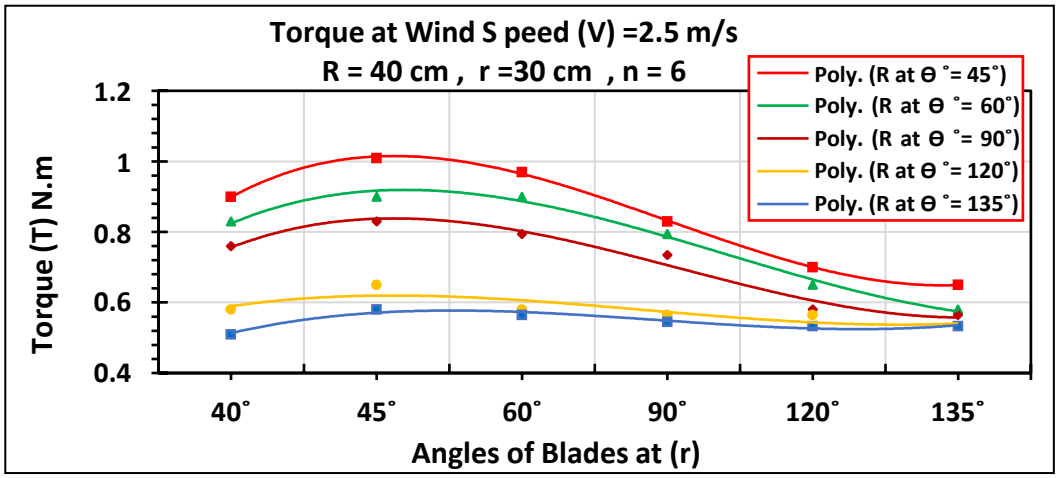

(a)

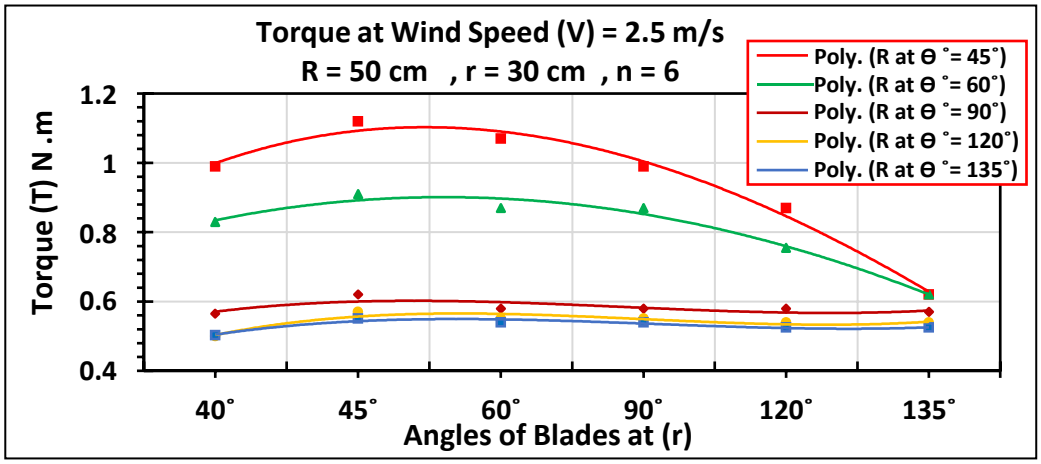

(b)

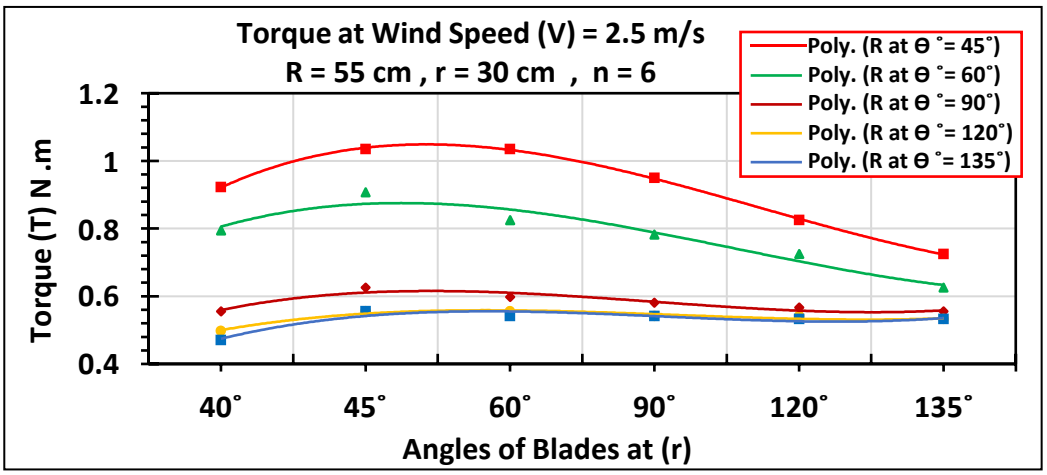

(c)

Fig. (5.31) Effect of angle of blades on the torque at several value of rotor radius (R) for (MBHYWT), when wind speeds (V) = 2.5 m/s, number of blades=6.

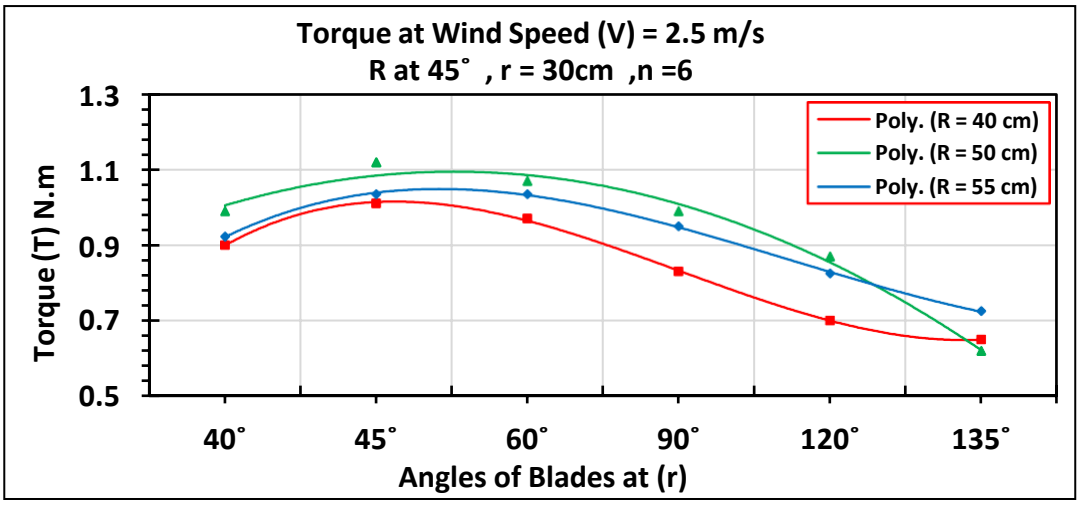

Fig. (5.32) Comparing effect of angle of blades on the torque at several value of radius of the rotor (R) of (MBHYWT), when wind speed (V) = 2.5 m/s, number of blades = 6.

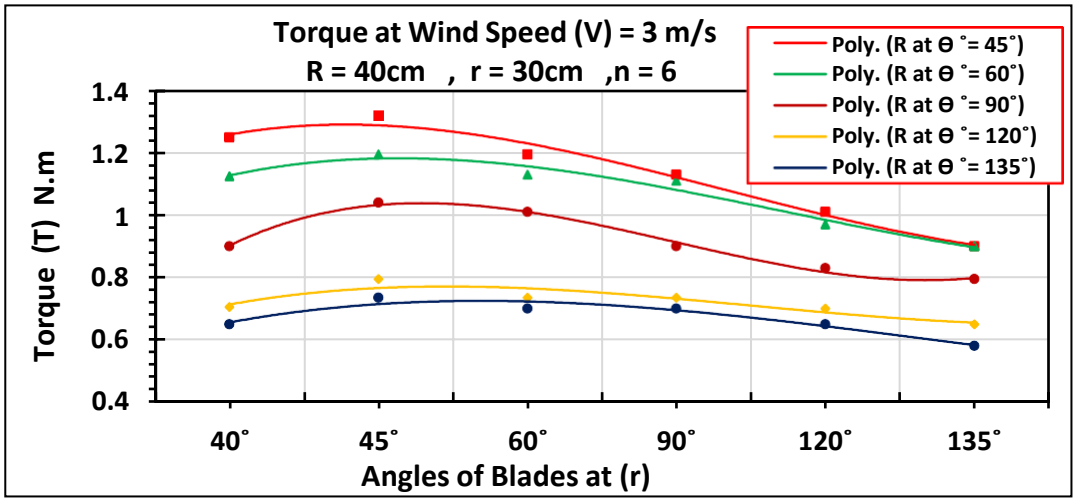

(a)

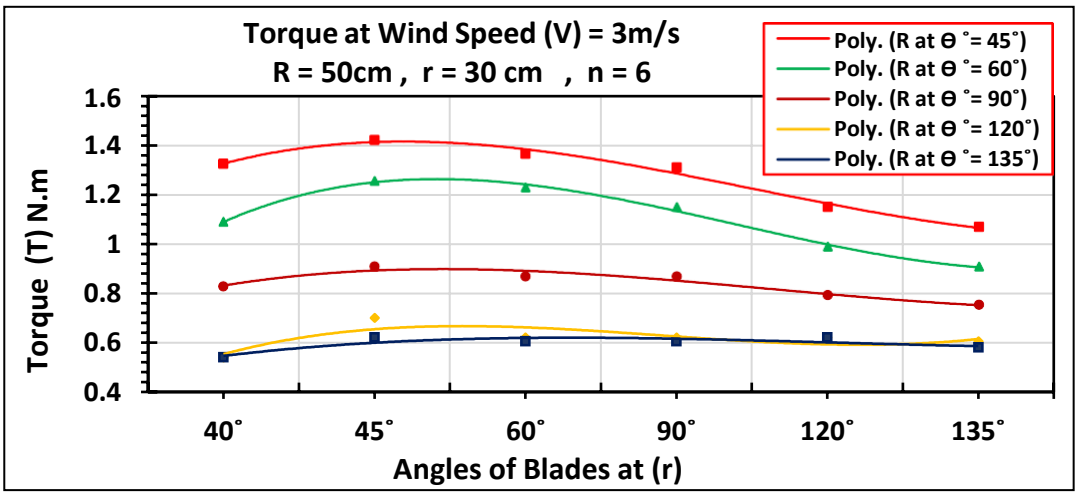

(b)

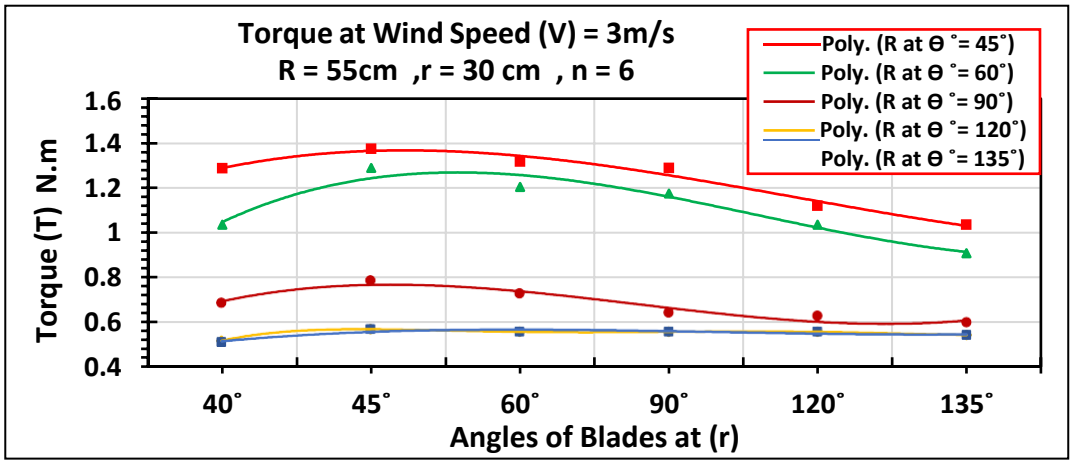

(c)

Fig. (5.33) Effect of angle of blades on the torque at several value of rotor radius (R) for (MBHYWT), when wind speeds (V) = 3 m/s, number of blades= 6.

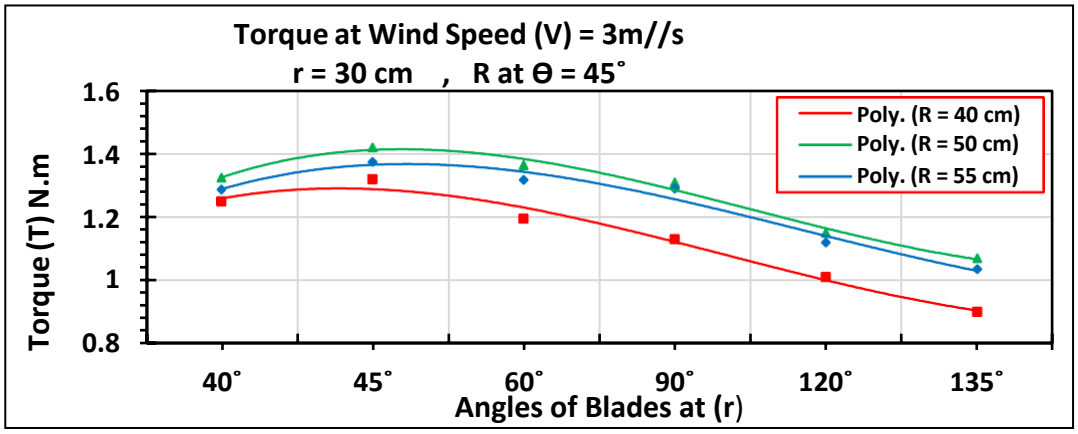

Fig. (5.34) Comparing effect of angle of blades on the torque at several value of radius of the rotor (R) for (MBHYWT), when wind speed (V) = 3 m/s, number of blades = 6.

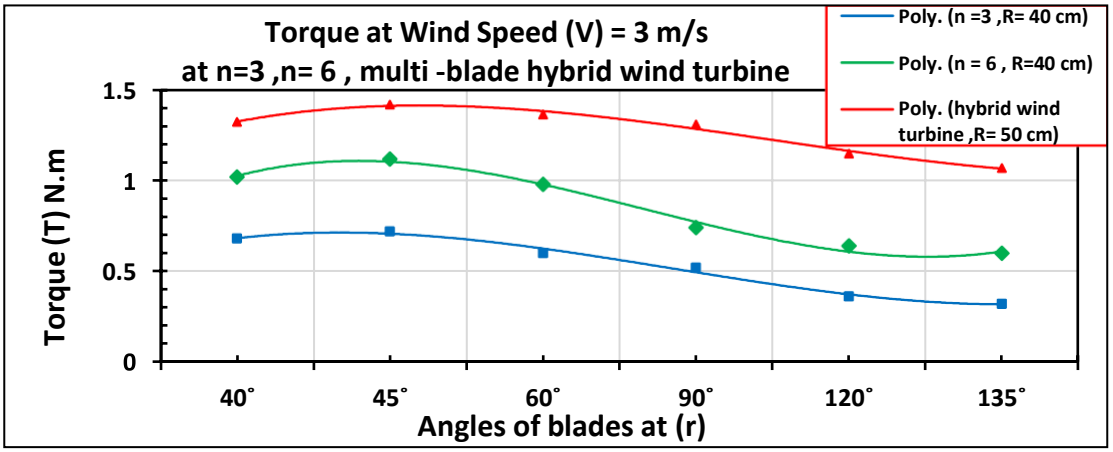

Fig. (5.35) Comparing effect of angle of blades on the torque at several value for a number of blades, when wind speed (V) = 3 m/s.

The variation of maximum torque when wind speed (V) = 3 m/s for the three types of turbine is illustrated in Figure (5.35). It is noted that increasing the blade number has a positive effect on the maximum torque output. It is noted that the maximum torque is produced by the multi-blade hybrid wind turbine (MBHYWT).

The results of the experimental work for all three cases of turbines in the appendix (A - 1) to (C - 9).

5.2. Wind Data Analysis Results.

In the current work, the wind data for the city of Al-Hilla are analyzed for the previous four years (1988, 1998, 2008, and 2018) respectively, as mentioned in chapter four. Velocity duration curve diagrams and power duration curve, depending on Weibull distribution in Fig. (5.36) and the frequency diagram in Fig. (5.37), it is found that V_R = 1.8 m/s, V_I = 0.75 m/s, $V_{O=}$ 2.5 m/s.

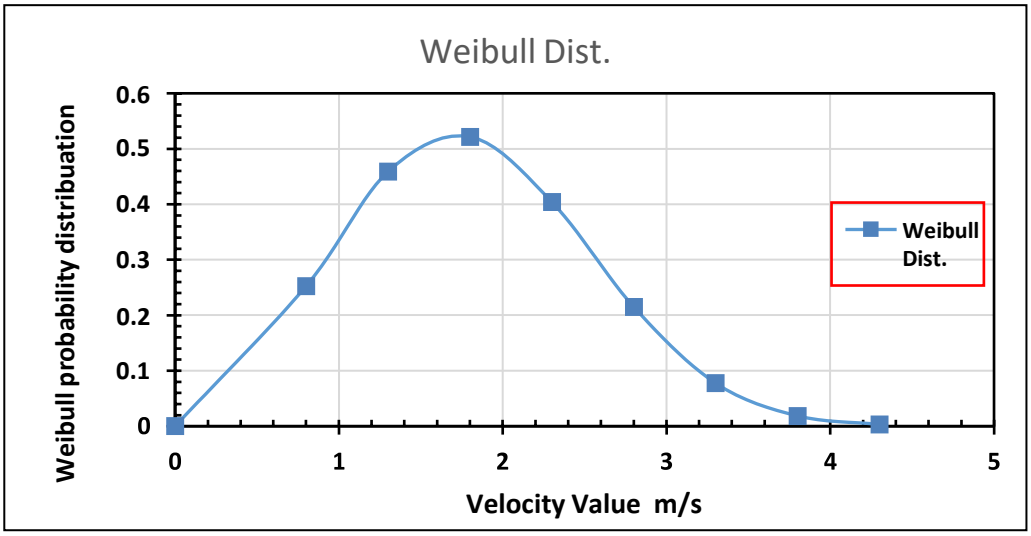

Fig. (5.36) Weibull distribution of wind speed for the city of Babylon from 1988 to 2018

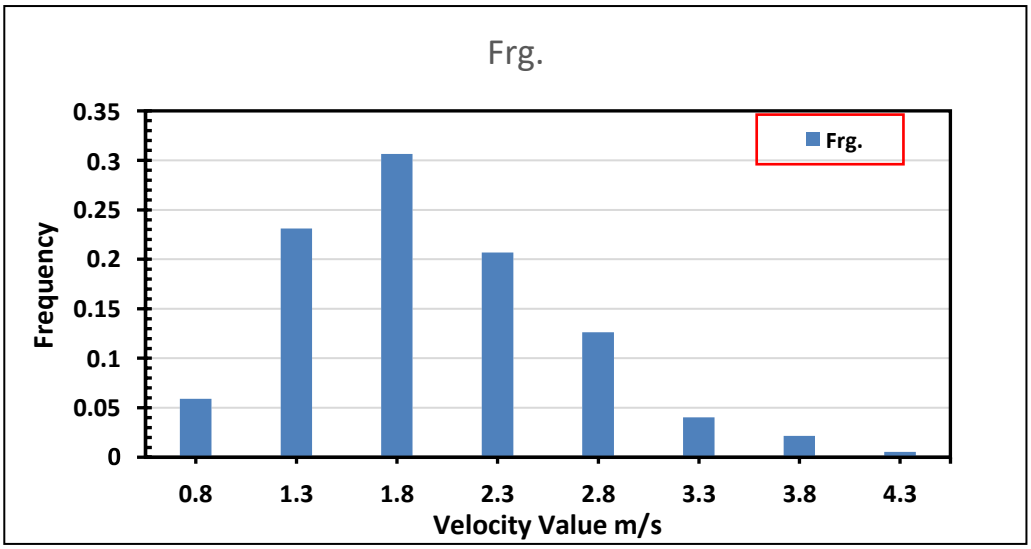

Fig. (5.37) Frequency of velocity from 1988 to 2018

From velocity duration curve diagrams power duration curve are drawn, where the areas under the curve represents the power, using equation (4.10). The resulting power from the use of wind energy for the previous years, are calculated and presented in Fig. (5.38), Fig. (5.39), Fig. (5.40) and Fig. (5.41) where they represent the histogram, diagrams of the wind speed duration curve and power duration curve respectively for Hilla city for the four years mentioned above.

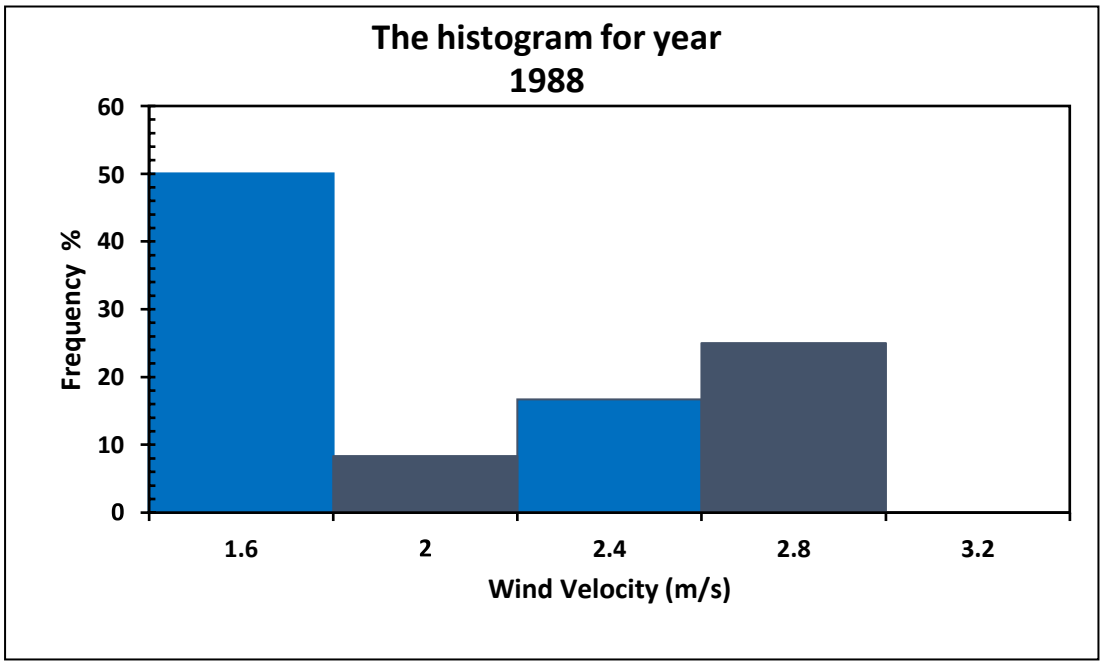

Fig. (5.38 -a)The histogram of the wind speed for Hilla city 1988 year

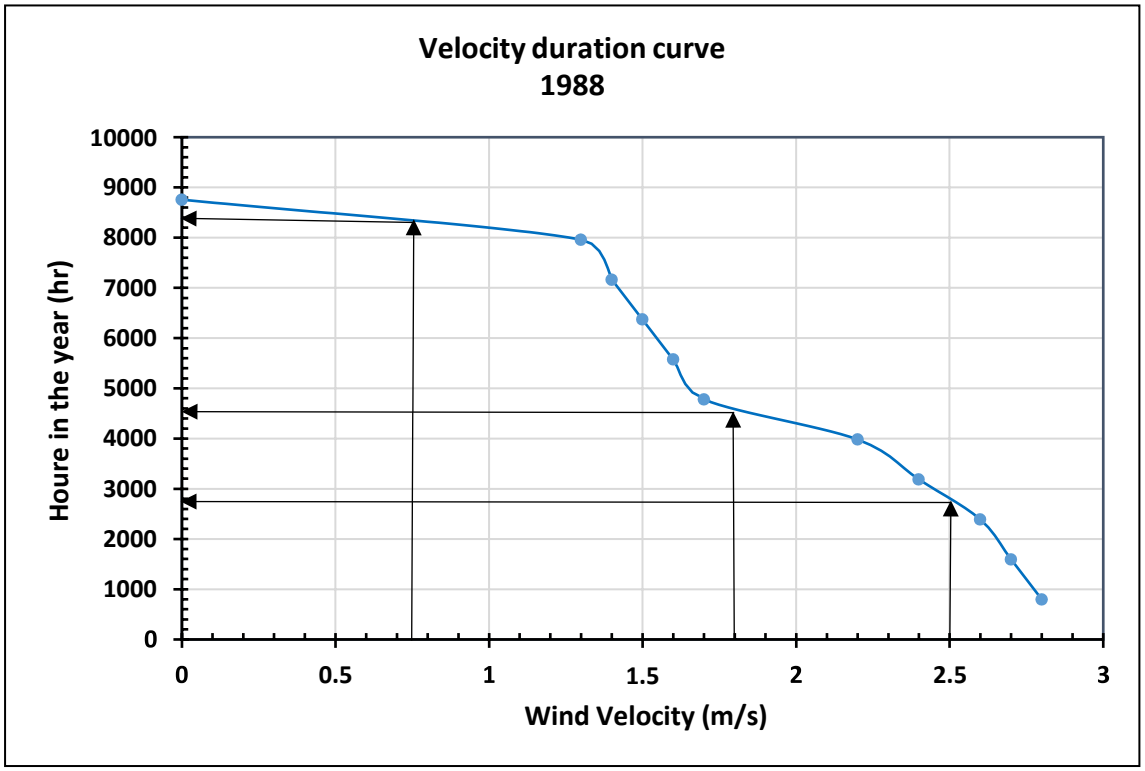

Fig. (5.38 –b) Velocity duration curve of the wind speed for Hilla city 1988 year.

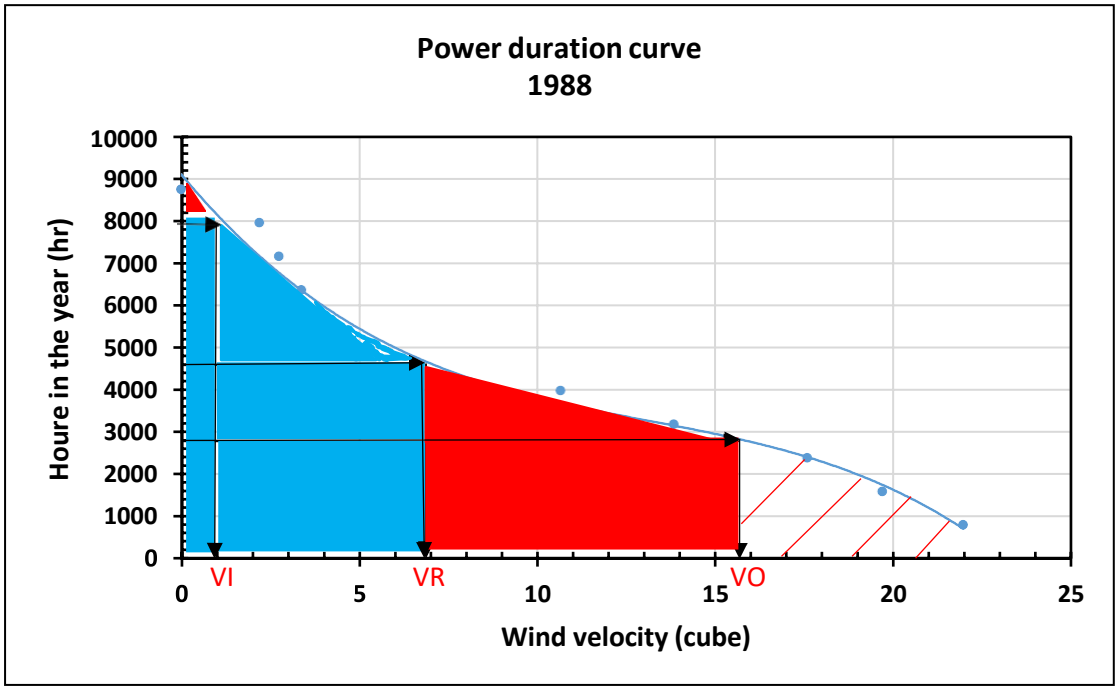

Fig. (5.38– c) Power duration curve of the wind speed for Hilla city 1988 year.

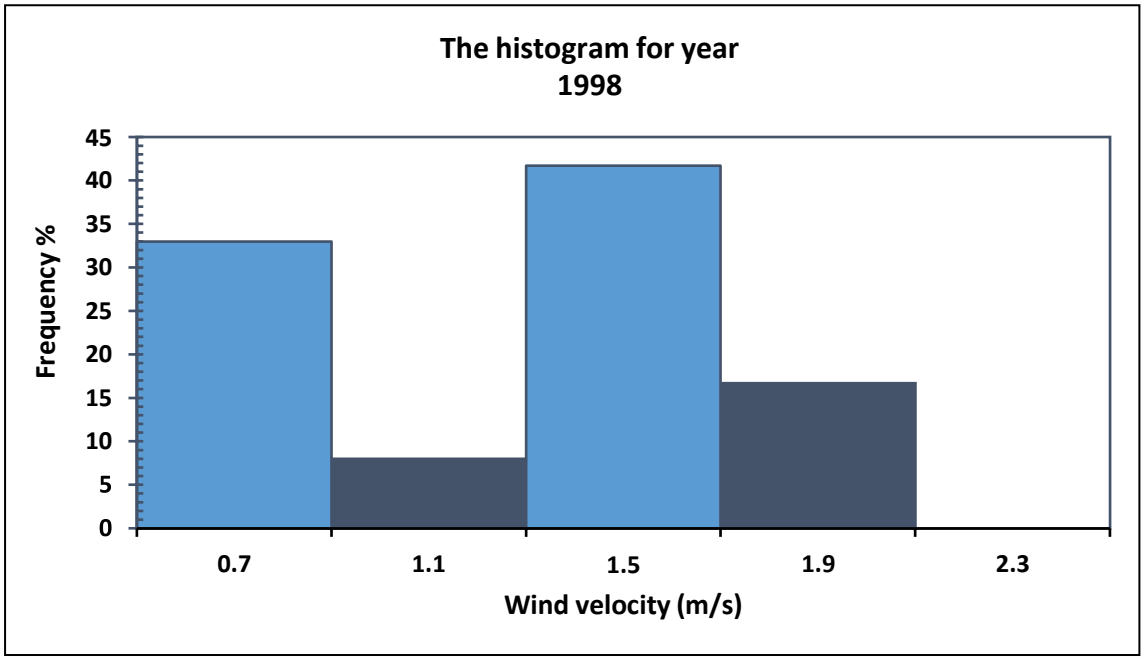

Fig. (5.39 –a) The histogram of the wind speed for Hilla city 1998 year.

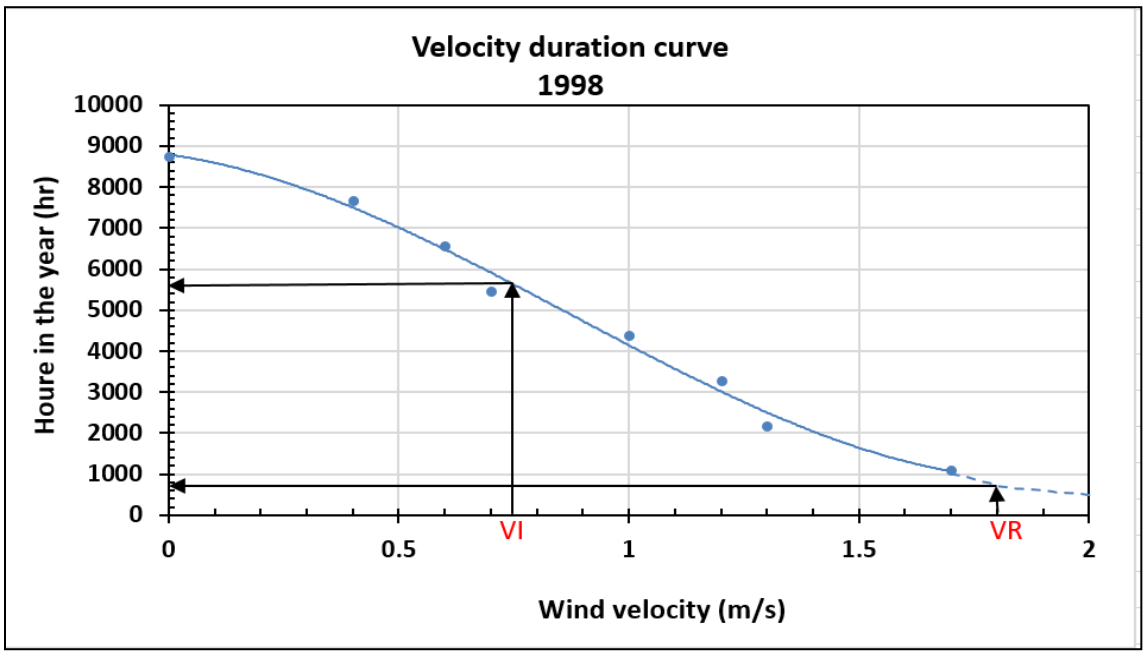

Fig. (5.39 –b) Velocity duration curve of the wind speed for Hilla city 1998 year.

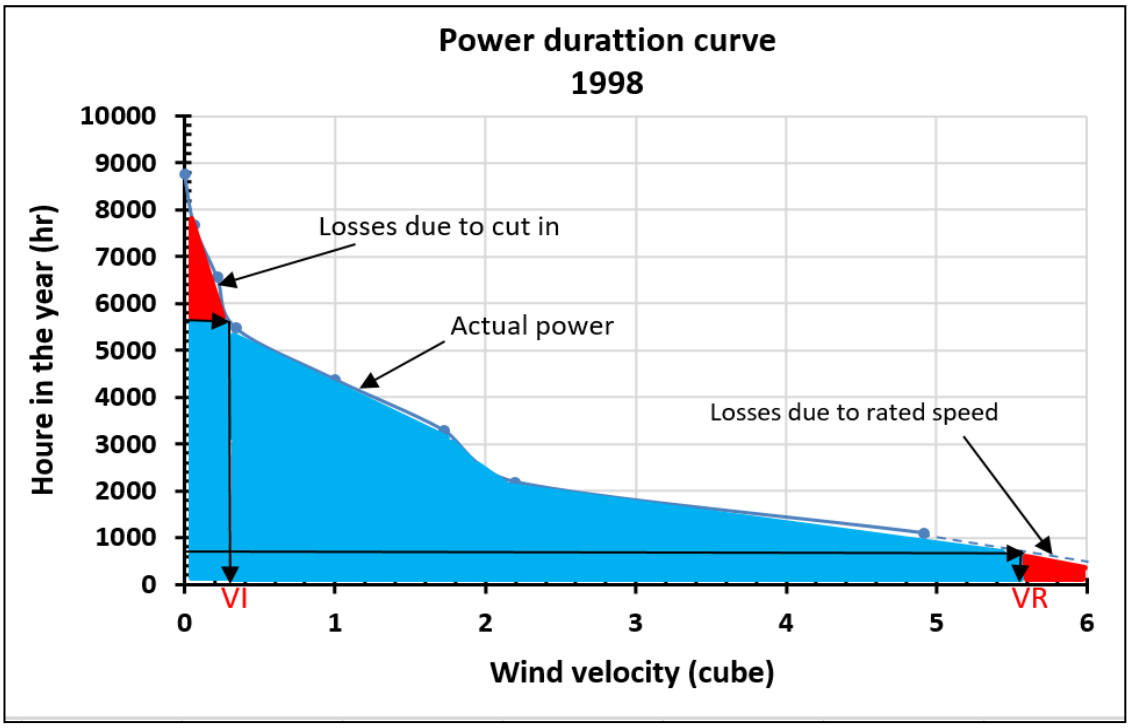

Fig. (5.39 – c) Power duration curve of the wind speed for Hilla city 1998 year.

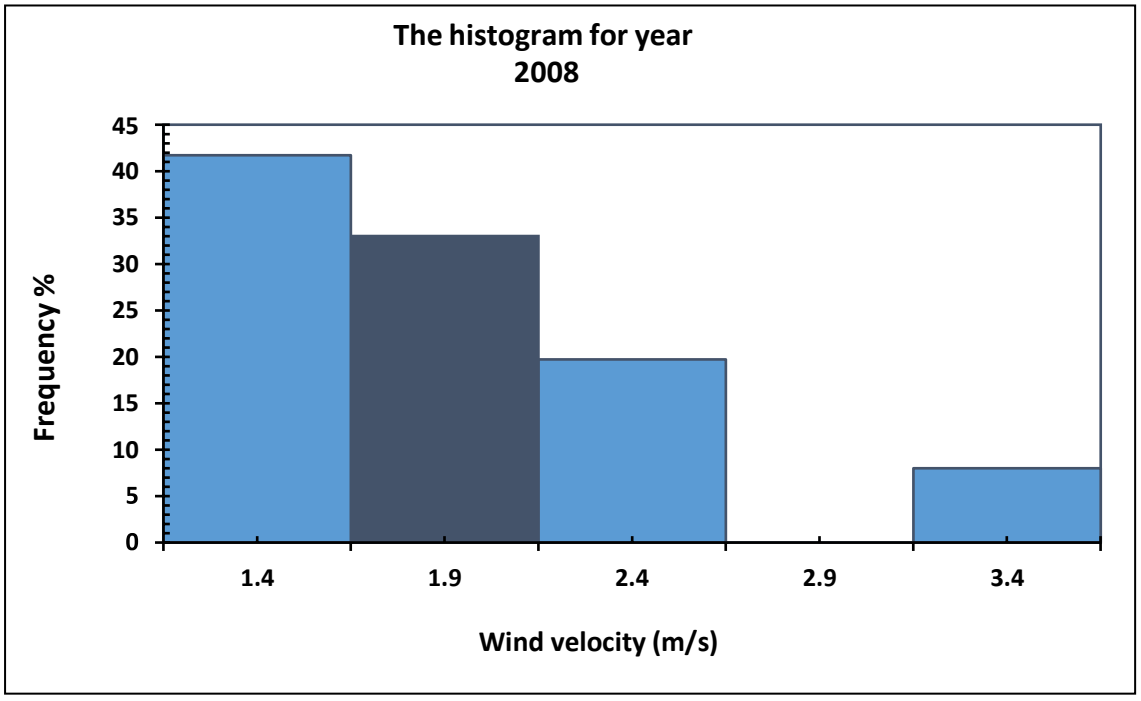

Fig. (5.40 – a) The histogram of the wind speed for Hilla city 2008 year.

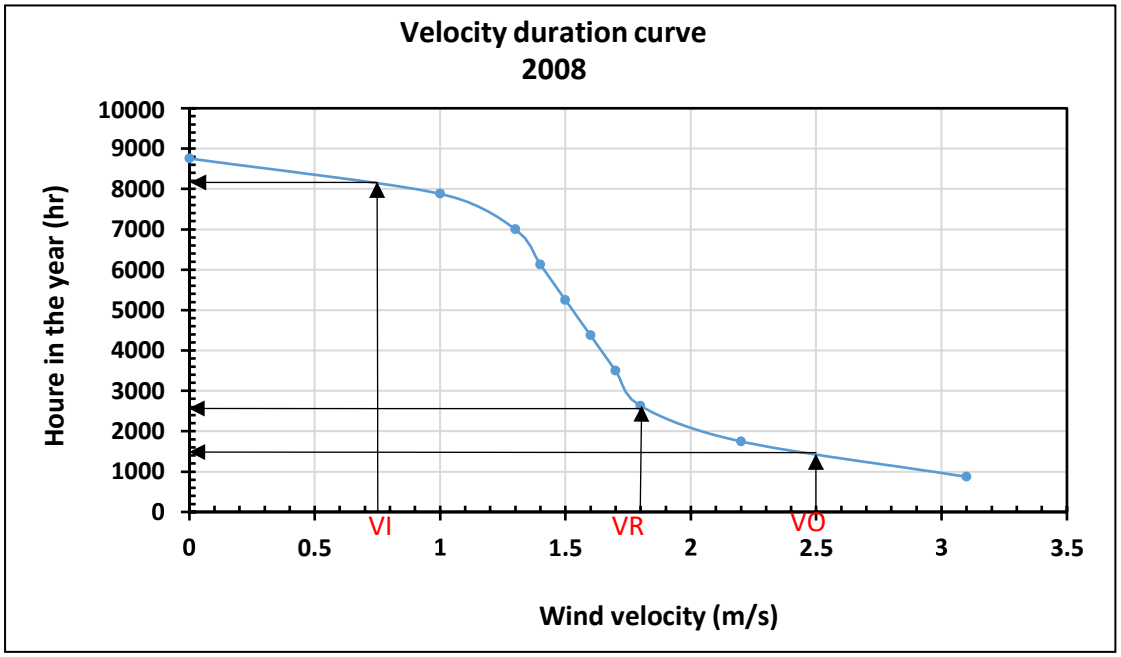

Fig. (5.40 –b) Velocity duration curve of the wind speed for Hilla city 2008 year.

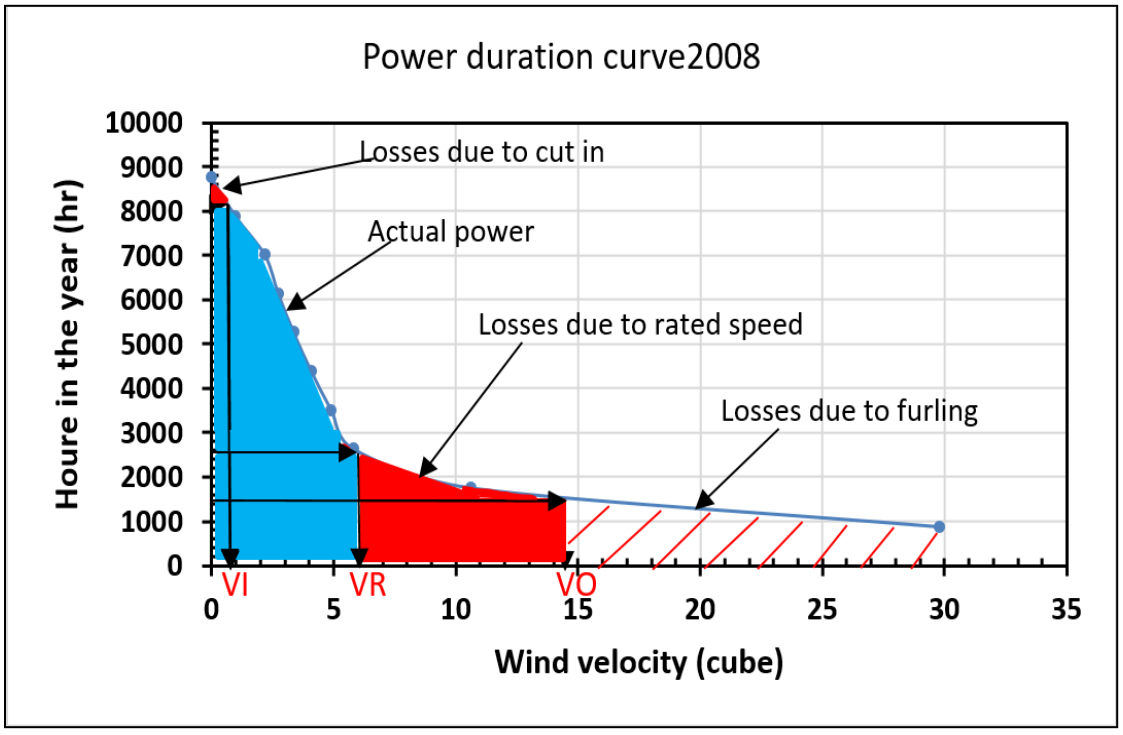

Fig. (5.40 –c) Power duration curve of the wind speed for Hilla city 2008 year.

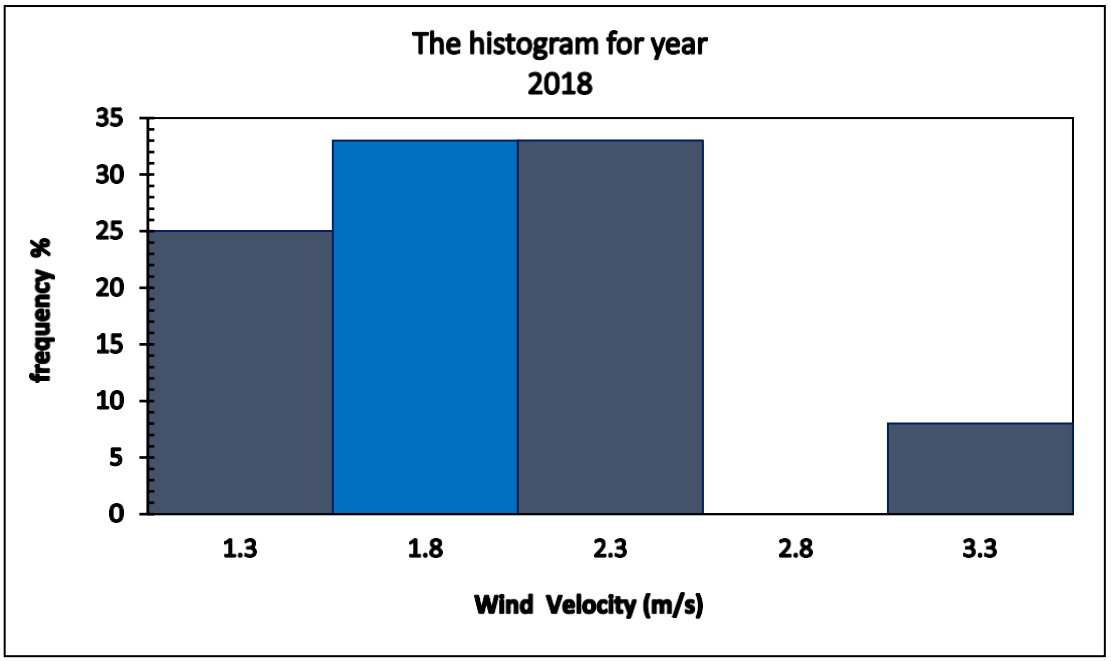

Fig. (5.41 – a) The histogram of the wind speed for Hilla city 2018 year.

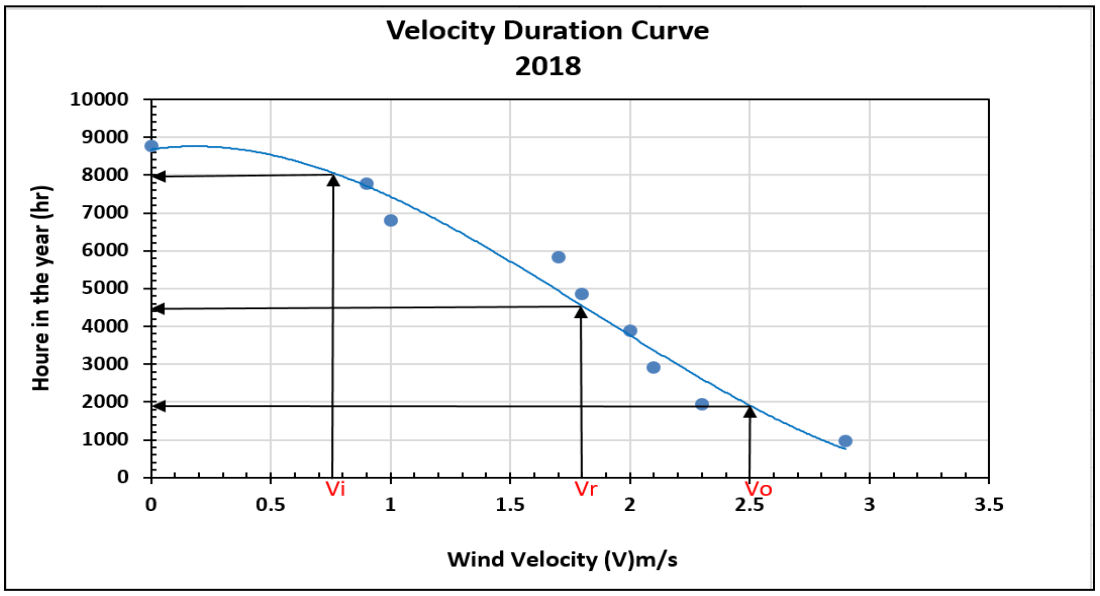

Fig. (5.41 – b) Velocity duration curve of the wind speed for Hilla city 2018 year.

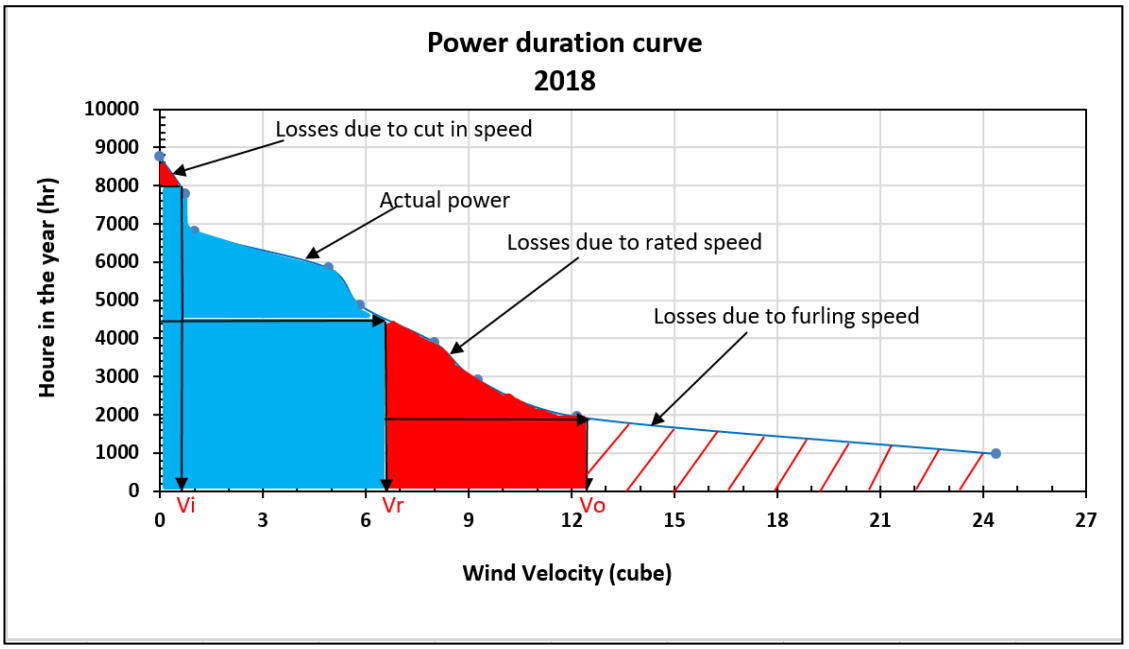

Fig. (5.41 – c) Power duration curve of the wind speed for Hilla city 2018 year.

Figs. (5.38-a),(5.39-a),(5.40 -a) and (5.41-a) represent the histogram of wind speed for the Hilla city for the four years, which represent a good and clear representation for the distribution of wind speed during the months of the year to determine the prevailing wind speed in the specific year. The information obtained from the histogram of speed is the basis on which wind turbines are designed in terms of the speed at which the turbine can start working, the speed that gives the best energy on a regular basis, and the high speeds at which the turbine must stop working to preserve it from crashing or damage with it.

Figs. (5.38-b), (5.39-b), (5.40-b) and (5.41-b) represent velocity duration curve of the wind speed for Hilla city for the past four years. This the curve shows the distribution of wind speed over the number of hours of the year. Depending on this curve, power duration curve for the Hilla city is drawn.

The wind power is usually proportional to the cube of the wind speed, and based on this fact and depending on the velocity duration curve drawing

power duration curve for the Hilla city, where it represents the relationship between the speed cubes corresponding to the number of hours per year. After subtracting the areas that are considered losses from the annual energy quantity of any city within the specifications of the turbine used. Average annual power of the Hilla city are calculated from the power duration curve for four different years as in Figs. (5.38-c), (5.39-c), (5.40-c) and (5.41-c) respectively.

After subtracting the areas that are considered losses, including the losses at high speeds (Energy losses due to the furling speed) at which the turbine stops in order to protect it from damage, losses at low speeds (Energy losses due to cut in speed) at which the turbine does not operate, and losses due to the normal speeds at which the turbine is designed to operate (Energy losses due to the rated speed), the net area under the curve has been calculated, the annual rate of the city of Al-Hilla, as shown in Table (5.1).

Table (5.1): The net area under the curve for the previous years.

The year	1988	1998	2008	2018
The area under the curve(m^3.hr/s^3)	45320	14514	34606	17850

Considering the density of air (1.2 kg/m^3), and using equation (4.10), the annual energy rate is:

$Power_{1988} = 0.5 \times 1.2 \times 45320 \times 3600 = 97891200$ kg/s^2

Annual power is divided by the number of seconds per year, to get the average annual power for Hilla city and for the previous four years, as in Table (5.2).

$P_{1988} = 97891200 \div 31536000 = 3.104$ Watt.

Table (5.2): The resulting power from the use of wind energy for the previous years

The year	1988	1998	2008	2018
The area (power) Watt	3.104	1	2.370	2.783

The speed of calm (∅) is calculated for the previous four years using equation (4.11), and found to be,

$$\emptyset_{1998} = \frac{2920}{8760} \times 100\% = 33.33\%$$

While (∅) for the years 1988, 2008 and 2018 it is 0%.

From the Table (5.2) the power generated from wind is rated between (2.78 – 3 W) it depended on value of the calm speeds, where the percentage of calm speeds for 1998 is about 33.3%, which indicated higher the percentage of (∅), so it is lower the resulting power.

CHAPTER SIX

CONCLUSIONS AND SUGGESTIONS

Conclusions and Suggestions for Future Work

6.1. Conclusion

In this thesis, the underlying concepts in the method of conversion of wind energy is presented. Thus, the rotor's actual power output is determined by the system performance and energy transported from the winds to the rotor; this performance is frequently referred to as the power coefficient (Cp). Additionally, effect of turbines design was examined on mechanical power generated at low wind speeds. Wind speed and rotor diameter are assumed as the parameters of design. The wind speeds varied 1.5 m/s, 2.5 m/s, and 3 m/s. The rotor's radius varied between (30 cm, 40 cm, and 50 cm), respectively. The blades are constructed entirely of PVC material. All testing are achieved indoors to exclude the influence of wind and other environmental factors. The main conclusions of this thesis are:

1- Wind turbine performance depends on wind speed, blades locations (radius of rotor and angle of blades), blade design and type of turbine.

2- The maximum value of the power coefficients of the hybrid turbine (Cp = 31.111%) is obtained at (R = 50 cm, r = 30 cm) and 1.5 m/s for blade radius and wind speed, respectively, specifically at TSR = 2.8, blade angle (Θ) = 45˚ and the number of blades (n = 6).

3- The maximum values of the Cp at all values of the effective parameters are noticed at 45˚ blade angle.

4- Meanwhile, the static torque coefficient (CTs) of the hybrid rotor is superior, the maximum torque noticed wind speed (V= 3m/s) at R= 50 cm equals to (1.42 N. m).

5- By analyzing the wind data for the city of Al-Hilla, it is found that the higher the percentage of calm speeds (Ø), the lower the resultant power.

6- VAWT is able to generate electricity for local use even at low wind speeds in Hilla city.

7- Maximum rated speed (V_R) is 1.8 m/s in Hilla city.

6.2. Suggestions for Future Work

Future studies should incorporate computer modelling of the rotor to determine its flow profile and to forecast its torque and power coefficient performance. The findings of these analyses may help us gain a better understanding of the wind turbine's fluid dynamic features.

1- CFD (Computational fluid dynamics) analysis could be used to compare the findings of testing with naturally occurring wind.
2- Blade turbine can be designed to control its angle online by including servo – motor prepared for this case.
3- Blade location (R) can be also controlled to vary online based on the design requirements.
4- Suggestions in (3) and (4) can be designed for one integrated design to investigate its performance.
5- Design an offline controller for the blade to provide the optimal projected area of blade for maximize the performance and minimize negative torque, respectively.

REFERENCES

References

[1] Mathew S 2006 Wind energy: fundamentals, resource analysis and economics Springer.

[2] Golding E (1976) the generation of electricity by wind power. Halsted Press, New York.

[3] Sorensen B (1995) History of, and recent progress in, wind-energy utilizatio Annual Review of Energy and the Environment 20(1): 387-424.

[4] Putnam PC (1948) Power from the wind. Van Nostrand, New York.

[5] Ramler JR, Donovan RM (1979) Wind turbines for electric utilities: Development status and economics. DOE/NASA/1028-79/23, NASA TM- 79170, AIAA-79-0965.

[6] Savonius SJ (1931) The S-rotor and its applications. Mechanical Engineering 53(5):333- 338.

[7] Kumar, R., Raahemifar, K. & Fung, A. S. A critical review of vertical axis wind turbines for urban applications. Renew. Sustain. Energy Rev. 89, 281–291 (2018(.

[8] Carrasco JM, Galván E, Portillo R. Chapter 4 – wind turbine applications. Altern Energy Power Electron 2011:177–230.

[9] Tummala A, Velamati RK, Sinha DK, Indraja V, Krishna VH. A review on small scale wind turbines. Renew Sustain Energy Rev 2016; 56:1351–71.

[10] Liu S, Ho Y. Wind energy applications for Taiwan buildings: what are the challenges and strategies for small wind energy systems exploitation? Renew Sustain Energy Re 2016; 59:39–55.

[11] Bedon G, Antonini EGA, Betta SD, Castelli MR, Benini E. Evaluation of the different aerodynamic databases for vertical axis wind turbines simulations. Renew Sustain Energy Rev 2014; 40:386–99.

[12] Global Wind Energy Council. Global wind energy statistics. Available on: ⟨http://www.gwec.net/global-figures/wind-in-numbers/⟩; 2015 [Accessed 15 March 2018].

[13] International Energy Agency. Technology roadmap wind energy, OECD/IEA-2013. Available on:⟨https://www.iea.org/publications/freepublications/publication/Wind_2013_Roadmap.pdf⟩; 2013 [Accessed 24 July 2016].

[14] Bahaj AS, Myers L, James PAB. Urban energy generation: influence of micro-wind turbine output on electricity consumption in buildings. Energy Build 2007; 39:154–65.

[15] Heagle ALB, Naterer GF, Pope K. Small wind turbine energy policies for residential and small business usage in Ontario, Canada. Energy Policy 2011; 39:1988–99.

[16] W.e. V. Global Statistics Retrieved from Wind Energy International)2018 (.

[17] Yudaev I V, Daus Y V, Zharkov A V and Zharkov V Y 2020 Private Solar Power Plants of Ukraine of Small Capacity: Features of Exploitation and Operating Experience Applied Solar Energy 56 54-62

[18] IEA 2014 Energy Technology Perspectives International Energy Agency.

[19] Archer C L and Jacobson M Z 2003 Spatial and temporal distributions of US winds and wind power at 80m derived from measurements J. Geophys. Res. Atmos. 108

[20] Fried, Wind Power to dominate power sector growth (2016). Retrieved from Global Wind Energy Council: https://gwec.net/wind-power-to-dominate-power sectorgrowth/

[21] Wind Europe, WIND ENERGY IN EUROPE IN 2018 Trend and Statistics (Wind Europe, Belgium, 2018). Available ONLINE: https://windeurope.org/about-wind/statistics/eu ropean/wind-energy-in-europe-in-2018/

[22] Saad, A. Elwardany, I. I. El-Sharkawy, S. Ookawara, and M. Ahmed, "Performance evaluation of a novel vertical axis wind turbine using twisted blades in multi-stage Savonius rotors," Energy Convers. Manag., vol. 235, no. November 2020, p. 114013, 2021, doi: 10.1016/j.enconman.2021.114013.

[23] Liew, A. R. Rosemizi, M. Z. Aihsan, I. Muzamir, and I. Baharuddin, "Wind Characterization by Three Blade Savonius Wind Turbine Using IoT," IOP Conf. Ser. Mater. Sci. Eng., vol. 932, no. 1, 2020, doi: 10.1088/1757-899X/932/1/012080.

[24] Al-Asbahi and L. Y. San, "Development of Vertical Axis Wind Turbines and Solar Power Generation Hybrid System," Int. J. Comput. Digit. Syst., vol. 90, no. 4, pp. 625–634, 2020, doi: 10.12785/ijcds/090410.

[25] Zahir Hussain et al., "Charging of car battery in electric vehicle by using wind energy," Mater. Today Proc., no. xxxx, 2020, doi: 10.1016/j.matpr.2020.08.341.

[26] Brandetti, D. De Tavernier, B. Leblanc, and C. Ferreira, "Experimental test of variable loads on a vertical-axis wind turbine," J. Phys. Conf. Ser., vol. 1618, no. 3, 2020, doi: 10.1088/1742-6596/1618/3/032037.

[27] Al-Ghriybah, M. F. Zulkafli, D. H. Didane, and S. Mohd, "Review of the recent power augmentation techniques for the savonius wind turbines," J. Adv. Res. Fluid Mech. Therm. Sci., vol. 60, no. 1, pp. 71–84, 2019.

[28] Vergaerde et al., "Experimental validation of the power enhancement of a pair of vertical-axis wind turbines," Renew. Energy, vol. 146, pp. 181–187, 2020, doi: 10.1016/j.renene.2019.06.115.

[29] Ayati, K. Steiros, A. M. Miller, S. Duvvuri, and M. Hultmark, "A double-multiple streamtube model for vertical axis wind turbines of arbitrary rotor loading," Wind Energy Sci., vol. 4, no. 4, pp. 653–662, 2019, doi: 10.5194/wes-4-653-2019.

[30] Gouda, K. B.M., and K. Jayaram, "Power Generation On Highway Using Vertical Axis Wind Turbine and Solar Energy," vol. 8, no. 1, pp. 5–8, 2019.

[31] Driss, "Evaluation of the Savonius Wind Rotor Performance for Different External Overlap Ratios," Int. J. Fluid Mech. Therm. Sci., vol. 1, no. 1, p. 14, 2015, doi:

10.11648/j.ijfmts.20150101.13.

[32] Bhayo, H. H. Al-Kayiem, and N. Z. Yahaya, “Performance investigation of the S-rotors,” IOP Conf. Ser. Mater. Sci. Eng., vol. 100, no. 1, 2015, doi: 10.1088/1757-899X/100/1/012043.

[33] Loganathan, H. Chowdhury, I. Mustary, and F. Alam, “An experimental study of a cyclonic vertical axis wind turbine for domestic scale power generation,” Procedia Eng., vol. 105, no. Icte 2014, pp. 686–691, 2015, doi: 10.1016/j.proeng.2015.05.057.

[34] Abdelsalam, M. A. Kotb, K. Yousef, and I. M. Sakr, “Performance study on a modified hybrid wind turbine with twisted Savonius blades,” Energy Convers. Manag., vol. 241, no. March, p. 114317, 2021, doi: 10.1016/j.enconman.2021.114317.

[35] Melani, F. Balduzzi, L. Brandetti, C. J. S. Ferreira, and A. Bianchini, “An experimental and numerical analysis of the dynamic variation of the angle of attack in a vertical-axis wind turbine,” J. Phys. Conf. Ser., vol. 1618, no. 5, 2020, doi: 10.1088/1742-6596/1618/5/052064.

[36] Jiang, P. Zhao, T. Stoesser, K. Wang, and L. Zou, “Experimental and numerical investigation of twin vertical axis wind turbines with a deflector,” Energy Convers. Manag., vol. 209, no. November 2019, p. 112588, 2020, doi: 10.1016/j.enconman.2020.112588.

[37] LeBlanc and C. Simao Ferreira, “Overview and design of pitchVAWT: Vertical axis wind turbine with active variable pitch for experimental and numerical comparison,” Wind Energy Symp. 2018, vol. 0, no. 210029, pp. 1–11, 2018, doi: 10.2514/6.2018-1243.

[38] Malge and T. Ganesha, “Study And Analysis of Savonious Vertical Axis Wind Turbine With Neodymium Permanent Magnet Rotor,” Int. Res. J. Eng. Technol., vol. 4, no. 8, pp. 438–443, 2017, [Online]. Available: https://irjet.net/archives/V4/i8/IRJET-V4I878.pdf.

[39] Anthony, V. Prasad, K. Raju, M. H. Alsharif, Z. W. Geem, and J. Hong, “Design of rotor blades for vertical axis wind turbine with wind flow modifier for low wind profile areas,” Sustain., vol. 12, no. 19, pp. 1–24, 2020, doi: 10.3390/su12198050.

[40] Chen, Z. Han, D. Zhou, Y. Bao, and Y. Zhao, “Investigation of V-shaped blade for the performance improvement of vertical axis wind turbines,” Appl. Energy, vol. 260, no. December 2019, p. 114326, 2020, doi: 10.1016/j.apenergy.2019.114326.

[41] Siddiqui, M. H. Khalid, R. Zahoor, F. S. Butt, M. Saeed, and A. W. Badar, “A numerical investigation to analyze effect of turbulence and ground clearance on the performance of a roof top vertical–axis wind turbine,” Renew. Energy, vol. 164, pp. 978–989, 2021, doi: 10.1016/j.renene.2020.10.022.

[42] Longo, P. Nicastro, M. Natalini, P. Schito, R. Mereu, and A. Parente, “Impact of urban environment on Savonius wind turbine performance: A numerical perspective,” Renew. Energy, vol. 156, pp. 407–422, 2020, doi:

10.1016/j.renene.2020.03.101.

[43] Vergaerde, T. De Troyer, S. Muggiasca, I. Bayati, M. Belloli, and M. C. Runacres, “Influence of the direction of rotation on the wake characteristics of closely spaced counter-rotating vertical-axis wind turbines,” J. Phys. Conf. Ser., vol. 1618, no. 6, 2020, doi: 10.1088/1742-6596/1618/6/062017.

[44] Darwish and R. Al-Dabbagh, “Wind energy state of the art: present and future technology advancements,” Renew. Energy Environ. Sustain., vol. 5, p. 7, 2020, doi: 10.1051/rees/2020003.

[45] Svorcan, Z. Trivković, T. Ivanov, M. Baltić, and O. Peković, “Multi-objective constrained optimizations of VAWT composite blades based on FEM and PSO,” FME Trans., vol. 47, no. 4, pp. 887–893, 2019, doi: 10.5937/fmet1904887S.

[46] Antar and M. Elkhoury, “Parametric sizing optimization process of a casing for a Savonius Vertical Axis Wind Turbine,” Renew. Energy, vol. 136, pp. 127–138, 2019, doi: 10.1016/j.renene.2018.12.092.

[47] Tian, Z. Mao, X. An, B. Zhang, and H. Wen, “Numerical study of energy recovery from the wakes of moving vehicles on highways by using a vertical axis wind turbine,” Energy, vol. 141, pp. 715–728, 2017, doi: 10.1016/j.energy.2017.07.172.

[48] VIVEK, “a Review on Vertical and Horizontal Axis Wind Turbine,” Int. Res. J. Eng. Technol., vol. 4, no. 4, pp. 2395–56, 2017, [Online]. Available: https://www.irjet.net/archives/V4/i4/IRJET-V4I449.pdf.

[49] Milas and N. Architecture, “Numerical Workflow for 3D Shape Optimization and Synthesis of Vertical-Axis Wind Turbines for Specified Operating.”

[50] Rogowski, R. Maroński, and J. Piechna, “Numerical Analysis of a Small-Size Vertical-Axis Wind Turbine Performance and Averaged Flow Parameters Around the Rotor,” Arch. Mech. Eng., vol. 64, no. 2, pp. 205–218, 2017, doi: 10.1515/meceng-2017-0013.

[51] Wong, W. T. Chong, N. L. Sukiman, S. C. Poh, Y. C. Shiah, and C. T. Wang, “Performance enhancements on vertical axis wind turbines using flow augmentation systems: A review,” Renew. Sustain. Energy Rev., vol. 73, no. November 2016, pp. 904–921, 2017, doi: 10.1016/j.rser.2017.01.160.

[52] Rezaeiha, I. Kalkman, and B. Blocken, “Effect of pitch angle on power performance and aerodynamics of a vertical axis wind turbine,” Appl. Energy, vol. 197, pp. 132–150, 2017, doi: 10.1016/j.apenergy.2017.03.128.

[53] Musgrove, “Vertical axis wind turbine.” pp. 0–5, 1979, doi: 10.22214/ijraset.2019.5679.

[54] Gang and W. C. Kau, “Unsteady Flow Numerical Simulation of Vertical Axis Wind Turbine,” Procedia Eng., vol. 99, pp. 734–740, 2015, doi: 10.1016/j.proeng.2014.12.595.

[55] Mathew S 2006 Wind energy: fundamentals, resource analysis and economics Springer.

[56] El-Askary, A. S. Saad, A. M. AbdelSalam, and I. M. Sakr, "Investigating the performance of a twisted modified Savonius rotor," *J. Wind Eng. Ind. Aerodyn.*, vol. 182, no. April, pp. 344–355, 2018, doi: 10.1016/j.jweia.2018.10.009.

[57] El-Askary, A.S. Saad, A.M. AbdelSalam, I.M. Sakr. "Experimental and theoretical studies for improving the performance of a modified shape Savonius wind turbine". J Energy Resour Technol. 2020 Dec 1; 142 (12).

[58] Jiang, P. Zhao, T. Stoesser, K. Wang, and L. Zou, "Experimental and numerical investigation of twin vertical axis wind turbines with a deflector," Energy Convers. Manag., vol. 209, no. November 2019, p. 112588, 2020, doi: 10.1016/j.enconman.2020.112588.

[59] Saad, A. Elwardany, I. I. El-Sharkawy, S. Ookawara, and M. Ahmed, "Performance evaluation of a novel vertical axis wind turbine using twisted blades in multi-stage Savonius rotors," Energy Convers. Manag., vol. 235, no. November 2020, p. 114013, 2021, doi: 10.1016/j.enconman.2021.114013.

[60] Guarienti, A. Kaufmann Almeida, A. Menegati Neto, A. R. de Oliveira Ferreira, J. P. Ottonelli, and I. Kaufmann de Almeida, "Performance analysis of numerical methods for determining Weibull distribution parameters applied to wind speed in Mato Grosso do Sul, Brazil," Sustain. Energy Technol. Assessments, vol. 42, no. January, 2020, doi: 10.1016/j.seta.2020.100854.

[61] Wais, "Two and three-parameter Weibull distribution in available wind power analysis," Renew. Energy, vol. 103, pp. 15–29, 2017, doi: 10.1016/j.renene.2016.10.041.

[62] Wais, "A review of Weibull functions in wind sector," Renew. Sustain. Energy Rev., vol. 70, no. February 2015, pp. 1099–1107, 2017, doi: 10.1016/j.rser.2016.12.014.

[63] Jung and D. Schindler, "Wind speed distribution selection – A review of recent development and progress," Renew. Sustain. Energy Rev., vol. 114, no. February, p. 109290, 2019, doi: 10.1016/j.rser.2019.109290.

[64] Carta, P. Ramírez, and S. Velázquez, "A review of wind speed probability distributions used in wind energy analysis. Case studies in the Canary Islands," Renew. Sustain. Energy Rev., vol. 13, no. 5, pp. 933–955, 2009, doi: 10.1016/j.rser.2008.05.005.

[65] Aririguzo and E. B. Ekwe, "Weibull distribution analysis of wind energy prospect for Umudike, Nigeria for power generation," Robot. Comput. Integr. Manuf., vol. 55, no. January, pp. 160–163, 2019, doi: 10.1016/j.rcim.2018.01.001.

[66] Soulouknga, S. Y. Doka, N.Revanna, N.Djongyang, and T.C.Kofane, "Analysis of wind speed data and wind energy potential in Faya-Largeau, Chad, using Weibull distribution," Renew. Energy, vol. 121, pp. 1–8, 2018, doi: 10.1016/j.renene.2018.01.002.

[67] Seguro and T. W. Lambert, "Modern estimation of the parameters of the Weibull wind speed distribution for wind energy analysis," J. Wind Eng. Ind. Aerodyn., vol. 85, no. 1, pp. 75–84, 2000, doi: 10.1016/S0167-6105(99)00122-1.

[68] Arslan, Y. M. Bulut, and A. Altin Yavuz, “Comparative study of numerical methods for determining Weibull parameters for wind energy potential,” Renew. Sustain. Energy Rev., vol. 40, pp. 820–825, 2014, doi: 10.1016/j.rser.2014.08.009.

[69] Akdağ and A. Dinler, “A new method to estimate Weibull parameters for wind energy applications,” Energy Convers. Manag., vol. 50, no. 7, pp. 1761–1766, 2009, doi: 10.1016/j.enconman.2009.03.020.

[70] El-Ghazali,"The influence of turbine geometry on the performance of c- section vertical axis wind turbine athesis submitted to the graduate school of applied sciences of by Abdalla El-Ghazali In Partial Fulfillment of the Requirements for the Degree of Master of Scie,” 2016.

APPENDIXES

Appendix (A): Results of the experimental work for six blades

Wind Speed (V) m/s	Radius of Rotor (R) cm	Blade Angle (˚)	Rotational speed (RPM)	Angular velocity (ω) (rad/s)	Tip Speed Ratio (λ)	Torque(T) (N.m)	Power coefficient (Cp)%
1.5	30	40˚	53.5	5.6175	1.124	0.39	11.592
		45˚	51.5	5.4075	1.082	0.45	12.875
		60˚	48.5	5.0925	1.019	0.39	10.508
		90˚	48.5	5.0925	1.019	0.39	10.508
		120˚	46.5	4.8825	0.977	0.36	9.3
		135˚	44	4.62	0.924	0.33	8.067
	40	40˚	50	5.25	1.398	0.44	12.222
		45˚	47	4.935	1.317	0.5	13.056
		60˚	45.5	4.7775	1.276	0.48	12.133
		90˚	44	4.62	1.234	0.44	10.756
		120˚	41	4.305	1.149	0.4	9.111
		135˚	39	4.095	1.093	0.396	8.58
	50	40˚	49	5.145	1.715	0.425	11.569
		45˚	45.5	4.7775	1.593	0.5	12.639
		60˚	37.5	3.9375	1.313	0.35	7.292
		90˚	37	3.885	1.295	0.35	7.194
		120˚	36	3.78	1.26	0.3	6
		135˚	35	3.675	1.225	0.25	4.861
2.5	30	40˚	58	6.09	0.731	0.555	3.854
		45˚	57	5.985	0.718	0.6	4.095
		60˚	51.5	5.4075	0.649	0.555	3.422
		90˚	52.5	5.5125	0.662	0.555	3.489
		120˚	47.5	4.9875	0.599	0.51	2.9
		135˚	47	4.935	0.592	0.51	2.869
	40	40˚	56	5.88	0.941	0.6	4.0228
		45˚	53.5	5.6175	0.899	0.74	4.739
		60˚	50.5	5.3025	0.849	0.68	4.111

		90˚	43.5	4.5675	0.731	0.6	3.125
		120˚	40.5	4.2525	0.681	0.56	2.715
		135˚	39.5	4.1475	0.664	0.56	2.648
	50	40˚	54	5.67	1.134	0.55	3.556
		45˚	52	5.46	1.092	0.725	4.514
		60˚	48.5	5.0925	1.019	0.65	3.774
		90˚	41.5	4.3575	0.872	0.55	2.733
		120˚	37.5	3.9375	0.788	0.45	2.020
		135˚	34	3.57	0.714	0.25	1.018
3	30	40˚	63	6.615	0.662	0.57	2.487
		45˚	60.5	6.3525	0.635	0.63	2.639
		60˚	57.5	6.0375	0.604	0.6	2.3895
		90˚	56	5.88	0.588	0.6	2.327
		120˚	50.5	5.3025	0.53	0.45	1.574
		135˚	46.5	4.8825	0.488	0.36	1.159
	40	40˚	66	6.93	0.924	1.02	4.663
		45˚	63.5	6.6675	0.889	1.12	4.926
		60˚	59.5	6.2475	0.833	0.98	4.039
		90˚	53.5	5.6175	0.749	0.74	2.742
		120˚	46.5	4.8825	0.651	0.64	2.061
		135˚	42.5	4.4625	0.595	0.6	1.766
	50	40˚	65	6.825	1.138	0.95	5.402
		45˚	62.5	6.5625	1.094	1	4.329
		60˚	52.5	5.5125	0.919	0.725	2.636
		90˚	47	4.935	0.823	0.65	2.116
		120˚	40.5	4.2525	0.709	0.55	1.543
		135˚	36.5	3.8325	0.639	0.4	1.011

Appendix (B): Results of the experimental work for three blades (n=3)

Wind Speed (V) m/s	Radius of Rotor (R) cm	Blade Angle (˚)	Rotational speed (RPM)	Angular velocity (ω) (rad/s)	Tip Speed Ratio (λ)	Torque(T) (N.m)	Power coefficient(Cp) %
1.5	30	40˚	47	4.935	0.987	0.33	8.6166667
		45˚	46	4.83	0.966	0.36	9.2
		60˚	43	4.515	0.903	0.33	7.8833333
		90˚	38	3.99	0.798	0.24	5.0666667
		120˚	36	3.78	0.756	0.18	3.6
		135˚	35	3.675	0.735	0.15	2.9166667
	40	40˚	42	4.41	1.176	0.36	8.4
		45˚	41	4.305	1.148	0.42	9.5666667
		60˚	39	4.095	1.092	0.36	7.8
		90˚	36	3.78	1.008	0.24	4.8
		120˚	33	3.465	0.924	0.16	2.9333333
		135˚	32	3.36	0.896	0.12	2.1333333
	50	40˚	42	4.41	1.47	0.35	8.1666667
		45˚	41	4.305	1.435	0.4	9.1111111
		60˚	36	3.78	1.26	0.3	6
		90˚	33	3.465	1.155	0.2	3.6666667
		120˚	31	3.255	1.085	0.15	2.5833333
		135˚	29	3.045	1.015	0.1	1.6111111
2.5	30	40˚	51	5.355	0.643	0.48	2.930901
		45˚	50	5.25	0.63	0.51	3.053022
		60˚	46	4.83	0.579	0.45	2.478335
		90˚	40	4.2	0.504	0.3	1.436716
		120˚	38	3.99	0.479	0.24	1.091904
		135˚	37	3.885	0.466	0.24	1.06317
	40	40˚	49	5.145	0.823	0.5	2.933295
		45˚	48	5.04	0.806	0.6	3.448119
		60˚	43	4.515	0.722	0.4	2.059293
		90˚	38	3.99	0.638	0.32	1.455872
		120˚	35	3.675	0.588	0.28	1.173318
		135˚	34	3.57	0.571	0.24	0.976967

	50	40˚	45	4.725	0.945	0.5	2.693843
		45˚	44	4.62	0.924	0.55	2.897377
		60˚	39	4.095	0.819	0.45	2.101197
		90˚	35	3.675	0.735	0.35	1.466648
		120˚	33	3.465	0.693	0.3	1.185291
		135˚	32	3.36	0.672	0.25	0.957811
3	30	40˚	54	5.67	0.567	0.51	1.907454
		45˚	53	5.565	0.557	0.6	2.202507
		60˚	50	5.25	0.525	0.51	1.766161
		90˚	44	4.62	0.462	0.42	1.279947
		120˚	41	4.305	0.431	0.33	0.937104
		135˚	39	4.095	0.409	0.27	0.729321
	40	40˚	52	5.46	0.728	0.68	2.449077
		45˚	51	5.355	0.714	0.72	2.543272
		60˚	47	4.935	0.658	0.6	1.953166
		90˚	43	4.515	0.602	0.52	1.548681
		120˚	39	4.095	0.546	0.36	0.972427
		135˚	37	3.885	0.518	0.32	0.820053
	50	40˚	50	5.25	0.875	0.65	2.250989
		45˚	49	5.145	0.858	0.7	2.37566
		60˚	43	4.515	0.752	0.55	1.638028
		90˚	40.5	4.253	0.708	0.45	1.262286
		120˚	37	3.885	0.648	0.3	0.768799
		135˚	36	3.78	0.63	0.3	0.748021

Appendix (C): Results of the experimental work for multi -blades hybrid turbine

1- At Wind Speed (V) = 1.5 m/s.

Wind Speed (V) = 1.5 m/s R = 40cm ,r = 30cm						
R at Θ˚	r at Θ˚	N (RPM)	ω (rad/s)	TSR(λ)	T(N.m)	C p %
45	40	52	5.46	2.548	0.9	26
	45	50	5.25	2.45	0.97	26.944
	60	48	5.04	2.352	0.9	24
	90	44	4.62	2.156	0.7	17.111
	120	42	4.41	2.058	0.58	13.533
	135	40	4.2	1.96	0.545	12.111
60	40	50	5.25	2.45	0.83	23.056
	45	48	5.04	2.352	0.9	24
	60	47	4.935	2.303	0.83	21.672
	90	43	4.515	2.107	0.65	15.528
	120	40	4.2	1.96	0.545	12.111
	135	37	3.885	1.813	0.51	10.483
90	40	45	4.725	2.205	0.65	16.25
	45	44	4.62	2.156	0.7	17.111
	60	43	4.515	2.107	0.65	15.528
	90	41	4.305	2.009	0.565	12.869
	120	39	4.095	1.911	0.533	11.548
	135	36	3.78	1.764	0.51	10.2
120	40	39	4.095	1.911	0.478	10.35666667
	45	37	3.885	1.813	0.51	10.48333333
	60	36	3.78	1.764	0.51	10.2
	90	35	3.675	1.715	0.499	9.702777778
	120	34	3.57	1.666	0.492	9.293333333
	135	33	3.465	1.617	0.485	8.891666667
135	40	35	3.675	1.715	0.449	8.730555556
	45	34	3.57	1.666	0.492	9.293333333
	60	33	3.465	1.617	0.485	8.891666667
	90	33	3.465	1.617	0.485	8.891666667
	120	32	3.36	1.568	0.482	8.568888889
	135	32	3.36	1.568	0.482	8.568888889

Wind Speed (V) = 1.5 m/s R = 50 cm ,r = 30cm						
R at Θ˚	r at Θ˚	N (RPM)	ω (rad/s)	TSR(λ)	T(N.m)	C p %
45	40	52	5.46	2.912	1.035	29.9
	45	50	5.25	2.8	1.12	31.11111111
	60	48	5.04	2.688	1.035	27.6
	90	46	4.83	2.576	0.9075	23.19166667
	120	43	4.515	2.408	0.725	17.31944444
	135	41	4.305	2.296	0.625	14.23611111
60	40	48.5	5.0925	2.716	0.95	25.59722222
	45	48	5.04	2.688	1.035	27.6
	60	46	4.83	2.576	0.95	24.27777778
	90	45	4.725	2.52	0.825	20.625
	120	41	4.305	2.296	0.625	14.23611111
	135	38	3.99	2.128	0.5665	11.95944444
90	40	39.5	4.1475	2.212	0.525	11.52083333
	45	39	4.095	2.184	0.581	12.58833333
	60	37.5	3.9375	2.1	0.555	11.5625
	90	37	3.885	2.072	0.555	11.40833333
	120	36	3.78	2.016	0.538	10.76
	135	35	3.675	1.96	0.538	10.46111111
120	40	35.5	3.7275	1.988	0.503	9.920277778
	45	35	3.675	1.96	0.538	10.46111111
	60	34	3.57	1.904	0.538	10.16222222
	90	33	3.465	1.848	0.521	9.551666667
	120	33	3.465	1.848	0.521	9.551666667
	135	32	3.36	1.792	0.518	9.208888889
135	40	34.5	3.6225	1.932	0.4975	9.535416667
	45	34	3.57	1.904	0.538	10.16222222
	60	33	3.465	1.848	0.521	9.551666667
	90	32	3.36	1.792	0.521	9.262222222
	120	33	3.465	1.848	0.521	9.551666667
	135	32	3.36	1.792	0.521	9.262222222

Wind Speed (V) = 1.5 m/s R = 55 cm ,r = 30cm						
R at Θ˚	r at Θ˚	N (RPM)	ω (rad/s)	TSR(λ)	T(N.m)	C p %
45	40	46.5	4.8825	2.76675	0.7825	20.21458333
	45	46	4.83	2.737	0.9075	23.19166667
	60	45	4.725	2.6775	0.7825	19.5625
	90	44	4.62	2.618	0.7825	19.12777778
	120	42	4.41	2.499	0.64	14.93333333
	135	39	4.095	2.3205	0.581	12.58833333
60	40	44.5	4.6725	2.64775	0.725	17.92361111
	45	44	4.62	2.618	0.7825	19.12777778
	60	43.5	4.5675	2.58825	0.725	17.52083333
	90	43	4.515	2.5585	0.725	17.31944444
	120	39	4.095	2.3205	0.581	12.58833333
	135	37	3.885	2.2015	0.555	11.40833333
90	40	38.5	4.0425	2.29075	0.5155	11.02597222
	45	38	3.99	2.261	0.5665	11.95944444
	60	37	3.885	2.2015	0.555	11.40833333
	90	36	3.78	2.142	0.555	11.1
	120	35	3.675	2.0825	0.538	10.46111111
	135	34	3.57	2.023	0.538	10.16222222
120	40	33.5	3.5175	1.99325	0.4825	8.979861111
	45	33	3.465	1.9635	0.524	9.606666667
	60	33	3.465	1.9635	0.524	9.606666667
	90	32	3.36	1.904	0.521	9.262222222
	120	32	3.36	1.904	0.521	9.262222222
	135	31	3.255	1.8445	0.5125	8.826388889
135	40	32.5	3.4125	1.93375	0.4825	8.711805556
	45	32	3.36	1.904	0.521	9.262222222
	60	31	3.255	1.8445	0.5125	8.826388889
	90	31	3.255	1.8445	0.5125	8.826388889
	120	32	3.36	1.904	0.521	9.262222222
	135	31	3.255	1.8445	0.5125	8.826388889

2 - At Wind Speed (V) = 2.5 m/s.

Wind Speed (V) = 2.5 m/s R = 40cm ,r = 30cm						
R at Θ˚	r at Θ˚	N (RPM)	ω (rad/s)	TSR(λ)	T(N.m)	C p %
45	40	51	5.355	1.4994	0.9	5.495
	45	50.5	5.3025	1.4847	1.01	6.107
	60	50	5.25	1.47	0.97	5.807
	90	47	4.935	1.3818	0.83	4.671
	120	44	4.62	1.2936	0.7	3.688
	135	43	4.515	1.2642	0.65	3.346
60	40	50	5.25	1.47	0.83	4.969
	45	49	5.145	1.4406	0.9	5.28
	60	48	5.04	1.4112	0.9	5.172
	90	46	4.83	1.3524	0.795	4.378
	120	43	4.515	1.2642	0.65	3.346
	135	42.5	4.4625	1.2495	0.58	2.951
90	40	48	5.04	1.4112	0.76	4.368
	45	47	4.935	1.3818	0.83	4.671
	60	46	4.83	1.3524	0.795	4.378
	90	45	4.725	1.323	0.735	3.96
	120	42	4.41	1.2348	0.58	2.917
	135	41	4.305	1.2054	0.565	2.773
120	40	44	4.62	1.2936	0.58	3.055
	45	43	4.515	1.2642	0.65	3.346
	60	42	4.41	1.2348	0.58	2.917
	90	41	4.305	1.2054	0.565	2.773
	120	41	4.305	1.2054	0.565	2.773
	135	39	4.095	1.1466	0.533	2.489
135	40	43	4.515	1.2642	0.51	2.626
	45	42	4.41	1.2348	0.58	2.917
	60	41	4.305	1.2054	0.565	2.773
	90	40	4.2	1.176	0.545	2.61
	120	39	4.095	1.1466	0.533	2.489
	135	39	4.095	1.1466	0.533	2.489

Wind Speed (V) = 2.5 m/s R = 50cm ,r = 30cm						
R at Θ˚	r at Θ˚	N (RPM)	ω (rad/s)	TSR(λ)	T(N.m)	C p %
45	40	51.5	5.4075	1.7304	0.99	6.104
	45	51	5.355	1.7136	1.12	6.839
	60	50	5.25	1.68	1.07	6.405
	90	48	5.04	1.6128	0.99	5.689
	120	46	4.83	1.5456	0.87	4.791
	135	42	4.41	1.4112	0.62	3.118
60	40	47.5	4.9875	1.596	0.83	4.72
	45	47	4.935	1.5792	0.91	5.121
	60	46	4.83	1.5456	0.87	4.791
	90	46	4.83	1.5456	0.87	4.791
	120	44	4.62	1.4784	0.755	3.977
	135	42	4.41	1.4112	0.62	3.118
90	40	43	4.515	1.4448	0.565	2.909
	45	42	4.41	1.4112	0.62	3.118
	60	41	4.305	1.3776	0.58	2.847
	90	41	4.305	1.3776	0.58	2.847
	120	40	4.2	1.344	0.58	2.778
	135	39	4.095	1.3104	0.57	2.662
120	40	40	4.2	1.344	0.5	2.395
	45	39	4.095	1.3104	0.57	2.662
	60	38	3.99	1.2768	0.551	2.507
	90	38	3.99	1.2768	0.551	2.507
	120	37	3.885	1.2432	0.54	2.392
	135	37	3.885	1.2432	0.54	2.392
135	40	39	4.095	1.3104	0.503	2.349
	45	38	3.99	1.2768	0.551	2.507
	60	37	3.885	1.2432	0.54	2.392
	90	37	3.885	1.2432	0.54	2.392
	120	36	3.78	1.2096	0.525	2.263
	135	36	3.78	1.2096	0.525	2.263

Wind Speed (V) = 2.5 m/s R = 55cm ,r = 30cm						
R at Θ˚	r at Θ˚	N (RPM)	ω (rad/s)	TSR(λ)	T(N.m)	C p %
45	40	49.5	5.1975	1.76715	0.9225	5.467
	45	49	5.145	1.7493	1.035	6.072
	60	48	5.04	1.7136	1.035	5.948
	90	47	4.935	1.6779	0.95	5.346
	120	45	4.725	1.6065	0.825	4.445
	135	43	4.515	1.5351	0.725	3.732
60	40	46.5	4.8825	1.66005	0.795	4.426
	45	46	4.83	1.6422	0.9075	4.998
	60	45	4.725	1.6065	0.825	4.445
	90	44	4.62	1.5708	0.7825	4.122
	120	43	4.515	1.5351	0.725	3.732
	135	41	4.305	1.4637	0.625	3.068
90	40	41.5	4.3575	1.48155	0.555	2.758
	45	41	4.305	1.4637	0.625	3.068
	60	40	4.2	1.428	0.5975	2.861
	90	39	4.095	1.3923	0.581	2.713
	120	38	3.99	1.3566	0.5665	2.577
	135	37	3.885	1.3209	0.555	2.459
120	40	38	3.99	1.3566	0.4975	2.263
	45	37	3.885	1.3209	0.555	2.459
	60	36	3.78	1.2852	0.555	2.392
	90	35.5	3.7275	1.26735	0.541	2.299
	120	35	3.675	1.2495	0.541	2.267
	135	34	3.57	1.2138	0.5325	2.168
135	40	36.5	3.8325	1.30305	0.47	2.054
	45	36	3.78	1.2852	0.555	2.392
	60	35	3.675	1.2495	0.541	2.267
	90	35	3.675	1.2495	0.541	2.267
	120	34	3.57	1.2138	0.5325	2.168
	135	34	3.57	1.2138	0.5325	2.168

3 - At Wind Speed (V) = 3 m/s.

Wind Speed (V) = 3 m/s R = 40cm ,r = 30cm						
R at Θ˚	r at Θ˚	N (RPM)	ω (rad/s)	TSR(λ)	T(N.m)	C p %
45	40	61	6.405	1.4945	1.25	5.281
	45	60	6.3	1.47	1.32	5.485
	60	58	6.09	1.421	1.195	4.8
	90	54	5.67	1.323	1.13	4.226
	120	51	5.355	1.2495	1.01	3.568
	135	49	5.145	1.2005	0.9	3.054
60	40	59	6.195	1.4455	1.125	4.597
	45	57	5.985	1.3965	1.195	4.718
	60	54	5.67	1.323	1.13	4.226
	90	53	5.565	1.2985	1.11	4.075
	120	50	5.25	1.225	0.97	3.359
	135	48	5.04	1.176	0.9	2.992
90	40	53	5.565	1.2985	0.9	3.304
	45	52	5.46	1.274	1.04	3.746
	60	51	5.355	1.2495	1.01	3.568
	90	49	5.145	1.2005	0.9	3.054
	120	47	4.935	1.1515	0.83	2.702
	135	46	4.83	1.127	0.795	2.533
120	40	47	4.935	1.1515	0.705	2.295
	45	46	4.83	1.127	0.795	2.533
	60	45	4.725	1.1025	0.735	2.291
	90	45	4.725	1.1025	0.735	2.291
	120	44	4.62	1.078	0.7	2.133
	135	43	4.515	1.0535	0.65	1.936
135	40	46	4.83	1.127	0.65	2.071
	45	45	4.725	1.1025	0.735	2.291
	60	44	4.62	1.078	0.7	2.133
	90	44	4.62	1.078	0.7	2.133
	120	43	4.515	1.0535	0.65	1.936
	135	42	4.41	1.029	0.58	1.687

Wind Speed (V) = 3 m/s R = 50 cm ,r = 30cm						
R at Θ˚	r at Θ˚	N (RPM)	ω (rad/s)	TSR(λ)	T(N.m)	C p %
45	40	58	6.09	1.624	1.325	5.323
	45	57	5.985	1.596	1.42	5.606
	60	56	5.88	1.568	1.365	5.294
	90	55	5.775	1.54	1.31	4.99
	120	52	5.46	1.456	1.15	4.142
	135	50	5.25	1.4	1.07	3.705
60	40	54.5	5.7225	1.526	1.09	4.114
	45	54	5.67	1.512	1.255	4.694
	60	53	5.565	1.484	1.23	4.515
	90	52	5.46	1.456	1.15	4.142
	120	49	5.145	1.372	0.99	3.36
	135	47	4.935	1.316	0.91	2.962
90	40	47.5	4.9875	1.33	0.83	2.731
	45	47	4.935	1.316	0.91	2.962
	60	46	4.83	1.288	0.87	2.772
	90	46	4.83	1.288	0.87	2.772
	120	45	4.725	1.26	0.795	2.478
	135	44	4.62	1.232	0.755	2.301
120	40	43.5	4.5675	1.218	0.54	1.627
	45	43	4.515	1.204	0.7	2.085
	60	42	4.41	1.176	0.62	1.804
	90	42	4.41	1.176	0.62	1.804
	120	42	4.41	1.176	0.62	1.804
	135	41	4.305	1.148	0.605	1.718
135	40	43	4.515	1.204	0.54	1.608
	45	42	4.41	1.176	0.62	1.804
	60	41	4.305	1.148	0.605	1.718
	90	41	4.305	1.148	0.605	1.718
	120	42	4.41	1.176	0.62	1.804
	135	40	4.2	1.12	0.58	1.607

Wind Speed (V) = 3 m/s R = 55cm ,r = 30cm						
R at Θ˚	r at Θ˚	N (RPM)	ω (rad/s)	TSR(λ)	T(N.m)	C p %
45	40	56	5.88	1.666	1.2875	4.994
	45	55	5.775	1.63625	1.375	5.238
	60	54	5.67	1.6065	1.3175	4.928
	90	53	5.565	1.57675	1.29	4.735
	120	50	5.25	1.4875	1.12	3.879
	135	48	5.04	1.428	1.035	3.441
60	40	53.5	5.6175	1.591625	1.035	3.835
	45	53	5.565	1.57675	1.29	4.735
	60	52	5.46	1.547	1.205	4.34
	90	51	5.355	1.51725	1.175	4.15
	120	48	5.04	1.428	1.035	3.441
	135	46	4.83	1.3685	0.9075	2.891
90	40	45	4.725	1.33875	0.6825	2.127
	45	44	4.62	1.309	0.7825	2.385
	60	43	4.515	1.27925	0.725	2.159
	90	42	4.41	1.2495	0.64	1.862
	120	41	4.305	1.21975	0.625	1.775
	135	40	4.2	1.19	0.5975	1.655
120	40	39	4.095	1.16025	0.5155	1.392
	45	38	3.99	1.1305	0.5665	1.491
	60	37	3.885	1.10075	0.555	1.422
	90	37	3.885	1.10075	0.555	1.422
	120	36	3.78	1.071	0.555	1.384
	135	35	3.675	1.04125	0.541	1.311
135	40	38.5	4.0425	1.145375	0.5095	1.359
	45	38	3.99	1.1305	0.5665	1.491
	60	37	3.885	1.10075	0.555	1.422
	90	36	3.78	1.071	0.555	1.384
	120	37	3.885	1.10075	0.555	1.422
	135	35	3.675	1.04125	0.541	1.311

Appendix (D): Published research

1-

Design Engineering

ISSN: 0011-9342 | Year 2021
Issue: 8 | Pages: 7085 - 7102

Wind Turbine Performance: Review

[1]Ikhlas Qanber Ayuz Fath Ali; [2]Salwan Obaid Waheed Khafaji ; [3]Dhirgham AL Khafaji

[1,2,3] Mechanical Engineering Department, University of Babylon, Iraq
E-mail: alnafs55@gmail.com, ekhlas.muhammad@student.uobabylon.edu.iq

Abstract. Increased environmental issues have contributed for requesting more energy options that are ecofriendly in its nature. As a clean source of green electricity, wind energy is available in vast amounts in certain parts of the world. This can be used if well harnessed correctly to overcome the difficulties of major strength problems. For places far away from integrated grid, vertical axis wind turbines provide promising alternatives. Local wind patterns, surrounding obstructions, power demand patterns, and number of other variables influence the actual output. The diameter of Rotor, mean wind speed, cut in speed, cut out speed, turbine performance, and Weibull shape parameters are the main characteristics of the wind turbine c. In this article, these characteristics are discussed to understand the main functions of these parameters and how it control to enhnce the output torque.

Nomenclature

Symbol	Description
VAWT	Vertical axial wind turbine
m	Mass of air
V	Velocity
E	Kinetic energy
ν	The air volume
A_T	A cross sectional area
ρ_a	The air density
P	Power
P_T	Powe of turbine
C_P	The power coefficient
F	Force
T	The rotor torque
C_T	The torque coefficient
λ	Tip speed ratio
ω	The angular velocity
N	The rotational speed
R	Radius of rotor
σ	Solidity
c	Chord length

Contents

2-

ISSN: 0974-5823 Vol. 7 No. 2 February, 2022

International Journal of Mechanical Engineering

Performance of Multi Buckets Vertical -Axis Wind Turbine with at Different Blades Angles

[*1]Ikhlas Qamber Ayuz. Fateh Ali, [1]Salwan Obaid Waheed Khafaji and [1]Dhirgham Al Kafaji

[1]Department of Mechanical Engineering, College of Engineering, University of Babylon, Iraq

Abstract

Utilizing wind energy in built-up locations to generate electricity via the turbines for home usage remains a challenge, despite extensive studies in this field. The variability and uncertainty in the wind conditions, manufacturing complexity, and the expenses are the main parameters that make the wind turbines unsuitable for domestic use. Vertical axis wind turbines (VAWTs) are suitable for use in built sites because to their outstanding features, attractiveness, low noise, and safety. To achieve these objectives, vertical axis wind turbines with multiple blades (blades are made from polyvinyl chloride (PVC) material) have been designed, manufactured and studied experimentally to investigate its performance. Turbine's blade is a half cylinder in its shape. The blades rotational speed of the blades, the resulted torque (T), and generated power (P) of each configuration of the suggested turbine were determined for different wind speeds (1.5m/s, 2.5m/s, and 3m/s) and rotor radius of (30cm, 40cm ,and 50cm), respectively. The graphical relation between coefficient of power (C_p) and the tip speed ratio (TSR) and between coefficient of power (C_p) and angles of the blades were constructed. It was noted that performance of wind turbine is largely depends on wind speed, blade locations, and blade angle. The maximum value of the power coefficients (Cp =13.056%) is noticed at 40cm and 1.5 m/s for blade radius and wind speed, respectively, specifically at TSR=1.3 and 45o blade angle**.** The maximum values of the Cp for all values of the effective parameters are noticed at 45o blade angle. In addition, higher values of Cp are achieved at the lower wind speeds and high blade radius, and that corresponds to higher TSR. Finally, VAWT is able to generate electricity for local use even at low wind speeds.

Keywords: wind turbine, power coefficient, wind speed, blade angle, blade location, tip speed ratio

Nomenclature

Symbol	Description
VAWT	Vertical axial wind turbine
HAWT	Horizontal
m	Mass of air
V	Velocity
E	Kinetic energy
v	The air volume
A_T	A cross sectional area
ρ_a	The air density
P	Power
P_T	Power of turbine
C_P	The power coefficient
F	Force
T	The rotor torque
C_T	The torque coefficient
TSR , λ	Tip speed ratio
ω	The angular velocity
N	The rotational speed
R	Radius of rotor

3-

ICECET 2022
International Conference on
Electrical, Computer and Energy Technologies
20-22 July 2022, Prague

06/06/2022

ACCEPTANCE LETTER

Dear ***Ekhlas Qanber Ayuz Fateh Ali, Salwan Obaid Waheed Khafaji, Dhirgham Al Kafaji,***

Thank you for your submission to the ICECET 2022 conference. We are pleased to inform you that your paper entitled **"ID-1004 Privacy-Preserving Short-term Power Consumption Forecasting Using K-anonymity "** has been accepted as a full paper for **oral presentation** by the conference committee of *International Conference on Electrical, Computer, and Energy Technologies (ICECET)*. The event will take place in Prague, Czech Republic on 20-22 July 2022 **online** and **physically.**

We strictly follow "no podium, no paper" policy and only the papers that are presented at the conference will be submitted to IEEE Explore for publication. **At least one author** of an accepted paper must register (as a full participant) and participate in ICECET 2022 online or physically for the paper to be included in the proceedings. If you have not yet registered online (using the credit card or bank transfer options), at least one author of each paper should register to the conference via the online registration page at https://www.ecres.net/icecet. If you have already registered, please do not make another registration. Kindly note that your registration becomes valid only after your payment.

According to the conference regulations, only those papers which have been duly registered and presented on the conference day are considered for submission to IEEE Explore. The conference program will be communicated in due course.

We look forward to seeing you for a fruitful research and innovation event and for a great time in the wonderful environment of Prague

Yours sincerely,

Dr. Simon Winberg
Chair

Web: http://www.icecet.com E-mail: icecet.conference@gmail.com

1/1

Participation in the 1st International Conference on Advances in Engineering Science and Technology (AEST - 2021), Iraq.

Certificate

OF PARTICIPATION

THIS CERTIFICATE IS PROUDLY PRESENTED TO

Ikhlas Q. A. Fateh Ali

For successful participation in the 1st International Conference on Advances in Engineering Science and Technology (AEST-2021), Iraq, with the STEPS Ltd, and Liverpool John Moores University, UK that was held online on 26-27th April 2021.

Prof. Dr. Jasim M.Salman
On behalf of the University of Babylon
Signature

R. S. Mohammed
On behalf of the Academic Steps Ltd
Signature

Appendix (E): Calibration

a- Calibration Anemometry device

The anemometer is calibrated with a digital device (hot wire anemometer) as shown in the figures (E-1) and (E-2) respectively . A hot wire anemometer is used to measure velocity.

Fig. (E – 1) Anemometry device

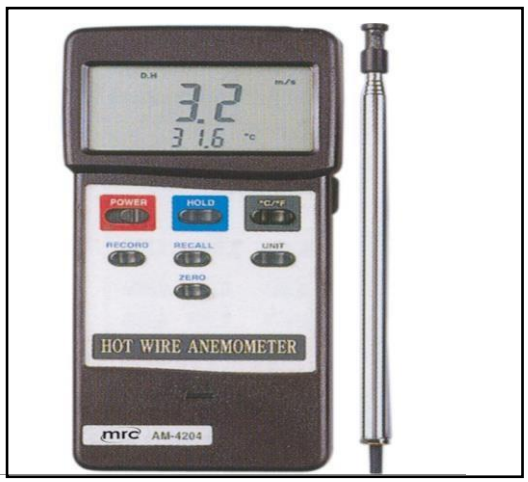

Fig. (E – 2) Hot wire anemometer

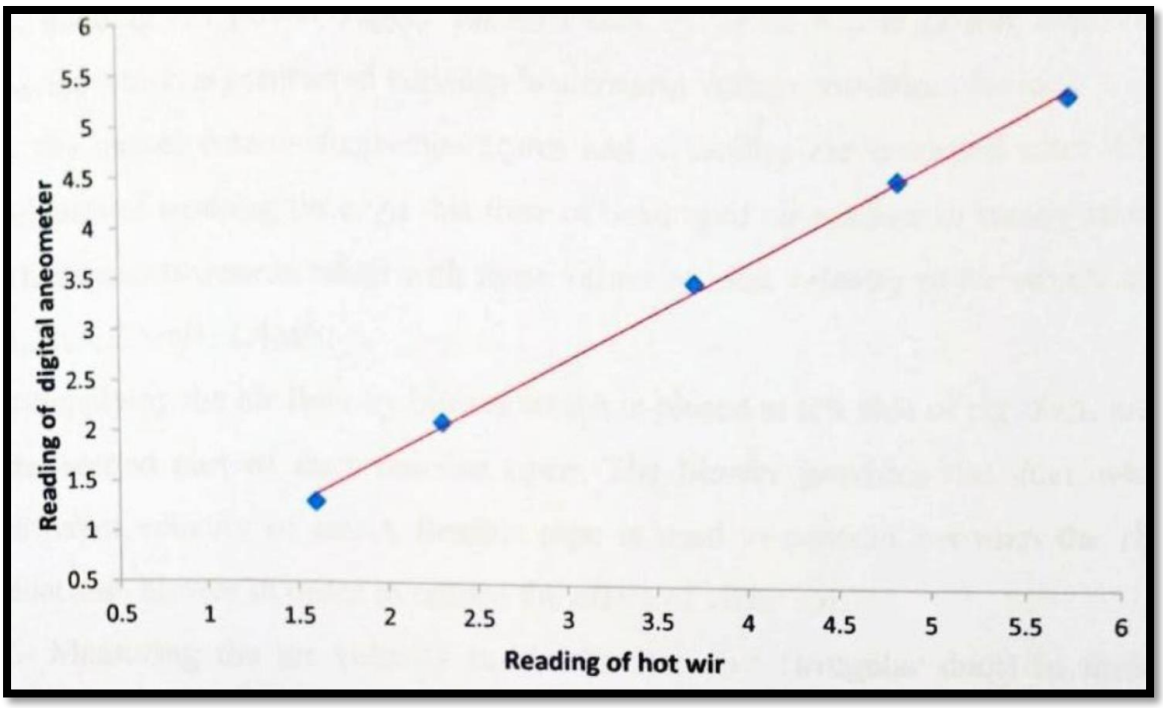

Fig. (E- 3) curve of velocity calibration

b- Rotational Speed (RPM)Calibration

Rotational Speed measurement device is calibrated with a digital calibration device type (Digital Laser RPM Tachometer) as shown in figs. (E-4) and (E- 5) respectively. Tachometer A device for measuring speed, the number of revolutions of rotation, whether mechanical or electronic, analog or digital. A tachometer is used to measure the speed of rotation of a shaft or wheel, usually in revolutions per minute (RPM). Tachometers are commonly used to measure revolutions per minute of machinery in automobiles, ships, aircraft, and all machinery and engines.

Fig. (E – 4) Rotational Speed measurement device

Fig. (E – 5) Digital Laser RPM Tachometer

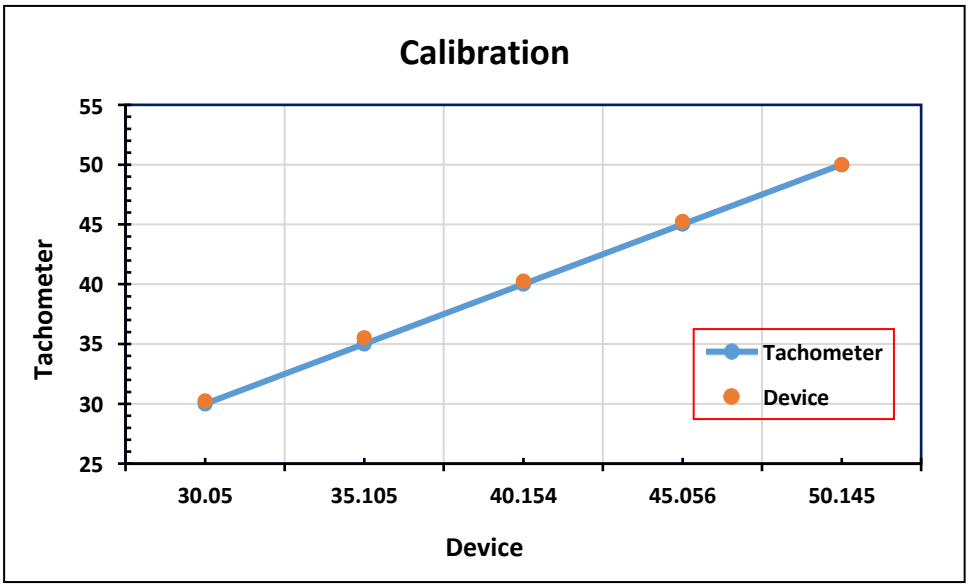

Fig. (E – 6) curve of RPM calibration

الخلاصة

أدت المخاوف البيئية المتزايدة إلى الطلب على المزيد من خيارات الطاقة الصديقة للبيئة. في جميع أنحاء العالم ، تعد طاقة الرياح أحد المصادر النظيفة والمتجددة للكهرباء الخضراء. الوقود الأحفوري هو أحد أهم مصادر الطاقة لدينا وكمياته آخذة في التناقص. ومع ذلك ، فإن الرياح هي مورد متجدد يمكن أن يكون مصدرًا للوقود. تستخدم توربينات الرياح لتسخير الرياح لتوليد الطاقة. بالنسبة للاستخدام المنزلي ، بالنسبة للاستخدام المنزلي ، فإن معظم توربينات الرياح ذات المحور الأفقي (HAWTs)غير جذابة نظرًا لتعقيد التصنيع والتكلفة. تعد توربينات الرياح ذات المحور الرأسي (VAWTs)مثالية للتطبيقات الحضرية نظرًا لتعدد استخداماتها وجمالياتها وانخفاض مستوى الضجيج والسلامة فيها. لتحسين أداء توربينات الرياح ذات المحور الرأسي ، توربينات الرياح متعددة الشفرات ذات المحور الرأسي (sim-Savonius) بستة أذرع بستة دلو دوار منزلق (نصف) مما يمنح المرونة لتغيير الزخم من خلال تغيير طول الذراع وزوايا الشفرات تم تصميمها واختبارها في هذه الدراسة تجريبياً وتصنيعها ودراستها للتحقق من أدائها. شفرة التوربين هي (شفرة نصف أسطوانة). تم اختبار توربينات الرياح الهجينة Savonius بسرعات رياح مختلفة (١,٥ م / ث ، ٢,٥ م / ث ، ٣ م / ث) ونصف قطر (٣٠ سم ، ٤٠ سم ، ٥٠ سم) لأول توربين ، (٤٠ سم ، ٥٠ سم ، ٥٥ سم) للتوربينات الهجينة عنفة. تم إنشاء العلاقة الرسومية بين عامل القدرة (Cp) ونسبة السرعة النهائية (TSR) وبين عامل القدرة (Cp) وزوايا الشفرة. من الملاحظ أن أداء توربينات الرياح يعتمد إلى حد كبير على سرعة الرياح ومواقع الريش وعدد الشفرات وزاوية الريش. تم ملاحظة القيمة القصوى لمعاملات القدرة للتوربين الهجين(Cp = 31.111 ٪ (عند (R = 50 cm ، (r = 30 cm و ١,٥ m / s لنصف قطر الشفرة وسرعة الرياح ، على التوالي ، وتحديداً عند TSR = 2.8 ، زاوية النصل (Θ) = 45 درجة وعدد الشفرات (ن) يساوي ستة ،حيث بلغت نسبة الزيادة في معامل القدرة بين التوربين الهجين متعدد الشفرات (MBHYVAWT) وتوربين الرياح ذو المحور العمودي الذي يحتوي على ستة شفرات (VAWT–b6) = ١,٣٨٣%، وبين (MBHYVAWT)و (VAWT-b3) = ٢,٧% كما تم تحليل قاعدة بيانات سرعة الرياح لمحافظة بابل للأعوام الـ ٣١ الماضية باستخدام (توزيع احتمالية Weibull) ، وتم الحصول على السرعة المقدرة (VR) وسرعة القطع (VI) وسرعة القطع (VO) للتوربين. سرعة القطع (VI) للتوربين هي الحد الأدنى لسرعة الرياح التي تبدأ عندها الآلة في إنتاج الطاقة. السرعة المقدرة للتوربين (VR) هي أقل سرعة رياح مطابقة لقوتها المقدرة. سرعة القطع (VO) للتوربين هي

سرعة الرياح التي يتم فيها إيقاف تشغيل التوربين (لا توجد طاقة في النظام). يتم تحديد منحنى مدة القدرة أيضًا بناءً على منحنى مدة السرعة ، والذي يتم رسمه بين قيم النسبة المئوية للسرعة والوقت. بمجرد أن يتم تكعيب محور السرعة ، سيكون لدينا منحنى قوة ، بحيث تتناسب المساحة الواقعة أسفل هذا المنحنى مع كمية الطاقة المتاحة سنويًا. وُجدت الطاقة لمدة أربع سنوات (١٩٨٨ و ١٩٩٨ و ٢٠٠٨ و ٢٠١٨) لتكون (٣,١٠٤ و ١ و ٢,٣٧٠ و ٢,٧٨٣) وات على التوالي.

جمهـــورية العـــــراق
وزارة التعليم العالي والبحث العلمي
جـــــامعـــة بابـــــــل
كليـــــــــة الهنـــدســـــــة
قســـم الهنـدســـة الميكانيكيـــة

اختبار نفق الرياح للدوار الرأسي الجديد متعدد الشفرات لتحسين الطاقة الاخرج في مدينة الحلة

رسالة
مقدمة الى كلية الهندسة / جامعة بابل وهي جزء من متطلبات نيل درجة ماجستير في الهندسة الميكانيكية / قدرة

أعدت من قبل
اخلاص قنبر أيوز محمد

بأشراف
أ.د. ضرغام عبد الحسن الخفاجي
أ.د. سلوان عبيد وحيد خفاجي

١٤٤٤ هـ **2022 م**